Modulation of T-cell responses to Murine Melanoma by Targeted-Cytokine Therapy.

Thesis

UNRESTRICTED

MODULATION OF T-CELL RESPONSES TO MURINE MELANOMA BY TARGETED-CYTOKINE THERAPY

Ph.D. Thesis

in

Immunology

by

Jürgen C. Becker, M.D.

THE OPEN UNIVERSITY
London

Submitted November, 2000

Sponsoring Establishment
Institute of Cancer Biology
THE DANISH CANCER SOCIETY
Strandboulevarden 49
2100 Copenhagen
Denmark

DATE OF SUBMISSION : 30 OCTOBER 2000
DATE OF AWARD : 9 JANUARY 2001

ProQuest LLC.
789 East Eisenhower Parkway
P.O. Box 1346
Ann Arbor, MI 48106 – 1346

Abstract

The present thesis describes the characterization of T cell responses to melanoma and its modulation by *in situ* cytokine therapy. Previous studies have shown that antibody cytokine fusion proteins, designated immunocytokines, achieve high cytokine concentrations in the tumor microenvironment and thereby effectively stimulate cellular immune responses against malignancies. Analysis of the T cell receptor repertoire of tumor infiltrating lymphocytes, as presented here, revealed operative differences in the immunomodulatory capacity of two proinflammatory cytokines, i.e., interleukin 2 and lymphotoxin α, if applied targeted to the tumor site. While interleukin 2 is boosting an already established T cell response and enables the re-circulation of clonally expanded T cells, lymphotoxin α's *modus operandi* is relying on newly recruited T cells. Via induction of a tertiary lymphoid organ at the tumor site lymphotoxin α immunocytokines allow the recruitment, priming, and activation of naïve T cells to harness an effective T cell response against the tumor.

List of Papers or Manuscript Included in the Thesis

1. Becker JC, Lode HN, thor Straten P, Reisfeld RA. Targeted-IL-2 Therapy for Melanoma by Immuno-cytokines. Dermatol.Therapy 10, 53-61. 2000.

2. thor Straten P, Guldberg P, Seremet T, Reisfeld RA, Zeuthen J, Becker JC. Activation of preexisting T cell clones by targeted interleukin 2 therapy. Proc Natl Acad Sci U S A 1998 Jul;95(15):8785-90.

3. Becker JC, Guldberg P, Andersen MH, Moerch U, Schrama D, Seremet T, Siedel C, Zeuthen J, Reisfeld RA, thor Straten P. 2000. *In situ* Cytokine Therapy: Redistribution of Clonally expanded T-cell Clones. *submitted*

4. Schrama D, thor Straten P, Fischer WH, Broecker EB, Reisfeld RA, Becker JC. 2000. Targeting of lymphotoxin-α to the tumor microenvironment elicits an efficient immune response by induction of a peripheral lymphoid-like tissue. *submitted*

List of Papers not Included in the Thesis

1. Becker JC, Kolanus W, Lonnemann C, Schmidt RE. Human natural killer clones enhance in vitro antibody production by tumour necrosis factor alpha and gamma interferon. Scand J Immunol 1990 Aug;32(2):153-62.

2. Becker JC, Dummer R, Hartmann AA, Burg G, Schmidt RE. Shedding of ICAM-1 from human melanoma cell lines induced by IFN-gamma and tumor necrosis factor-alpha. Functional consequences on cell- mediated cytotoxicity. J Immunol 1991 Dec;147(12):4398-401.

3. Becker JC, Dummer R, Schmidt RE, Burg G, Hartmann AA. Shedding of soluble intercellular adhesion molecule 1 (ICAM-1) from melanoma cells and the effect on cellular cytotoxicity. Immun Infekt 1992 Apr;20(2):62-3.

4. Becker JC, Dummer R, Von Wussow P, Burg G, Schmidt RE. Non-MHC-restricted T-cell interaction with B cells: role of the T-cell receptor. Scand J Immunol 1992 Aug;36(2):177-81.

5. Becker JC, Dummer R, Schwinn A, Hartmann AA, Burg G. Circulating intercellular adhesion molecule-1 in melanoma patients: induction by interleukin-2 therapy. J Immunother 1992 Aug;12(2):147-50.

6. Dummer R, Becker JC, Boser B, Hartmann AA, Burg G. Successful therapy of metastatic eccrine poroma using perilesional interferon alfa and interleukin 2. Arch Dermatol 1992 Aug;128(8):1127-8.

7. Dummer R, Posseckert G, Nestle F, Witzgall R, Burger M, Becker JC, Schafer E, Wiede J, Sebald W, Burg G. Soluble interleukin-2 receptors inhibit interleukin 2-dependent proliferation and cytotoxicity: explanation for diminished natural killer cell activity in cutaneous T-cell lymphomas in vivo? J Invest Dermatol 1992 Jan;98(1):50-4.

8. Becker JC, Schwinn A, Dummer R, Burg G, Broecker EB. Tumour-infiltrating lymphocytes in primary melanoma: functional consequences of differential IL-2 receptor expression. Clin Exp Immunol 1993 Jan;91(1):121-5.

9. Becker JC, Schwinn A, Dummer R, Burg G, Broecker EB. Lesion-specific activation of cloned human tumor-infiltrating lymphocytes by autologous tumor cells: induction of proliferation and cytokine production. J Invest Dermatol 1993 Jul;101(1):15-21.

10. Becker JC, Termeer C, Schmidt RE, Broecker EB. Soluble intercellular adhesion molecule-1 inhibits MHC-restricted specific T cell/tumor interaction. J Immunol 1993 Dec;151(12):7224-32.

11. Becker JC, Brabletz T, Czerny C, Termeer C, Broecker EB. Tumor escape mechanisms from immunosurveillance: induction of unresponsiveness in a specific MHC-restricted CD4+ human T cell clone by the autologous MHC class II^+ melanoma. Int Immunol 1993 Dec;5(12):1501-8.

12. Dummer R, Becker JC, Eilles C, Schafer E, Borner W, Burg G. T cells migrate to tumour sites after extracorporeal interleukin 2 stimulation and reinfusion in a patient with metastatic melanoma. Br J Dermatol 1993 Apr;128(4):399-403.

13. Becker JC, Gillitzer R, Broecker EB. A member of the melanoma antigen-encoding gene (MAGE) family is expressed in human skin during wound healing. Int J Cancer 1994 Aug;58(3):346-8.

14. Becker JC, Winkler B, Klingert S, Broecker EB. Antiphospholipid syndrome associated with immunotherapy for patients with melanoma. Cancer 1994 Mar;73(6):1621-4.

15. Becker JC, Broecker EB. Prevention of anergy induction in cloned T cells by interleukin 12. Exp Dermatol 1994 Dec;3(6):283-9.

16. Becker JC, Czerny C, Broecker EB. Maintenance of clonal anergy by endogenously produced IL-10. Int Immunol 1994 Oct;6(10):1605-12.

17. Rünger TM, Klein CE, Becker JC, Broecker EB. The role of genetic instability, adhesion, cell motility, and immune escape mechanisms in melanoma progression. Curr Opin Oncol 1994 Mar;6(2):188-96.

18. Schultz ES, Dummer R, Becker JC, Zillikens D, Burg G. Influence of various cytokines on the interleukin-2-dependent lysis of melanoma cells in vitro. Arch Dermatol Res 1994;286(2):73-6.

19. Becker JC, Broecker EB. Lymphocyte-melanoma interaction: role of surface molecules. Recent Results Cancer Res 1995;139:205-14.

20. Becker JC, Brabletz T, Kirchner T, Conrad CT, Broecker EB, Reisfeld RA. Negative transcriptional regulation in anergic T cells. Proc Natl Acad Sci U S A 1995 Mar;92(6):2375-8.

21. Becker JC, Nikroo A, Brabletz T, Reisfeld RA. DNA loops induced by cooperative binding of transcriptional activator proteins and preinitiation complexes. Proc Natl Acad Sci U S A 1995 Oct;92(21):9727-31.

22. Bröcker EB, Becker JC. Immunology of melanoma. Hautarzt 1995 Nov;46(11):818-28.

23. Dummer R, Gore ME, Hancock BW, Guillou PJ, Grobben HC, Becker JC, Oskam R, Dieleman JP, Burg G. A multicenter phase II clinical trial using dacarbazine and continuous infusion interleukin-2 for metastatic melanoma. Clinical data and immunomonitoring. Cancer 1995 Feb;75(4):1038-44.

24. Dummer W, Becker JC, Schwaaf A, Leverkus M, Moll T, Broecker EB. Elevated serum levels of interleukin-10 in patients with metastatic malignant melanoma. Melanoma Res 1995 Feb;5(1):67-8.

25. Yebra M, Filardo EJ, Bayna EM, Kawahara E, Becker JC, Cheresh DA. Induction of carcinoma cell migration on vitronectin by NF-kappa B- dependent gene expression. Mol Biol Cell 1995 Jul;6(7):841-50.

26. Becker JC, Varki N, Gillies SD, Furukawa K, Reisfeld RA. Long-lived and transferable tumor immunity in mice after targeted interleukin-2 therapy. J Clin Invest 1996 Dec;98(12):2801-4.

27. Becker JC, Pancook JD, Gillies SD, Mendelsohn J, Reisfeld RA. Eradication of human hepatic and pulmonary melanoma metastases in SCID mice by antibody-interleukin 2 fusion proteins. Proc Natl Acad Sci U S A 1996 Apr;93(7):2702-7.

28. Becker JC, Pancook JD, Gillies SD, Furukawa K, Reisfeld RA. T cell-mediated eradication of murine metastatic melanoma induced by targeted interleukin 2 therapy. J Exp Med 1996 May;183(5):2361-6.

29. Becker JC, Varki N, Gillies SD, Furukawa K, Reisfeld RA. An antibody-interleukin 2 fusion protein overcomes tumor heterogeneity by induction of a cellular immune response. Proc Natl Acad Sci U S A 1996 Jul;93(15):7826-31.

30. Becker JC, Varki N, Broecker EB, Reisfeld RA. Lymphocyte-mediated alopecia in C57BL/6 mice following successful immunotherapy for melanoma. J Invest Dermatol 1996 Oct;107(4):627-32.

31. Montgomery AM, Becker JC, Siu CH, Lemmon VP, Cheresh DA, Pancook JD, Zhao X, Reisfeld RA. Human neural cell adhesion molecule L1 and rat homologue NILE are ligands for integrin alpha v beta 3. J Cell Biol 1996 Feb;132(3):475-85.

32. Pancook JD, Becker JC, Gillies SD, Reisfeld RA. Eradication of established hepatic human neuroblastoma metastases in mice with severe combined immunodeficiency by antibody-targeted interleukin-2. Cancer Immunol Immunother 1996 Feb;42(2):88-92.

33. Reisfeld RA, Gillies SD, Mendelsohn J, Varki NM, Becker JC. Involvement of B lymphocytes in the growth inhibition of human pulmonary melanoma metastases in athymic nu/nu mice by an antibody- lymphotoxin fusion protein. Cancer Res 1996 Apr;56(8):1707-12.

34. Stromblad S, Becker JC, Yebra M, Brooks PC, Cheresh DA. Suppression of p53 activity and p21WAF1/CIP1 expression by vascular cell integrin alphaVbeta3 during angiogenesis. J Clin Invest 1996 Jul;98(2):426-33.

35. thor Straten P, Becker JC, Seremet T, Broecker EB, Zeuthen J. Clonal T cell responses in tumor infiltrating lymphocytes from both regressive and progressive regions of primary human malignant melanoma. J Clin Invest 1996 Jul;98(2):279-84.

36. Becker JC, Terheyden P, Broecker EB. Molecular basis of T-cell dysfunction in melanoma. Melanoma Res 1997 Aug;7 Suppl 2:S51-S57.

37. Reisfeld RA, Becker JC, Gillies SD. Immunocytokines: a new approach to immunotherapy of melanoma. Melanoma Res 1997 Aug;7 Suppl 2:S99-106.

38. Lode HN, Xiang R, Becker JC, Gillies SD, Reisfeld RA. Immunocytokines: a promising approach to cancer immunotherapy. Pharmacol Ther 1998 Dec;80(3):277-92.

39. Terheyden P, Kampgen E, Runger TM, Broecker EB, Becker JC. Immunochemotherapy of metastatic uveal melanoma with interferon alfa- 2b, interleukin-2 and fotemustine. Case reports and review of the literature. Hautarzt 1998 Oct;49(10):770-3.

40. Terheyden P, Hornschuh B, Karl S, Becker JC, Broecker EB. Lichen planus associated with Becker's nevus. J Am Acad Dermatol 1998 May;38(5 Pt 1):770-2.

41. Trcka J, Kampgen E, Becker JC, Schwaaf A, Broecker EB. Immunochemotherapy of malignant melanoma. Epifocal administration of dinitrochlorobenzene (DNCB) combined with systemic chemotherapy with dacarbazine (DTIC). Hautarzt 1998 Jan;49(1):17-22.

42. Wagner SN, Schultewolter T, Wagner C, Briedigkeit L, Becker JC, Kwasnicka HM, Goos M. Immune response against human primary malignant melanoma: a distinct cytokine mRNA profile associated with spontaneous regression. Lab Invest 1998 May;78(5):541-50.

43. Becker JC, Guldberg P, Zeuthen J, Broecker EB, thor Straten P. Accumulation of identical T cells in melanoma and vitiligo-like leukoderma. J Invest Dermatol 1999 Dec;113(6):1033-8.

44. Conrad CT, Ernst NR, Dummer W, Broecker EB, Becker JC. Differential expression of transforming growth factor beta 1 and interleukin 10 in progressing and regressing areas of primary melanoma. J Exp Clin Cancer Res 1999 Jun;18(2):225-32.

45. Fischer WH, thor Straten P, Terheyden P, Becker JC. Function and dysfunction of CD4(+) T cells in the immune response to melanoma. Cancer Immunol Immunother 1999 Oct;48(7):363-70.

46. Terheyden P, Siedel C, Merkel A, Kampgen E, Broecker EB, Becker JC. Predominant expression of Fas (CD95) ligand in metastatic melanoma revealed by longitudinal analysis. J Invest Dermatol 1999 Jun;112(6):899-902.

47. thor Straten P, Becker JC, Guldberg P, Zeuthen J. In situ T cells in melanoma. Cancer Immunol Immunother 1999 Oct;48(7):386-95.

48. thor Straten P, Guldberg P, Gronbaek K, Hansen MR, Kirkin AF, Seremet T, Zeuthen J, Becker JC. In situ T cell responses against melanoma comprise high numbers of locally expanded T cell clonotypes. J Immunol 1999 Jul;163(1):443-7.

49. Becker JC, thor Straten P. T-cell clonality in immune responses. Immunol Today 2000 Feb;21(2):107.

50. Hofmann UB, Westphal JR, Waas ET, Becker JC, Ruiter DJ, Van Muijen GN. Coexpression of Integrin alphavbeta3 and Matrix Metalloproteinase-2 (MMP-2) Coincides with MMP-2 Activation: Correlation with Melanoma Progression. J Invest Dermatol 2000 Oct;115(4):625-32.

51. Hofmann UB, Westphal JR, Zendman AJ, Becker JC, Ruiter DJ, Van Muijen GN. Expression and activation of matrix metalloproteinase-2 (MMP-2) and its co-localization with membrane-type 1 matrix metalloproteinase (MT1-MMP) correlate with melanoma progression [In Process Citation]. J Pathol 2000 Jul;191(3):245-56.

52. Moerch U, Schrama D, Guldberg P, Seremet T, Zeuthen J, Becker JC, thor Straten P. Comparative delineation of T cell clonotypes in coexisting syngeneic B16 melanoma. Cancer ImmunolImmunother 49, 426-432. 2000.

53. Terheyden P, thor Straten P, Broecker EB, Kampgen E, Becker JC. CD40-ligated dendritic cells effectively expand melanoma-specific CD8+ CTLs and CD4+ IFN-gamma-producing T cells from tumor-infiltrating lymphocytes. J Immunol 2000 Jun;164(12):6633-9.

54. Termeer CC, Schirrmacher V, Broecker EB, Becker JC. Newcastle disease virus infection induces B7-1/B7-2-independent T-cell costimulatory activity in human melanoma cells. Cancer Gene Ther 2000 Feb;7(2):316-23.

55. thor Straten P, Guldberg P, Moerch U, Becker JC. Anti-melanocyte T cell responses - methodology versus biology. J Invest Dermatol 2000 Apr;114(4):738-9.

56. thor Straten P, Kirkin AF, Siim E, Dahlstrom K, Drzewiecki KT, Seremet T, Zeuthen J, Becker JC, Guldberg P. Tumor infiltrating lymphocytes in melanoma comprise high numbers of T- cell clonotypes that are lost during in vitro culture. Clin Immunol 2000 Aug;96(2):94-9.

57. Vetter CS, thor Straten P, Terheyden P, Zeuthen J, Broecker EB, Becker JC. Expression of CD94/NKG2 subtypes on tumor-infiltrating lymphocytes in primary and metastatic melanoma. J Invest Dermatol 2000 May;114(5):941-7.

Preface and Acknowledgements

The work summarized in the present Thesis was conducted in the years 1996 to 2000 at the Department of Tumor Cell Biology, The Danish Cancer Society, Strandboulevarden 49, 2100 Copenhagen, Denmark; the Department of Dermatology, Julius Maximilians University, Josef-Schneider-Str. 2, 97080 Wuerzburg, Germany; and The Scripps Research Institute, Department of Immunology, 10550 North Torrey Pines Road, La Jolla, California 92037, USA. The work was supervised by Professor Jesper Zeuthen, Head of Department, Department of Tumor Cell Biology, The Danish Cancer Society and Professor P. Moss, C.R.C. Institute for Cancer Studies, University of Birmingham B13 2TA, United Kingdom.

The present Thesis is structured into three parts: (i) a general introduction, (ii) an overview on targeted cytokine therapy, and (iii) the compilation of three experimental studies. Although there is some methodological overlap, each study can be read more or less independently.

Five persons have been deeply involved in the present work; Per thor Straten, Ralph A. Reisfeld, Jesper Zeuthen, Jes Forchhammer, and Eva-Bettina Broecker.

I first met Per thor Straten in 1992 at an EORTC melanoma group meeting in Lyon; he just had started to participate in a project on tumor infiltrating lymphocytes conducted by Jesper Zeuthen's group at the Danish Cancer Society. Most of the time we spent together at that meeting he was nagging about two things that he hates to travel and that formalin-fixed tissue samples were hard to work with; thus, I decided that it would be a lot easier to meet him in Copenhagen on a regular bases than to try to get Per to leave Copenhagen, and that I should provide him with some snap-frozen tissue samples. These decisions proved to be the right: the data of our first collaboration was published in THE JOURNAL OF CLINICAL INVESTIGATION and I am currently writing these acknowledgements sitting in an office at the Danish Cancer Society. Although I have not managed yet to learn Danish, Per and I are connected by an understanding not bound by language barriers. This understanding is sometimes even further improved by a glass of HAVANNA CLUB.

I met Ralph A. Reisfeld when he picked me up at the airport in San Diego in 1994. He is actually the conceptual father of the immunocytokines. At that time, I started to work on the characterization of an interleukin 2 immunocytokine in his group at The

Scripps Research Institute and, as it is obvious from this Thesis, I am still continuing to work in this field, though not in La Jolla anymore. Initially, Ralph had some problems to adjust to my working attitude, i.e. that I went to the beach and practiced surfing when there wasn't anything to do in the lab; however, as soon as he realized that I stayed in the lab when there actually was something to do, we became very good friends. I sincerely hope that I will have the opportunity to spend some additional time working under his direct supervision.

I met Jesper Zeuthen, like Per, at an EORTC melanoma group meeting, which was held in San Miniato in 1993. I was presenting some data on immune escape mechanisms of melanoma and ended my presentation with a cartoon from THE FAR SIDE by Gary Larson. The reaction from the audience was deep silence and some irritated looks; only one person was laughing – Jesper. He was equally amused when I asked him if he would agree on supervising me as a Ph.D. student.

However, without the help from Jes Forchhammer I never would have been able to successfully (at least I hope for a good ending) pass through the process of conducting this Thesis. His explanations of the necessary regulations, his kind reminders on deadlines, as well as his ongoing support and encouragement were always there to keep me on track.

Eva-Bettina Broecker joined me at the Department of Dermatology at the Julius Maximilians University in 1992; actually she was appointed as the head of the department, whereas I was just finishing my internship. She was not only teaching me Dermatology and Cancer Therapy, but also encouraged and fostered my scientific career. Without her I would probably be working in private practice taking care of athlete's foot and pimples – and by now being bored to death. She created an environment that allows combining clinical work and basic sciences. Although I sometimes get tired of this combination, as it is rather labor intensive and time consuming, it offers the opportunity to carry ideas born during the practical care of patients into the lab and *vice versa*. Moreover, it is nice to successfully treat athlete's foot once in a while, especially if experiments in the lab don't work out.

I like to extend my thanks to David Schrama, Claudia Siedel, Per Guldberg, Mads Hald Andersen, Lars Østergard Pedersen, Tina Seremet, Jim Pancook, Dorothy Markowitz, Yessica van Leuven, Angela Merkel, Holger Lode, Alex McLealan, as

well as all the people in the labs in Copenhagen, Würzburg, and La Jolla not mentioned here.

Although Claudia S. Vetter was not directly involved in the practical work, she was the one who had to tolerate all my bad moods when things didn't work; thank you for being there.

Authorship Declaration

The work described in the present Thesis is my own with the following exceptions:

- Per thor Straten and Per Guldberg, both at the Danish Cancer Society, established the RT-PCR/DGGE based clonotype mapping.
- Ralph A. Reisfeld at The Scripps Research Institute, La Jolla, California provided the IL-2 and the lymphotoxin α immunocytokines
- David Schrama at the Department of Dermatology, University of Wuerzburg, Germany conducted the animal experiments for the lymphotoxin α immunocytokine study
- Claudia Siedel, Angela Merkel and Tina Seremet provided technical assistance for most of the described experiments.

Contents

Introduction

CELLULAR IMMUNE RESPONSES

The Immune system is a remarkably adaptive defense system that has evolved in vertebrates to protect them from invading pathogenic microorganisms and cancer[1]. An enormous variety of cells and molecules capable of specifically recognizing and eliminating a large variety of antigens act together in a dynamic network. Functionally, an immune response can be dived into a recognition and an effector phase. Once a pathogen has been recognized, the immune system enlists the participation of a variety of cells and molecules to mount an appropriate response to eliminate or neutralize the danger. Subsequent exposure to the same pathogen induces a memory response, characterized by a more rapid and heightened immune reaction.

Immunity includes both non-specific and specific components. The non-specific component, innate immunity, is a set of disease resistance mechanisms that are not specific to a particular pathogen[2]. In contrast, the specific component, adaptive immunity, displays a high degree of specificity as well as the remarkable property of memory[3]. Since the initiation of an adaptive immune response requires some time, innate immunity provides the first line of defense during the critical period just after the host's exposure to a pathogen. Innate and adaptive immunity do not operate in total independence of each other, but cooperate to produce effective immune responses. For example, the action of phagocytes can generate 'danger' signals that stimulate and direct adaptive immune responses; furthermore, they display the phagocytosed antigen in a manner that it can be recognized by antigen-specific T cells. *Vice versa* when encountering appropriately presented antigen, some T cells synthesize and secrete cytokines that activate macrophages, e.g., increase their ability to kill ingested microbes.

Adaptive immunity relies on antigen specificity which allows to distinguish subtle differences among antigens. This specificity is based on a tremendous diversity in its recognition molecules[4]. Immune responses involve two major groups of cells: lymphocytes and antigen-presenting cells (APC). Lymphocytes are produced in the bone marrow, circulate in the blood and lymphatic system, and reside in various

lymphoid organs[5]. Lymphocytes, e.g. B and T cells, produce and/or display antigen-binding surface receptors which allow them to mediate the defining immunologic attributes. B lymphocytes mature within the bone marrow; when they leave it, each B cell expresses a unique antigen-binding receptor which is a membrane bound antibody molecule. When a naïve B cell first encounters antigen that matches its antigen receptor this interaction causes the cell to divide rapidly; its progeny differentiate into memory and effector B cells, i.e., plasma cells. Although plasma cells only live for a few days, they secrete enormous amounts of antibody, which are the major effector molecules of humoral immunity.

Cellular immunity is largely based on T lymphocytes. T cells also arise from the bone marrow; unlike B cells, however, they migrate to the thymus for maturation. During this process the T cell comes to express its unique antigen-binding molecule, called the T-cell receptor (TCR), on the membrane[6]. In contrast to membrane-bound antibodies on B cells, which can recognize antigen alone, the majority of TCR can only recognize antigen that is bound to cell membrane proteins called major histocompatibility complex (MHC) molecules. When a T cell encounters antigen in the context of a MHC molecule, it undergoes clonal expansion and differentiates into memory and various effector T cells, e.g., helper (T_h) and cytotoxic T lymphocytes (CTL). While the T_h cells provides help to activate B cells, antigen-presenting cells and CTL, the CTL has a vital function in monitoring the cells of the body and eliminating any cell that displays antigen, such as virus infected cells, tumor cells, and cells of a foreign tissue graft.

Activation of both the humoral and cell-mediated branches of the immune response requires help from T_h cells, which is provided both by direct cell-cell contacts as well as by the production of cytokines. Thus, it is essential that activation of T_h cells is carefully regulated, as an inappropriate T_h-cell response could have fatal consequences. To ensure a tight regulation of T_h cells, naïve cell can only get activated when recognizing antigen that is presented by MHC class II molecules together with appropriate co-stimulatory molecules on the surface of APC[7]. These specialized cells, which include macrophages, B cells and dendritic cells internalize antigen by phagocytosis or endocytosis, process it and then display a part of the antigen, bound to a MHC class II molecule on their surface. Although APC encounter and incorporate antigen in many different compartments, the interaction with T_h cells

is largely confined to secondary lymphoid organs, i.e., lymph nodes, since the circulation and homing capacities of naïve T_h cells restrict their presence to the peripheral blood and such organs.

MAJOR HISTOCOMPATIBILITY COMPLEX

The MHC is a collection of genes arrayed within a long continuous stretch of DNA on chromosome 6 in humans and on chromosome 17 in mice[8]. The MHC is referred to as the HLA complex in humans and the H-2 complex in mice. The proteins encoded in the MHC encompass three different classes: (I) glycoproteins expressed by almost all nucleated cells presenting peptide antigens to CTL, (II) glycoproteins expressed primarily on APC presenting peptide antigens to T_h cells, and (III) secreted proteins possessing immune function, including the complement system components C2 and C4, as well as proinflammatory cytokines such as TNFα, lymphotoxin and heat shock proteins.

Both class I and II MHC genes are highly polymorphic; within a species each gene exists in many different alleles. The MHC loci are closely linked, e.g., the recombination frequency within the murine H-2 complex is less than 0.5%; thus, most individuals inherit the alleles encoded by the closely linked loci as of two sets, the haplotype, one set from each parent. In outbred populations, the offspring are generally heterozygous at many loci and will express both maternal and paternal MHC alleles. If mice, however, are inbred each H-2 locus will be homozygous because the maternal and paternal haplotypes are identical. Certain inbred mouse strains have been designated prototype strains, and the MHC haplotype expressed by these strains is designated by an arbitrary italic superscript. The mouse strain C57BL/6J used in the majority of experiments described in this Thesis has the same haplotype as the prototype strain B10, i.e., H-2^b.

Class I molecules contain a large (45kD) polymorphic α-chain noncovalently associated with the much smaller β_2-microglobulin (12kD). These molecules are encoded by genes in the A, B and C regions of the human leukocyte antigen (HLA) complex and the K and D/L regions of the murine H-2 complex. These are referred to as *classical class I molecules*. Additional genes within the HLA and H-2 complex, designated HLA-E, -F, -G, and -H in humans and Q_a and Tl_a in mice encode the so

called *non-classical class I genes*. Although these non-classical MHC molecules are not directly involved in antigen-presentation to CTL, they have a highly specialized role in controlling immune responses to self-antigens[9]. Class II MHC molecules are heterodimeric glycoproteins, consisting of an α- and a β-chain. There are three class II gene loci in humans (DR, DP, and DQ) and two in mice (IA and IE).

MHC molecules also function as antigen-recognition molecules: although they do not possess the fine specificity for antigen characteristic for T-cell receptors, each MHC molecules can bind only a defined spectrum of antigenic. Hence, a given MHC molecule can bind numerous different peptides, and some peptides can bind to several different MHC molecules. Class I and class II molecules exhibit some common peptide-binding features. Both class I and II peptide ligands are held in a largely extended conformation along the length of the peptide-binding cleft[10]. The cleft in class I molecules, however, is blocked at both ends, whereas the cleft is open in class II molecules. As a result of this difference, class I molecules bind peptides that typically contain 8-10 amino acid residues, while the open groove of class II molecules accommodates slightly longer peptides of 13-18 amino acids. Another difference is that class I binding requires that the peptides contain certain amino acid residues, anchor residues, near the N and C termini; there is no such requirement for class II peptide binding.

ANTIGEN PROCESSING AND PRESENTATION

The formation of peptide-MHC complexes requires that a protein antigen is degraded by a sequence of events called antigen processing. Intracellular and extracellular antigens present different challenges, i.e., the latter being eliminated by secreted antibodies, whereas intracellular antigens are more effectively eliminated by CTL. Thus, the immune system uses two different antigen presenting pathways enabling the initiation of immune responses against intracellular as well as extracellular antigens[11,12]: endogenous antigens are processed in the cytosolic pathway and presented on the membrane with class I MHC molecules; exogenous antigens are processed in the endocytic pathway and presented on the membrane with class II MHC molecules (Figure 1) However, it should be noted that intracellular antigens can also be directed into the endocytic pathway, a phenomenon known as cross

presentation. Cross presentation is of particular importance to ensure T_h assistance for CTL responses[13].

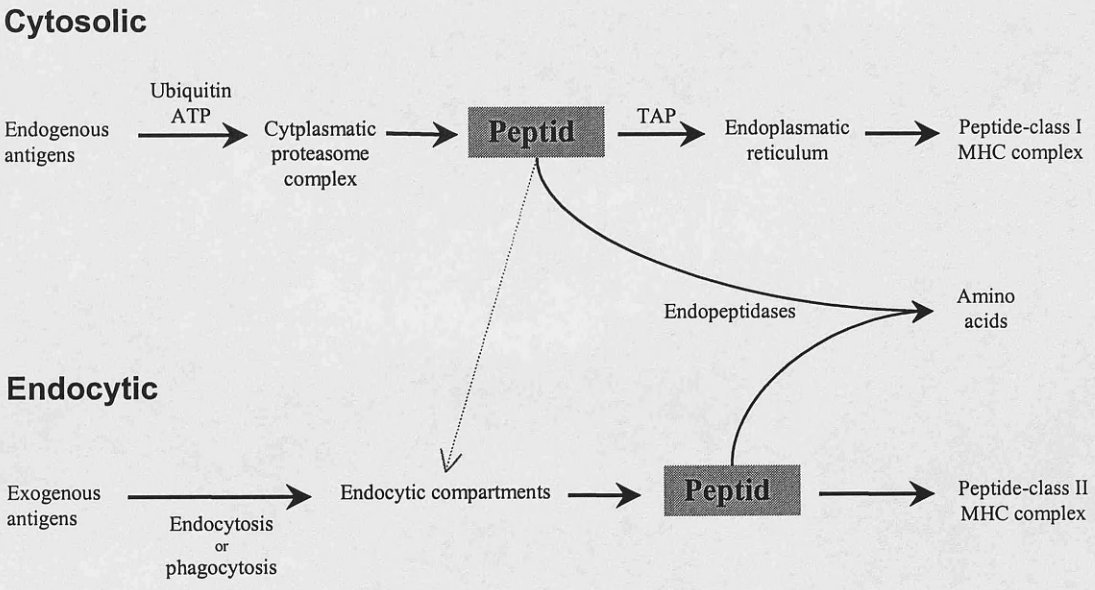

Figure 1. Cytosolic and endocytic pathways for antigen processing

In eukaryotic cells, protein levels are carefully regulated; denatured, misfolded, or otherwise abnormal proteins have a very short half-life[11]. Those proteins targeted for proteolysis often get covalently linked to ubiquitin via a lysine-amino group near the amino terminus of the protein. Ubiquitin-protein conjugates are degraded by a multifunctional protease complex, called the proteasome. The immune system utilizes this general pathway of protein degradation after modification of the proteasome by the addition of two subunits: LMP2 and LMP7. These subunits are encoded within the MHC gene cluster and are induced by IFN-γ. Subsequently, peptides are transported across the membrane of the rough endoplasmic reticulum by the ATP-binding transporter associated with antigen processing (TAP)[14]. The genes for TAP1 and TAP2 also map within the class II MHC region. Notably, both the LMP and the TAP genes are polymorphic and alleleic differences in LMP-mediated proteolytic cleavage or in the transport of different peptides may contribute to the observed variation among outbred individuals in their response to different endogenous antigens. The calnexin-associated class I MHC chain binds to β2-microglobulin, dissociates from calnexin, and binds to calreticulin and to tapasin, which is associated with TAP. This class I MHC complex then captures an antigenic peptide, which allows the dissociation of the MHC-peptide complex from the chaperones[14]. Finally, the class I

MHC molecule-peptide complex is transported through the Golgi complex to the plasma membrane.

APC internalize antigen by phagocytosis, pinocytosis, or endocytosis and subsequently degrade it to peptides within compartments of the endocytic processing pathway which involve three increasingly acidic compartments: endosomes (pH 6.0-6.5), endolysosomes (pH 5.0-6.0), and lysosomes (pH 4.5-5.0)[12]. Class II MHC molecules are only capable of binding peptides generated in the endocytic processing pathway as newly synthesized α and β chains associate with the invariant Ii chain within the rough endoplasmic reticulum. This complex is routed to compartments of the endocytic processing pathway where the Ii chain is degraded to the class II-associated invariant chain peptide (CLIP) occupying the antigen binding cleft. Within the lysosomes HLA-DM catalyzes the replacement of CLIP by antigenic peptides[15].

THE T-CELL RECEPTOR

The membrane bound TCR heterodimers consisting of an α and β chain or a γ and δ chain display a remarkable similarity in their domain structure to that of immunoglobulins; thus, they are classified as members of the immunoglobulin superfamily[16]. Each chain has two domains containing an intra-chain disulfide bond that spans 60 to 75 amino acids (Figure 2). The amino-terminal domain in both chains exhibits marked sequence variation, but the remainder of each chain are conserved. The variable domains have three hypervariable regions, which appear to be equivalent to the complementary determining regions (CDR) in immunoglobulin light and heavy chains. Adjacent to the constant domain, each TCR chain contains a short connecting sequence, in which a cysteine residue forms a disulfide link with the other chain. The transmembrane domains of each chain contain positively charged amino acid residues, which enables the TCR heterodimer to interact with chains of the signal-transducing CD3 complex[17].

CD3 is a complex of five invariant polypeptide chains that associate to form three dimers: a γε-and a δε-heterodimer, as well as a ξξ-homodimer; the latter can be replaced by a ξη-heterodimer (Figure 2). The ξ and η chains, which are encoded by the same gene, differ in their carboxyl-terminal ends because of differences in RNA splicing. The cytoplasmic chains contain a motif called the immunoreceptor tyrosine-

based activation motif (ITAM). These sites interact with tyrosine kinases and thereby play an important role in signal transduction[18].

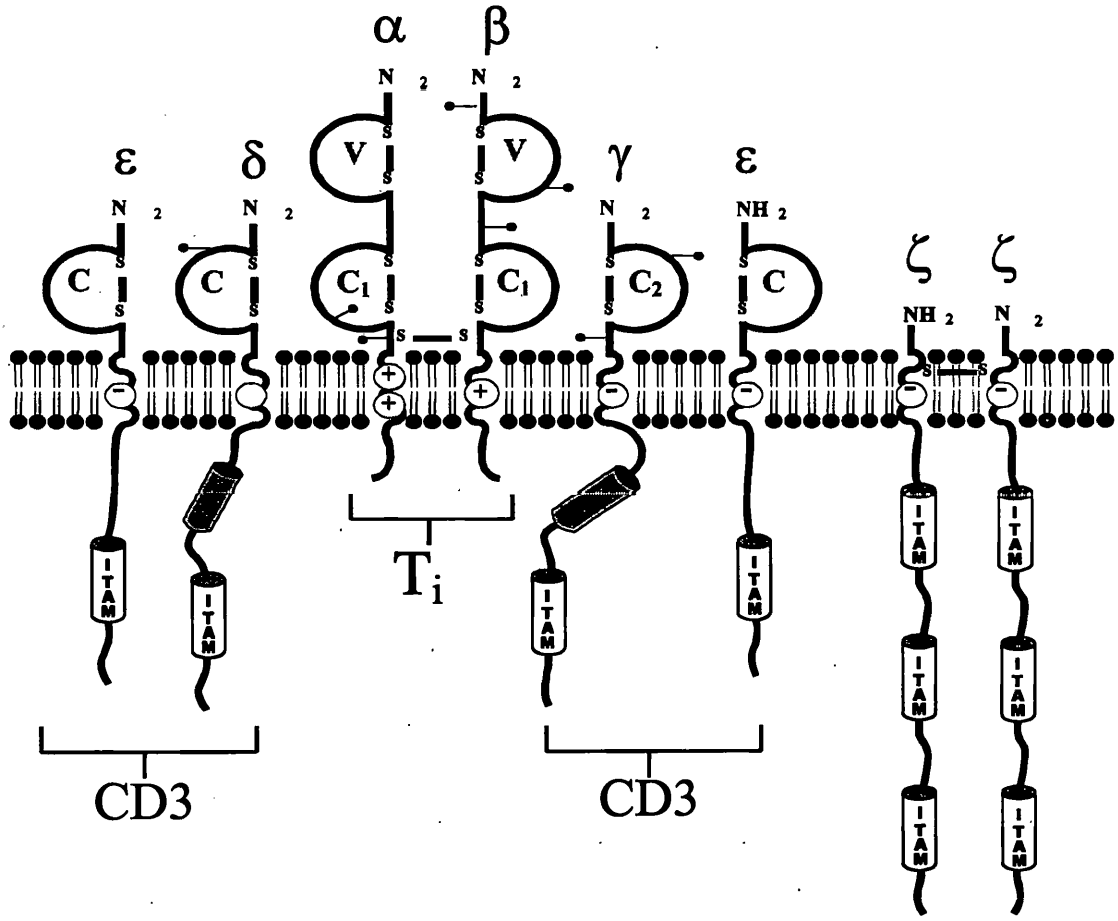

Figure 2. Schematic diagram of the TCR-CD3 (with the kind permission of J. Dietrich)

The genes encoding the αβ and γδ TCR are expressed only in cells of the T-cell lineage (Figure 3). Their germ-line organization is very similar to that of the immunoglobulin genes, separate V, D, and J segments rearrange during T-cell maturation to form functional genes, which encode the TCR (Figure 4)[4,19]. In the mouse, the α-, β-, and γ-chain gene segments are located on chromosomes 14, 6, and 13, respectively[20]. The δ-chain gene segments map on chromosome 14 between the V_α and J_α segments. Mouse germ-line DNA contains approximately 100 Vα and 50 Jα gene segments and only a single Cα segment; for the δ chain there are ~10 V, two D, two J, and one C gene segments; The β-chain gene family has about 20 V gene segments and two almost identical repeats of D, J, and C segments, each repeat consisting of one D_β, six J_β and one C_β; The γ-chain gene family contains seven V_γ segments and tree different J_γ /C_γ repeats.

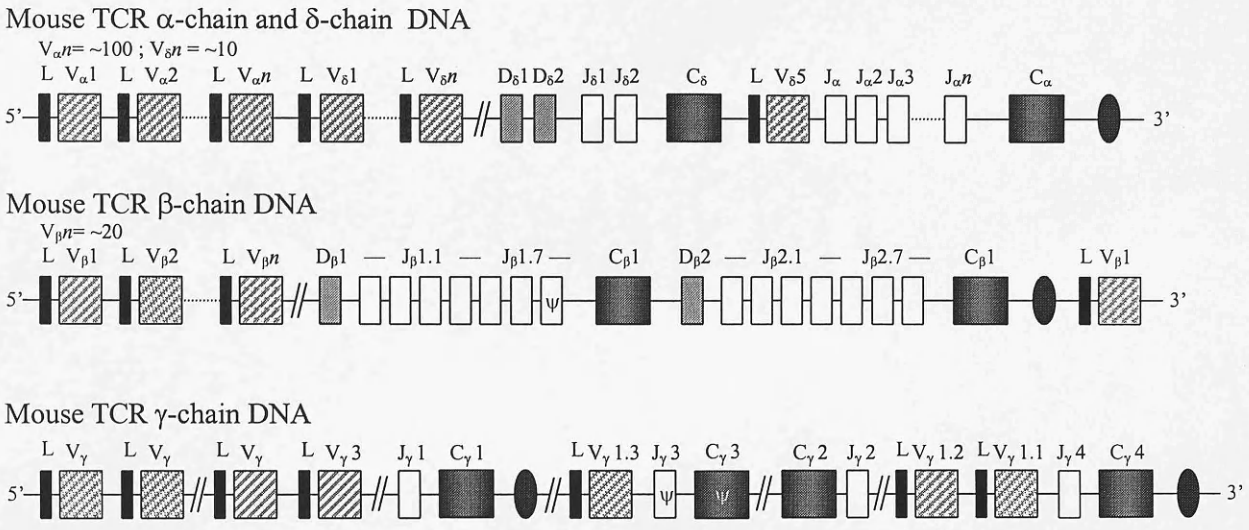

Figure 3. Germ-line organization of murine TCR α-, β-, γ-, and δ-chain gene segments.

The mechanisms of TCR DNA rearrangement are similar to that of Ig-gene rearrangements[4]. Conserved heptamer and nonamer recognition signals sequences (RSS) containing either 12-bp or 23-bp spacer sequences flank each S, D, and J gene segment with the 12-bp RSS being joined to a 23-bp RSS. The V-(D)-J recombination, which takes place at the junctions between RSS and coding sequences, is catalyzed by two recombination-activating enzymes, designated RAG 1 and RAG-2 [21]. These enzymes recognize the heptamer and nonamer recognition signals and enable the deletional or inversional V-J and V-D-J joining. RAG 1/2 introduces a nick on one DNA strand between the coding and signal sequences followed by a transesterification resulting in a hairpin at the coding sequence and a flush 5' phosphorylated double-strand break at the signal sequence.

Rearrangements of the TCR β-chain genes exhibit allelic exclusion[22]. The organization of the β-chain segments in two clusters implies that if a non-productive arrangement occurs, a second rearrangement is attempted at the other allele. Once, however, a productive rearrangement for one β-chain allele takes place, the rearrangement of the other allele is inhibited. Allelic exclusion appears less stringent for the TCR α-chains; hence, there are rare occasions in which more than one α chain is expressed on the membrane of a given T cell.

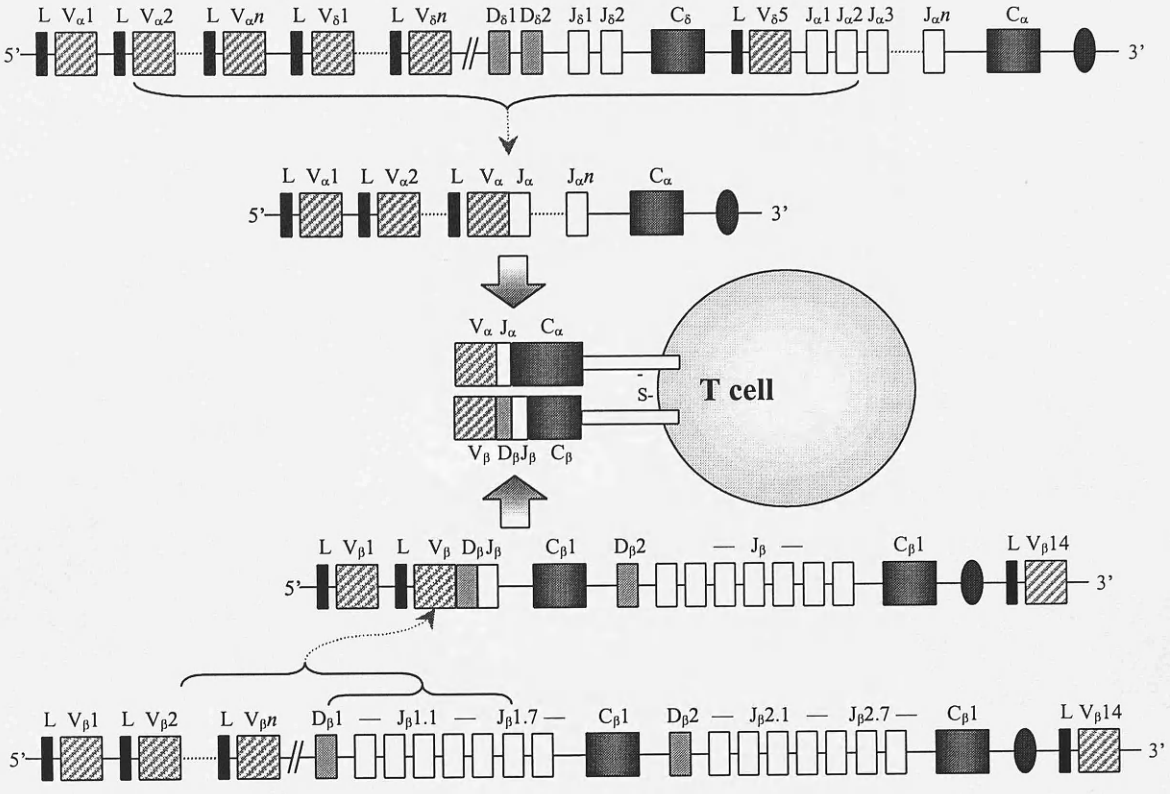

Figure 4. Example of gene rearrangements that yield a functional gene encoding the αβ T-cell receptor

Several mechanisms operate during TCR gene rearrangement to generate a high degree of diversity[4]. Combinatorial joining generates a large number of random combinations for all the TCR chains, e.g., more than 50 V_β, two D_β and 12 J_β gene segments can give 1.2×10^3 possible combinations (Figure 5a). Moreover, the joining of gene segments exhibits junctional flexibility (Figure 5b); although this generates many nonproductive rearrangements, resulting from creation of in-frame stop codons or substitutions of amino acids that render the product nonfunctional, it also increases diversity by encoding several alternative amino acids at each junction. Furthermore, nucleotides may be added at the junction between gene segments during rearrangement (Figure 5c). Variation in endonuclease cleavage leads to the addition of further nucleotides that are palindromic. Such P-region nucleotide addition can occur in the genes encoding for all TCR chains. Addition of N-region nucleotides, catalyzed by a terminal deoxynucleotidyl transferase, generates further junctional diversity; as many as six nucleotides can be added by this mechanism[23].

These mechanisms enable that despite the fact that each junctional region in a TCR encodes only 10-20 amino acids, an enormous diversity can be generated, i.e. more than 10^{13} possible amino acid sequences. Thus, it is not surprising that the diversity is

most pronounced in the CDR 3 where diversity is generated by junctional flexibility during joining of V, D, and J segments which allows introduction of P and N nucleotides at any of these junctions (Figure 5d).

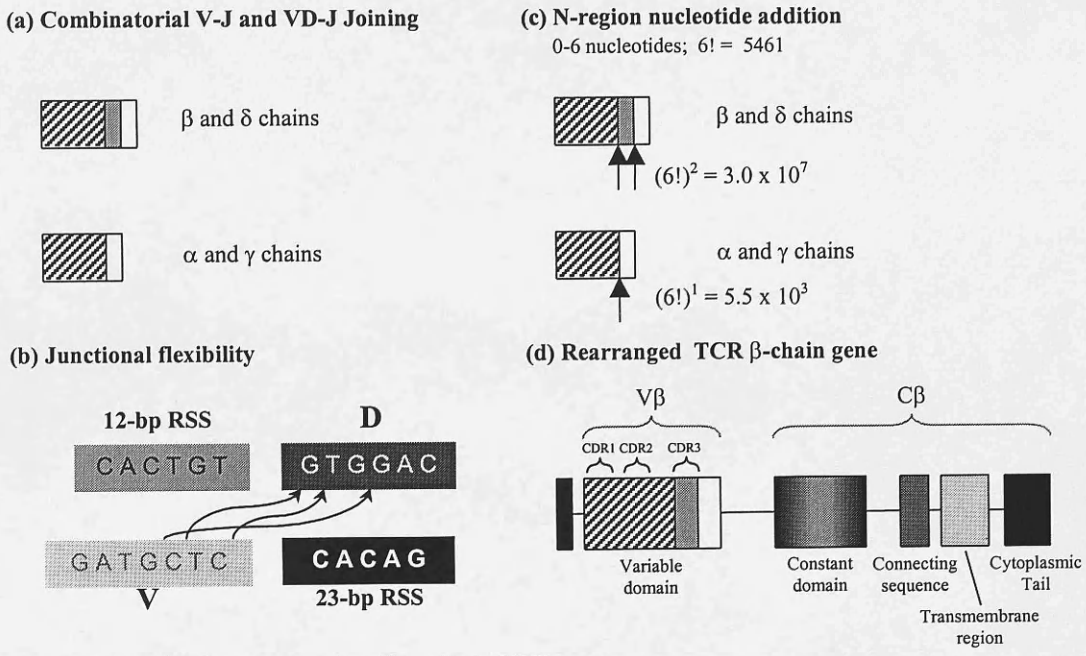

Figure 5. Mechanisms generating diversity in TCR genes.

TCR-MEDIATED T CELL ACTIVATION

As outlined above, amino acid sequence comparisons suggest that TCR heterodimers are immunoglobulin-like in structure, including regions with homology to the Ig CDR 1, 2, and 3. Early studies proposed that CDR 1 and 2 are the parts of the TCR responsible for interaction with the MHC molecule whereas CDR 3 should contact the peptide. Recently, the crystal structure of the TCR showed that this is not completely correct[16]. The orientation of the TCR to the MHC/peptide complex suggests an interaction of all CDR with the peptide.

The affinity of TCR/MHC-peptide interactions have a dissociation constant in the range of 10^{-4} to 10^{-6} M, orders of magnitude weaker than comparable antibody-antigen interactions. This finding is consistent with the scanning nature of T cell recognition and suggests that antigen-independent adhesion precedes TCR engagement[24]. Notably, although TCR/MHC-peptide interactions are characterized by a short half life, cellular interactions between T lymphocytes and target cells may last

for hours during which the T cell polarizes multiple TCR at the interaction site[25,26]. The observation that very few MHC/peptide complexes are sufficient to induce T-cell activation provided the rationale for a model of serial TCR triggering. According to this model, the TCR encounters the MHC/peptide for a short time, reaches an activation threshold upon which the TCR is removed, and another TCR becomes activated by interaction with the MHC/peptide complex[27]. Hence, the ability of an MHC/peptide complex to induce T-cell activation depends on the kinetics of the MHC/TCR interaction in combination with the number of TCR available on the T-cell surface as well as the number of ligands on the target cell.

Ligation of the TCR with the MHC/peptide complex leads to clustering of the TCR/CD3 complex with CD45 and CD4 or CD8. Signal transduction is initiated by an activation of protein tyrosine kinases of the src and syk families. $p56^{lck}$ tyrosine kinase is associated with CD4/CD8 that become aggregated with the TCR/CD3 upon activation, and $p59^{fyn}$ becomes associated with the CD45 molecule that likewise co-localizes with the TCR/CD3 complex[18]. This close encounter enables the $p56^{lck}$/ $p59^{fyn}$ mediated phosphorylation of tyrosine residues of ITAM present in the CD3 subunits, which allows activation of the ξ-associated protein 70 (ZAP-70). The activation of $p56^{lck}$, $p59^{fyn}$ and Zap70 leads to the phosphorylation of several proteins initiating different signaling pathways[28]. The nuclear targets for these signaling pathways are transcription factors such as AP-1 and NFAT.

A naïve T cell requires a co-stimulatory signal in order to reach a state of proliferation and clonal expansion. For example, a co-stimulatory signal may be provided by ligation of CD28 expressed by the T cell and B7-1 (CD80) or B7-2 (CD86) expressed on the APC[29]. Activation and signaling of the CD28 molecule induce an increase in the expression and stability of the IL2 mRNA. It also reduces the number of TCR/MHC-peptide interactions necessary for T-cell activation. Early events in CD28-mediated signal transduction include the activation of AP-1 and NFAT; thus, an integration of TCR and CD28 activation signals occurs on the level of transcriptional control[30]. In addition, other membrane-bound or soluble molecules participate in the activation of T cells either by direct signaling or by increasing the affinity of cell to cell interaction. All of these molecules are assembled to form the immunological synapse[31].

CLONOTYPE MAPPING

The rearrangement of the TCR gene segments creates a DNA sequence unique to that cell and its progeny. The large number of possible configurations of the rearranged genes makes this new sequence a marker that is specific for each T cell clone. These unique DNA sequences can be used to detect and characterize specific T cell responses. Reverse transcription (RT) coupled polymerase chain reaction (PCR) has been the method of choice in most laboratories analyzing the expression of TCR BV regions[32]. TCR transcripts are amplified with a set of primers covering the variable region families, together with a common constant region primer. This approach allows to proceed directly through steps of cloning or sequencing. However, the validity of semi-quantitative RT-PCR is highly dependent on parameters such as primer stability in duplex formation, specificity and discrimination of non-targets. Furthermore, it is imperative that all reactions work well and are being carried out within the linear range of amplification. Thus, the major obstacle in semi-quantitative RT-PCR analyses of multi-gene families is to select primers that work equally well and do not cross-react within the different families. The first primer panels for TCR α/β chains were published almost a decade ago[33]; since then the genomic DNA sequences of TCRAB regions have been completely elucidated, and the classification of different BV/AV sequences into the relevant families has been updated[20]. Obviously, primer panels for amplification of these multi-gene families had to be updated to ensure that all members of the different families are amplified. Most of the previously published primer panels either did not optimally match each sub-member of the different families, or show potential cross-reactivity to other families. All available TCR BV sequences were used to construct library files according to each BV family and aligned them to detect sequence stretches of optimal consensus in which primer sequences could be selected[32]. All primer sequences were tested for match to non-relevant BV families, aiming at a minimum of 5 mismatches. Moreover, primers were tested for their ability to amplify the BV region in question with high efficiency.

In general, methods for detection of T-cell clonality are based on RT-PCR followed by single strand conformation polymorphism, PCR heteroduplex analysis or CDR3 size determination[34]. All these methods require steps of either blotting and

hybridisation or re-amplification using end-labelled probes followed by computerised data analysis. However, the method used in the present Thesis is based on denaturing gradient gel electrophoresis (DGGE). It detects the presence of T-cell clonotypes, covering the BV regions 1-24 for the human or 1-18 in the murine system, and facilitates the possibility to produce full and detailed clonotype maps.

DGGE reveals small deletions, small insertions and point mutations with a detection efficiency close to 100%[35]. The method relies on the fact that the melting properties of DNA molecules are highly dependent on their nucleotide composition. During electrophoresis in a denaturing gradient gel, the DNA molecule will partially melt at a sequence-dependent concentration of denaturants, and the resulting partial separation of the DNA duplex will retard the electrophoretic mobility of the molecule in the gel. Even single base pair changes in a DNA sequence can be revealed in DGGE by a shift of the position at which the molecule stalls. In a polyclonal T-cell population, all TCR DNA sequences will, in theory, differ from each other in their melting properties and will therefore be revealed as a smear in the denaturing gradient gel. In contrast, any population of clonally expanded T cells will be revealed as a distinct band that can be recovered for further analysis. Using the computer algorithm MELT87 melting maps for each amplified TCR BV region were calculated to establish the ability to be resolved in DGGE using standardised conditions. For most of the BV-regions a suitable melting profile could be obtained by the attachment of a 50 bp "GC-clamp" to the 5′-end of the constant region primer.

Most analyses of T-cell clonality focus on the examination of tissues for the presence of clonotypic T cells. An important aspect is therefore related to the sensitivity of the method. Clonotypic transcripts constituting as low as 2.5% of the BV region in question can easily be visualised in the gel by ethidium bromide staining. Assuming that all regions are expressed at equal levels, this means that a T-cell clone can be detected in a mixed population at a fraction of 0.1 %.

MELANOMA

Melanocytes originate from the neural crest and migrate during embryogenesis to the skin where they reside within the basal epidermal layer separated from each other by several keratinocytes. The prime function of melanocytes is the production of

melanin, offering UV protection. Malignant transformation of melanocytes gives rise to melanoma; this tumor has a fatal prognosis if not cured by surgical excision prior to metastatic dissemination[36]. The presence of even micro-metastases in the sentinel lymph node deteriorates prognosis[37,38].

There is a consensus that melanoma cells are antigenic since they express tumor-associated antigens, which are recognized by syngeneic T cells[39]. Indeed, the presence of tumor reactive CTL in the sentinel lymph node has been demonstrated[40]. Furthermore, cellular components that should be able to reject the tumor, i.e., T lymphocytes and macrophages, are infiltrating both primary and metastatic tumors. Nevertheless, the prognosis of melanoma, if not cured by surgical resection, is one of the most unfavorable in medicine. The coexistence of tumor specific immunity with a progressing tumor remains a major paradox of tumor immunology[41]. This enigma is most evident in partially regressing melanoma, where efficient eradication of tumor cells occurs in close vicinity to uncontrolled tumor growth[42].

Multiple melanoma associated antigens (MAA) recognized by T cells have been characterized and HLA class I and class II restricted peptides have been identified[43]. These antigens can be divided into three different groups: cancer-testis antigens, melanocyte differentiation antigens, and mutated or aberrantly expressed antigens. Several of these proteins give rise to more than one antigenic peptide; hence, the number of antigenic peptides has exceeded fifty and is still increasing. Some of these peptides only induce cytotoxicity against peptide loaded target cells, but not melanoma cells expressing both the relevant protein and the required MHC molecules; hence, it is not known whether these peptides are actually processed and presented naturally or if additional signals are necessary to stimulate the effector cells[44].

Several studies have focused on the characterization of the T-cell response against malignant melanoma *in situ*, and evidence has been provided for the presence of clonally expanded T cells in both primary and metastatic lesions[45]. However, this T-cell response is obviously inadequate to control tumor growth. This notion raises the question of how melanoma cells escape immune surveillance. Possible mechanisms include the reduction or even complete loss of MHC class I expression or the impaired signaling capacity through the TCR/CD3 complex among tumor infiltrating lymphocytes (TIL) due to downregulation of the CD3 ζ-chain[41]. In

addition, melanoma cells are known to secrete a number of different cytokines, some of which may suppress cellular immune responses[46].

Over the past years immunologists and oncologists aimed at boosting ongoing or at inducing new T-cell responses to melanoma[43,47,48]. Several trials were based on the systemic administration of immunomodulatory cytokines such as Interleukin-2 (IL2). Although some beneficial effects were observed, the general results were not encouraging, as the response rates were limited and the side effects severe. One of the major obstacles was that the systemic administration neglected the paracrine nature of cytokines. This limitation can be overcome by means of fusion proteins consisting of a tumor-specific antibody and a cytokine. In a murine tumor model targeted IL2 therapy has been shown that the eradication of established metastases is due to specific CTL responses[49].

Scientific Results

AIMS OF THE STUDY

The primary aim of the present study was to scrutinize the T-cell responses to melanoma and its modulation by *in situ* cytokine therapy. For this purpose a syngeneic murine melanoma model, i.e., a subline of B16-melanoma in C57BL/6J mice with clinically relevant sites of metastases such as skin, lung, and liver was established. The analysis of the T-cell response was based on TCR clonotype maps of TIL, secondary lymphoid organs such as draining lymph nodes or spleen, and peripheral blood.

The present Thesis is introduced by a review on *in situ* cytokine therapy by tumor-specific antibody cytokine fusion proteins, designated immunocytokines (Paper 1). Immunocytokines achieve high cytokine concentrations in the tumor microenvironment and thereby effectively stimulate cellular immune responses. Proof of concept is presented indicating that immunocytokine-induced activation and expansion of immune effector cells in the tumor microenvironment can effectively eradicate established tumor metastases..

Since it was unclear whether this therapeutic effect was due to a boost of a preexisting or to an induction of a new T cell response clonotype mapping of TIL in treated and untreated animals was performed (Paper 2). The obtained results demonstrated an over-expression of several TCR BV families in tumors after IL2 immunocytokine treatment. DGGE analysis of selected TCR BV regions, however, revealed the presence of clonotypic T-cells in tumors from both treated and untreated animals. Thus, targeted-IL2 therapy does not induce clonal T-cell responses *de novo*, rather it acts as an activator for an already existing population of clonotypic T-cells.

Immunity to tumors relies on re-circulating antigen-specific T cells. The observation that the therapeutic effect of IL2 immunocytokines is not restricted to tumors expressing the targeted antigen, but extends to antigen negative variants of the tumor if present in the same animal suggested the re-circulation of activated T cells (Paper 3). Analysis of the T-cell infiltrate by quantitative RT-PCR demonstrated the presence of highly expressed TCR BV-regions in both tumor variants; clonotype

mapping further revealed that the high expression of these regions were caused by clonal expansions and, notably, that these specific clonotypic TCR transcripts were identical in both tumors. Thus, therapeutic T-cell clones activated locally by targeted-IL2 therapy re-circulate and mediate eradication of distant tumor sites not subjected to *in situ* cytokine therapy.

Although the IL2 immunocytokine was able to boost a pre-existing T-cell response, the induction of additional tumor-specific T cells was not achieved. Since it has been reported that tumor-antigen-specific T cells can be rendered anergic by the tumor, priming of additional T cells may be particularly critical. Therefore, the efficacy of targeting cytokines to the tumor site that are likely to promote the induction of new tumor-specific T cells was tested. Lymphotoxin-α (LTα) was chosen because it is a potent mediator of proinflammatory and tumoricidal activities as well as of lymphoid genesis. The final study describes that the use of an antibody-LTα fusion protein offers an effective treatment resulting in the eradication of established metastases (Paper 4). This is achieved by an improved T-cell response, which is most likely evoked by the induction of peripheral lymphoid tissue at the tumor site. In fact, the functional significance of this tertiary lymphoid tissue at tumor sites was confirmed by immunohistologic and electron microscopic analyses of endothelial/lymphocyte interactions as well as TCR clonotype mapping providing evidence for the induction of new T-cell clones among TIL.

TARGETED-IL2 THERAPY FOR MELANOMA BY IMMUNO-CYTOKINES

Summary

A major goal of tumor immunotherapy is the induction of tumor-specific T cell responses that are effective in eradicating disseminated tumors, as well as mounting a persistent tumor-protective immunity. Recombinant antibody-cytokine fusion proteins are immunocytokines that achieve high cytokine concentrations in the tumor microenvironment and thereby effectively stimulate cellular immune responses against malignancies. The activation and expansion of immune effector cells, such as CD8+ T lymphocytes by IL2 immunocytokines resulted in the eradication of established pulmonary and hepatic metastases of murine melanoma in syngeneic mouse models. The effective eradication of metastases by immunocytokines resulted in significant prolongation in life span of mice over that of controls receiving equivalent mixtures of antibody and IL2. Proof of concept was established indicating that immunocytokine-induced activation and expansion of immune effector cells in the tumor microenvironment can effectively eradicate established tumor metastases. These results suggest that antibody-targeted delivery of cytokines provides means to elicit effective immune responses against established tumors in the immunotherapy of neoplastic disease.

Introduction

After the discovery of antibodies by Emil von Behring in 1890, their use as "magic bullets" to specifically direct substances to pathogenic targets was initially proposed by Paul Ehrlich, who employed the term immunotherapy as early as 1900[50]. Progress in this field began to accelerate in 1974 with the development of specific monoclonal antibodies directed against well-characterized antigens by Cesar Milstein and Georges F. Köhler, who immortalized antibody-producing cells by hybridization with long-lived myeloma cells resulting in hybridomas. Isolation and propagation of one hybridoma clone would thus yield large quantities of monoclonal antibodies specific for one single antigenetic determinant [51]. This key development was followed by the introduction of recombinant DNA technologies that facilitated the engineering of novel antibody molecules with the unique targeting abilities of monoclonal antibodies. It is remarkable that it took almost one century, from the time Ehrlich first envisioned "therapia magna sterilisans" with "magic" substances like antibodies that exclusively affected harmful pathogens, to the first approval of a monoclonal antibody by the Food and Drug Administration for adjuvant immunotherapy of human B-cell Lymphoma in late 1997[52].

Most immunotherapeutic approaches using monoclonal antibodies are based on the concept of targeting tumor-associated antigens that are expressed to a greater extent on the surface of tumor cells than on normal cells and tissues. Once the antibody recognized a malignant cell tumor growth and dissemination should be suppressed via the natural effector mechanisms of antibodies. These include the complement-dependent cellular cytotoxicity (CDC) following activation of the complement cascade in proximity to the tumor cells with the formation of the membrane attack complex consisting of the complement components C5-C9 and the generation of chemotactic fragments, e.g. C3a and C5a. The latter have the ability to attract phagocytic cells, such as monocytes, macrophages or natural killer (NK) cells which can use their Fc receptors to lyse tumor cells mediated by antibody-dependent cellular cytotoxicity (ADCC)[53]. An alternative approach aimed at the induction of tumor regression via the anti-idiotype network. Specifically, immune competent hosts are vaccinated with an anti-idiotypic antibody mimicking the antigenic determinant of the

original immunogen, which ideally is recognized by B-cells and followed by a humoral response leading to the endogenous production of tumor-specific anti-idiotypic antibodies[54].

First clinical data were obtained by using monoclonal antibodies in patients with B-cell lymphoma[52] and several solid tumors, including colon carcinoma[55] and neuroblastoma[56]. Despite the intellectual appeal described above, the general therapeutic efficacy of tumor reactive mAbs has been rather disappointing. An obvious conclusion to be drawn from these results was, that in spite of their exquisite specificity and apparent ability to target tumor cells, antibodies alone were either not sufficiently cytotoxic or could not adequately harness the patients' own effector mechanisms. Consequently, a broad research effort was initiated to improve the cytotoxicity of antibodies by conjugating them with radioisotopes, cytotoxic drugs or potent toxins[57-59]. Clinical trials applying these constructs revealed that although a sizeable rate of remissions could be induced in patients with Non-Hodgkin lymphomas and myeloid leukemia, the therapeutic efficacy in solid tumors still remained very low. One of the major obstacles thwarting antibody based cancer therapy is the heterogeneity of target antigen expression within the tumor. Furthermore, mAbs do not sufficiently penetrate large tumor masses due to their pharmacokinetic characteristics[60].

Since becoming available in recombinant form, IL2 has been used as an *in vivo* T cell growth factor either alone or in combination with *in vitro* activated lymphocytes in the treatment of patients with advanced renal cell carcinoma or melanoma[61,62]. The aim of this partially successful approach is to generate or propagate tumor-reactive lymphocytes. Forni *et al* demonstrated that injection of a physiological dose of IL2 directly into tumors caused suppression of their growth[63]. The major advantage of an *in situ* application is that it avoids certain forms of toxicity associated with the systemic use of cytokines. Cancer patients receiving systemic IL2, often experience potentially life-threatening side effects that limit the total amount that can be administered[64]. Recently, *in situ* cytokine therapy has been developed further by transferring cytokine genes into tumor cells[65]. The expected goal is that *in vivo* injection of tumor cells transduced with cytokine genes will produce effective local concentrations of the cytokine to generate an anti-tumor response via the immune

system of the host, but systemic concentrations too low to produce significant side effects.

We reasoned that by using the targeting ability of tumor specific monoclonal antibodies we could develop a technically more simple strategy to achieve effective concentrations of IL2 in the tumor microenvironment[66]. Recombinant fusion proteins consisting of tumor-specific antibodies and cytokines were developed for this purpose. The novelty of this approach lies in its attempt to induce a tumor specific cellular immune response by means of elements derived from the antibody immune response. We named these antibody-cytokine fusion proteins immunocytokines, since they can direct cytokines to the tumor microenvironment and induce tumor-specific immune responses. This overview summarizes some of our results obtained in a series of studies that evaluated the efficacy of immunocytokines in eradicating established metastases in a syngeneic animal model of melanoma.

Immunocytokines

The rationale for constructing recombinant antibody cytokine fusion proteins is to achieve optimal biological effectiveness by using the unique targeting ability of antibodies to direct multifunctional cytokines to the tumor microenvironment. The hypotheses that needed to be tested with this approach were: (i) that such fusion proteins effectively direct cytokines to tumor sites and thereby stimulate and expand immune effector cells sufficiently to achieve efficient tumor cell lysis; and (ii) that low dose levels of the fusion protein will be more effective than equivalent mixtures of antibody and cytokine in suppressing tumor growth or ideally in eradicating established metastasis. Should these hypotheses prove correct, one might anticipate that lower effective dose levels of the antibody-cytokine fusion protein are required that may be less toxic than the relatively high levels of cytokines used thus far in systemic clinical applications and that this will ultimately result in a more effective immunotherapy of cancer.

The first successful constructions of antibody-cytokine fusion proteins that retained full cytokine activity were those of chimeric anti-ganglioside GD2 antibody (ch14.18) with recombinant human tumor necrosis factor beta (TNF-β)[67] and IL2[68]. Several other groups used the concept of increasing antibody-mediated host anti-tumor responses by genetic linkage of cytokines to the heavy chains. Thus, Tao and Levy [69]

reported the effective use of a fusion protein consisting of an idiotype-antibody and granulocyte/macrophage colony stimulating factor (GM-CSF) as a vaccine for murine B-cell lymphoma. Specifically, such a fusion protein was demonstrated to induce an idiotype-specific antibody response, which was effective in protecting mice from challenges with B-cell lymphoma cells. A different strategy was followed by Sabzevari *et al*, who used an antibody-cytokine fusion protein to target recombinant human IL2 into the tumor microenvironment[70]. These initial data were obtained in a xenograft model of human neuroblastoma in mice with severe combined immunodeficiency disease (SCID), reconstituted with human lymphokine activated killer (LAK) cells. These data clearly demonstrated for the first time the superior effect of the fusion protein in contrast to equivalent amounts of IL2. A human melanoma xenograft model was employed to confirm this therapeutic effect and to establish its specificity[71]. A similar strategy was followed by Hornick *et al*, who generated fusion proteins comprised of a human/mouse chimeric antibody specific for B-cell lymphoma (chCLL-1) and rhIL2 or GM-CSF, respectively[72]. These fusion proteins were demonstrated to maintain both antigen binding and cytokine activity *in vitro* and *in vivo*. However, these initial studies yielded only limited information on immune mechanisms involved in the treatment effect of antibody-cytokine fusion proteins. Thus, extended efforts were made to establish the *in vivo* function of such constructs, including the effective eradication of micrometastases and the delineation of immune mechanisms involved in preclinically relevant syngeneic animal models.

The immunocytokines, which are currently used in preclinical evaluations, were constructed by following one common strategy. The coding sequences for the cytokines were generated by RT-PCR with primers that include designated restriction sites used for cloning purposes. Once generated, these cytokine genes are fused with the human Cγ1 gene at the carboxyl end of the heavy chain of an antibody. Gillies *et al* inserted the fused genes of either an anti-ganglioside GD2 (ch14.18) or an anti-EGF-receptor (ch225) antibody and recombinant human IL2 into the vector pdHL2, which encodes the dihydrofolate reductase gene[68]. The same vector carried the gene encoding for the light chain of the ch14.18/ch225 antibody in a separate expression unit. Both expression units were driven by a metallothionine promoter. The expression plasmid was transduced into the immunoglobulin-nonproducer murine

hybridoma cell line Sp2/0-Ag14 cells by protoplast fusion and selected in the presence of increasing concentrations of methotrexate (100 nM to 5 μM).

Tao and Levy[69] and Chen *et al.*[73] fused the carboxyl terminal of the heavy chain of a 38C13 mouse B-cell lymphoma idiotypic antibody with the genes encoding either GM-CSF, IL2 or IL4. By contrast to the work of Gillies, the plasmids encoding heavy and light chains were co-transfected separately into immunoglobulin non-secreting plasmocytoma Ag8.653 cells by electroporation and selected for G418 resistance. Hornick *et al* used a vector with two expression units that contained the genes encoding the light and heavy chain of a human mouse chimeric antibody, specifically recognizing a human major histocompatibility complex class II variant that is strongly expressed on human B-cell non-Hodgkin's lymphoma, chronic lymphocytic leukemia and multiple myeloma[72]. The heavy chain was fused with human GM-CSF and IL2 and the fusion proteins were expressed in non-secreting NS0 murine myeloma cells in the absence of glutamine, since glutamine synthetase was used as a selection marker. All the fusion proteins described were purified by making use of the Fc-portion of the antibody molecule, which selectively binds Protein-A Sepharose. Following elution at low pH, pure preparations of the antibody-cytokine fusion proteins were obtained and used for further characterization.

This brief review focuses entirely on antibody-IL2 fusion proteins and the *in vivo* results obtained in the authors' laboratories. Evaluation of biological activities of interleukin-2 fusion proteins indicated that fusion of IL2 to the carboxy terminal of the immunoglobulin heavy chain fully maintained IL2 activity when measured in proliferation assays with IL2 dependent mouse or human T-cell lines. In these assays, the IL2 activity of both constructs, ch14.18-IL2 and ch225-IL2, was compared to that of commercially available rhIL2. These fusion proteins proved remarkably stable throughout their purification and during subsequent storage for over four years at -20°C, or lyophilized. A comparison of the binding activity of the ch14.18-IL2 fusion protein with that of the ch14.18 antibody revealed essentially identical GD2 binding, as determined by both direct and competitive binding assays[68,70]. Dissociation constants, calculated from Scatchard analysis of saturation binding curves, were 18 nM and 24 nM for ch14.18 and its IL2 fusion protein, respectively.

In summary, these findings indicate that these immunocytokines were biologically functional and combine the targeting ability of antibodies with the

immunomodulatory properties of cytokines. These data encouraged us to critically evaluate the anti-tumor activity of these immunocytokines as tools to deliver effective amounts of IL2 to the tumor microenvironment capable of local activation of suitable effector cells.

In vivo Studies

Human melanoma is a neuroectodermal malignancy that is characterized by the expression of various gangliosides, including disialoganglioside GD2. A classical melanoma model used to study various immunotherapeutic approaches in an immunocompetent host is the B16 melanoma cell line in C57BL6/J mice. In contrast to the human situation, all mouse melanoma cell lines, including B16, lack the expression of the ganglioside GD2. In order to test the hypothesis, that targeted IL2 therapy with the anti-GD2 antibody-IL2 fusion protein ch14.18-IL2 is effective in a syngeneic melanoma model, B16 melanoma cells were transfected with human genes encoding for the two enzymes in the last stages of GD2 biosynthesis, i.e. a-1,4-N-acetylgalactosaminyltransferase and a-2,8-sialyltransferase[74,75]. This transduction resulted in a cell line that expressed GD2, as demonstrated by specific binding of anti-GD2 antibodies (14G2a, ch14.18) and the ch14.18-IL2 fusion protein. These tumor cells formed experimental pulmonary and hepatic metastasis following intravenous or intrasplenic injection, respectively[76]. The question whether such hepatic and pulmonary micrometastases are specifically targeted by the ch14.18-IL2 fusion protein was addressed in biodistribution experiments using ^{125}I labeled ch14.18-IL2. Specifically, ten days after induction of hepatic or pulmonary metastases, mice were injected with 5 μCi of ^{125}I labeled ch14.18-IL2 fusion protein and the amount of radioactivity assessed 12 hr after injection in lungs and livers, respectively. An effective localization of tumor-specific ch14.18-IL2 was observed only in metastasis-bearing organs, as compared to naïve organs, indicating effective targeting *in vivo*.

The effect of the antibody-IL2 immunocytokine on disseminated established pulmonary melanoma metastasis was tested by treating C57BL6/J mice one week after tumor cell inoculation with 8 μg ch14.18-IL2 fusion protein injected intravenously for seven days. This treatment completely eradicated pulmonary metastases in the vast majority of animals, as confirmed by histologic examination of serial sections of lung specimens. Animals with residual macroscopic disease

revealed a dramatic decrease in tumor load, as compared to mice receiving either no treatment or injections of an equivalent mixture of ch14.18 antibody and IL2. Similar results were obtained when animals bearing established hepatic metastases were treated intravenously with 8 μg ch14.18-IL2 fusion protein for seven days. This treatment also resulted in a complete regression of micrometastases in the majority of mice. Specificity of this treatment was demonstrated by using a non-specific ch225-IL2 fusion protein targeting the human EGF-receptor, which failed to exert any anti-tumor effect[76].

Survival studies following the induction of hepatic or pulmonary melanoma metastases indicated a dramatic increase in life span only in mice treated with the ch14.18-IL2 fusion protein. This was demonstrated by a doubling in life span of fusion protein treated mice as compared to control animals receiving either injections with PBS or an equivalent mixture of ch14.18 antibody and IL2, which revealed a median survival of only 41 or 44 days, respectively.

A third clinically relevant metastatic site in human melanoma, in addition to lung and liver, is the skin. Thus, we tested the effect of antibody-IL2 fusion protein on established subcutaneous tumors. Ten days after inoculation of tumor cells, mice were treated over a period of seven days by intravenous injection of 16 μg ch14.18-IL2 fusion protein. Objective responses were observed in all treated animals as compared to untreated controls. Three out of eight animals had a complete tumor rejection, and five out of eight showed a partial regression. Even if treatment was delayed as long as 35 days, resulting in large subcutaneous tumors (~1,000 mm^3), ch14.18-IL2 was able to induce a temporary partial response with subsequent delay of future growth[77].

One of the major obstacles of antibody-based immunotherapies is the heterogeneity of antigen expression within the malignancy. However, successful treatment with an antibody-IL2 fusion protein may be achieved with only a small percentage of tumor cells being targeted by the fusion protein. This leads to the hypothesis that by increasing IL2 concentrations in the tumor microenvironment with an immunocytokine, using a tumor-associated antigen as a docking site, cellular immune responses mediated by T and/or NK cells are induced, which are completely independent of the target antigen. In order to test the hypothesis that antibody-IL2 fusion protein treatment can overcome heterogeneity of the docking site antigen, pulmonary metastases were induced that were heterogeneic in GD2 expression by

admixing GD2-positive and -negative B16 melanoma cells at a ratio of 5:1. Treatment with ch14.18-IL2 dramatically reduced the number of metastatic foci on the lungs of five out of eight animals and induced a complete eradication of metastases in three out of eight animals (Figure 6). If only GD2-negative cells were used for inoculation, ch14.18-IL2 displayed no anti-tumor effect, proving the requirement of a docking site for directing the immunocytokine to the tumor microenvironment[77].

Figure 6. Effect of ch14.18-IL2 on heterogeneous metastases. Pulmonary metastases were induced by i.v. injection of either 5 x 10^6 B16 melanoma cells alone (lower left specimen) or the mixture of 5 x 10^6 B78-D14 and 1 x 10^6 B16 cells (upper and lower right specimen). Treatment with 8 µg ch14.18-IL2 fusion protein was initiated 1 wk after tumor cell inoculation (upper and lower left specimen). Control animals (lower right specimen) received PBS over the same period instead. A representative lung specimen for each group is shown. Figure taken from .

The immune response induced in tumor bearing animals receiving treatments with the ch14.18-IL2 immunocytokine was found to be T-cell-dependent. This was established by histological and functional characterization of the effector cells and *in vivo* analyses of mice with distinct immune defects or mice depleted of T-cell subpopulations.

First, histomorphological and immunohistochemical analyses of subcutaneous tumors from mice that received the ch14.18-IL2 immunocytokine demonstrated an inflammatory response in subcutaneous tumors, whereas such cellular infiltrates were not found in control mice treated with an equivalent antibody/IL2 mixture. Morphological and immunohistochemical evaluations of the cellular infiltrates indicated predominance of lymphocytes intermixed with occasional granulocytes and macrophages and strong staining for $CD8^+$ T-cells, but to a lesser extent for $CD4^+$ T-cells. Staining of tumor specimens with a specific marker for NK cells, revealed only an occasional presence of NK cells that were primarily located in the periphery of the tumor, in contrast to T-cells that infiltrated the tumor microenvironment[77].

This immunohistological characterization of inflammatory infiltrates in GD2-positive B78-D14 s.c. tumors provides strong evidence for a T-cell-mediated mechanism and argues against a relevant role for NK-cells in tumor eradication. However, more rigorous proof of this mechanism was established by using mouse strains that were defective in distinct compartments of their cellular immune system[76]. These included C57BL/6 *scid/scid*, which lack mature T- and B-cells due to a defect in gene rearrangement of the T-cell receptor and immunoglobulins and C57BL/6 *beige/beige* mice that carry the autosomal recessive *beige* gene inducing a selective impairment of functional NK-cells. Established pulmonary melanoma metastases were induced in both of these strains of mice and subsequently treated with the immunocytokine. The treatment was completely successful in the *beige/beige* mice, which are known to have a fully functional T-cell repertoire, in contrast to the *scid/scid* strain in which the effect of the fusion protein was abrogated, despite the presence of functional NK-cells. These experiments clearly demonstrated the involvement of T-cells in the immune response induced by immunocytokine treatment, as opposed to NK-cells, which appear to be ineffective in this tumor model. The involvement of a distinct T-cell subpopulation in the eradication of established melanoma metastases was established *in vivo* by depletion of $CD4^+$ and/or $CD8^+$ T-cells. In order to exclude a contribution by NK-cells to the treatment effect of the immunocytokine, C57BL/6 *beige/beige* mice were used, since NK-cells are known to partially substitute for absent T-cells in certain functional aspects. Eradication of established pulmonary melanoma metastases following treatment with the immunocytokine was only observed in non-depleted controls and in mice depleted of $CD4^+$ T-cells. Depletion of $CD8^+$ or both $CD8^+$ and $CD4^+$ T-cells abrogates the effect of immunocytokine therapy, which suggests that only the presence of CD8+ T-cells is mandatory for an effective immune response in this melanoma model.

A third line of evidence indicating an involvement of $CD8^+$ T-cells was provided by functional *in vitro* cytotoxicity studies of effector cells obtained from successfully treated mice bearing established pulmonary metastases. Specifically, only splenocytes from mice that received the tumor-specific ch14.18-IL2 immunocytokine therapy displayed a cytolytic response against tumor target cells in a standard chromium release assay. This is in contrast to splenocytes of mice treated with a non-specific immunocytokine, e.g. ch225-IL2, which produced only background cytolytic activity.

The cytotoxic activity observed with $CD8^+$ and $CD4^+$ T-cells, purified from splenocytes of ch14.18-IL2 treated mice, was only detectable in the $CD8^+$ T-cell fraction. In addition, blocking of MHC class I antigens on tumor target cells by $H\text{-}2K^b/H\text{-}2D^b$ antibodies, completely inhibited the cytolytic response of both $CD8^+$ T-cells and non-separated splenocytes. This finding clearly demonstrated MHC class I restriction of the cytolytic response, a classical feature of tumor-specific $CD8^+$ T-cells[78].

A further proof for a T-cell mediated immune response was the demonstration of a long-lived and transferable immunity following successful therapy with the ch14.18-IL2 immunocytokine. Specifically, it was shown that mice cured of established subcutaneous tumors or pulmonary metastasis by immunocytokine therapy completely rejected a subsequent i.v. challenge with melanoma cells in 50% of all mice up to four months after initial treatment. In the remaining 50% of mice, a significant reduction in metastasis was observed. This was in contrast to mice that were initially treated with an equivalent mixture of antibody and cytokine or that received cryotherapy of their s.c. tumors, suggesting that neither IL2 nor the release of tumor antigens recognized by T-cells are sufficient to induce the long-lived protective immunity only observed in mice subjected to targeted-IL2 therapy. It is important to note that challenges with an unrelated tumor cell line (EL4), that also expresses the GD2 antigen, initially used as a docking site for the immunocytokine, induced fulminate metastases in the same mice that could be fully protected against challenge with murine melanoma cells. This finding clearly demonstrated that not yet defined tumor antigens recognized by T-cells are required for the induction of protective immunity which are independent of the GD2 docking antigen that was simply used to deliver IL2 into the tumor microenvironment. The adoptive transfer of T-cell subpopulations from immune mice into T-cell deficient *scid/scid* mice indicated that only $CD8^+$ T-cells were able to efficiently protect these animals from challenge with melanoma cells, whereas $CD4^+$ T-cells were completely ineffective in this regard. Using this model, it was also possible to demonstrate the homing of $CD8^+$ CTL into s.c. melanoma metastases following passive transfer (Figure 7)[78].

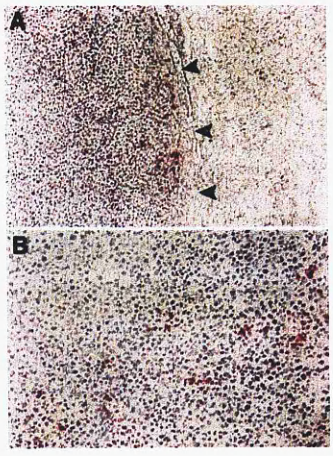

Figure 7. Homing of passively transferred CD8+ T cells to subcutaneous tumors. C57BL/6 *scid/scid* mice were injected s.c. with 5 x 10^6 B78-D14 cells. After 18 days, 3 x 10^7 lymphocytes obtained from immunocompetent C57BL/6 mice which had previously rejected B78-D14 tumors following ch14.18-IL2 treatment, were admistered i.v.. Twenty-four hr later, 8 µm sections of these tumors were prepared and subjected to immunostaining with anti-CD8 antibodies. Arrowheads mark the border between tumor and surrounding tissue. Magnification: (A) 80x, (B) 200x. Figure taken from reference 78.

The data obtained in the murine melanoma system provided proof of concept that targeted-IL2 therapy with an immunocytokine can engage a T-cell-mediated immune response followed by a long-lived transferable protective immunity. However, a successful anti-tumor T cell response involves induction, recruitment, and effector function of T cells. Antibody-directed IL2 therapy may influence this process in a number of different ways. First, the tumor cells themselves might interact with naive T cells with IL2 acting as the second co-stimulatory signal in the activation of cytotoxic T cells. A recent model proposed by J. Sprent for the activation of naïve T cells provides the rationale for this mechanism According to this model, high-avidity interactions between peptide-MHC class I complexes and the T cell receptor promote strong crosslinking of T-cell receptor-CD3 complexes, which in turn leads to strong signaling; thereby stimulating the production of cytokines, such as IL2, and receptors thereof; costimulation boosts the T cell receptor mediated signal. If the intensity of signaling is below a certain threshold, e.g., when the density of peptide-MHC complexes or the level of costimulation is low, the responding T cells express only IL2 receptors, but no IL2[79,80]. Hence, these T cells fail to proliferate unless exposed to exogenous IL2. The second possible scheme for the establishment of T cell activation is based on tumor antigens being processed by antigen-presenting cells. It has been shown that preactivated macrophages, dendritic cells and granulocytes express receptors for IL2 and that *in vitro* culture with IL2 causes functional changes in these

cells[81]. After arriving at the tumor site these cells may be activated by the antibody-targeted IL2 to kill the tumor cells and subsequently present the tumor antigens to T cells. The obvious infiltration of mononuclear cells within the tumor after administration of the antibody-IL2 fusion protein supports this hypothesis. In addition, antibody-IL2 fusion proteins are likely to be involved in the recruitment and activation of primed cytotoxic T cells and the activation of their effector function. This is particularly obvious in view of the demonstrated effect of antibody-IL2 fusion proteins on large subcutaneous tumors.

Perspectives

The preclinical data obtained with IL2 immunocytokines in the described melanoma model established proof of concept that directing IL2 into the tumor microenvironment effectively activates immune cells to eradicate established metastasis. Considering the efficiency of the IL2 immunocytokine and its immune mechanisms, it is very likely that its clinical application will lead to further improvements in the outcome of patients subjected to immunotherapies. In this regard, it will be of interest to assess whether immunocytokines might also be useful when applied in combinations with other experimental approaches currently under clinical investigation. These include the use of gene therapy with cytokine transduced autologous tumor cells or dendritic cells pulsed with tumor-associated peptides, which are currently used as cellular vaccines aimed at the induction of a long lasting T-cell mediated tumor-protective immunity[82,83]. In both cases, an increase of the cellular immune response could be achievable by directing cytokines into the tumor microenvironment. Thus, to test the efficacy of applying immunocytokines in conjunction with cellular vaccines will be a major goal to improve the immunotherapy for cancer.

ACTIVATION OF PRE-EXISTING T-CELL CLONES BY TARGETED INTERLEUKIN-2 THERAPY

Summary

The induction of an immunological anti-tumor response capable of eradicating metastatic tumors is the ultimate goal of immunotherapy. We have recently shown that this can be achieved by IL2 therapy directed to the tumor microenvironment by a recombinant antibody-IL2 fusion protein. It is not known, however, whether this curative treatment is associated with a predominance of T-cells carrying specific TCR BV or the presence of clonally expanded T-cells. To address this question we have used a quantitative RT-PCR method to analyze the TCR BV region repertoire in TIL of treated and untreated animals. As controls the TCR BV region repertoire was analyzed in blood and skin from disease-free animals. The results indicate an overexpression of TCR BV5 in the tumors of all treated mice and an additional overexpression of individual regions in each tumor. Direct sequencing of these TCR BV regions did not reveal any evidence of clonal expansions. However, since clonal expansions could exist as subpopulations in highly expressed regions, not detectable by direct sequencing, a DGGE assay was used for clonal analysis of TCR BV PCR products. DGGE analysis of selected TCR BV regions revealed the presence of clonotypic T-cells in tumors from both treated and untreated animals. These data indicate that targeted-IL2 therapy in this model does not induce clonal T-cell responses *de novo*, rather it acts as an activator for an already existing population of clonotypic T-cells.

Introduction

Melanoma is a highly malignant tumor but several lines of evidence suggest that it is capable of eliciting a specific immune response, i.e., a number of melanoma associated antigens have been identified and the presence of clonotypic T-cells has been demonstrated in melanoma lesions[42,84-86]. Therefore, several immunomodulatory therapeutic approaches were initiated to improve the prognosis of melanoma patients. IL2 is one of the most potent antitumor cytokines known, and was recently approved for treatment of metastatic melanoma[61]. However, objective responses induced by systemic IL2-therapy are still insufficient, and the associated side effects are severe[87]. These findings are due to the fact that a systemic application of IL2 disregards the paracrine nature of this cytokine under physiological conditions[88].

As a means to target IL2 directly to the tumor site we have recently shown that human IL2 can be genetically engineered as a fusion protein with the chimeric mouse-human monoclonal antibody 14.18 which recognizes the ganglioside GD_2, retaining both antigen binding and cytokine activity[68]. Furthermore we have shown that treatment with this antibody-IL2 fusion protein can eradicate human hepatic and pulmonary melanoma metastases in SCID mice[71] as well as autologous murine B16 melanomas[76]. Although it was shown in these studies that tumor eradication was dependent on $CD8^+$ T-cells, it is not known whether tumor clearance is associated with a clonal expansion of T-cells. Furthermore, it remains to be established whether such a clonal expansion would be due to a de novo induction or to the activation and expansion of preexisting T cell clones. Here, we demonstrate both the overexpression of certain TCR BV regions as well as the clonal expansion of T-cells in melanoma lesions subsequent to targeted-IL2 therapy. However, clonally expanded T-cells were also detectable prior to therapy, suggesting that antibody-IL2 targeted therapy act as an activator rather than an inducer of an anti-tumor T-cell response.

Experimental Procedures

Cell lines, antibodies and immunocytokines

The murine melanoma cell lines, B16 G.3.12 and B78-D14, have been described previously[68]. B78-D14 was derived from B16 melanoma cells by transfection with genes coding for β-1,4-N-acetylgalactosaminyltransferase and α-2,8-sialyltransferase inducing a constitutive expression of the gangliosides GD2 and GD3. B16 melanoma cells were maintained as monolayers in RPMI 1640 medium supplemented with 10% fetal calf serum and 2mM L-glutamine and were passaged as necessary. The culture medium for B78-D14 cells was further supplemented with 400 μg G418 and 50 μg Hygromycin B per μl.

Mouse/human chimeric antibodies directed against the EGF receptor (ch225) or GD2 (ch14.18) were constructed by joining the cDNA for the variable region of the murine antibodies with the constant regions of the γ1 heavy chain and the κ light chain as previously described[71]. The antibody-IL2 fusion proteins, ch225-IL2 and ch14.18-IL2, were constructed by fusion of a synthetic sequence coding for human IL2 to the carboxyl end of the human Cγ1 gene as described[68]. The fused genes were inserted into the vector pdHL2, which encodes for the dihydrofolate reductase gene. The resulting expression plasmids were introduced into Sp2/0-Ag14 cells and selected in Dulbecco's modified Eagle's medium supplemented with 10% fetal bovine serum and 100 nM methotrexate. The fusion proteins were purified over a protein A-Sepharose affinity column.

All other antibodies used are commercially available and have been described in detail by the manufacturer (Pharmingen, La Jolla, CA)

Animals

C57BL/6J mice were obtained from Jackson Laboratory at the age of 4 - 6 weeks. These animals were housed under specific pathogen-free conditions and all experiments were performed according to National Institute of Health guidelines for care and use of laboratory animals.

Subcutaneous tumors

Tumors were induced by s.c. injection of 5 x 10^6 tumor cells in RPMI 1640, which resulted in tumors of approximately 40 µl volume within 14 d.

Immunohistology

Frozen sections were fixed in cold acetone for 10 minutes followed by removal of endogenous peroxidase with 0.03% H_2O_2; and blocking of collagenous elements with 10% species specific serum in 1% BSA/PBS. The antibodies where then overlaid onto serial sections, at predetermined dilutions (usually 20 µg/ml) and the slides were incubated in a humid chamber for 30 minutes. With PBS washes between every step, a biotinylated link antibody was applied for 10 minutes followed by a streptavidin-linked enzyme, i.e. either peroxidase or alkaline phosphatase, for 10 minutes. After another wash, the substrate was added and the slides were incubated in the dark for 20 minutes. After a wash in PBS, the slides were counter stained, mounted and viewed using an Olympus BH2 microscope with photographic capabilities.

RNA extraction and cDNA synthesis

RNA was extracted using the method of Chomczynski and Sacchi as described[89]. cDNA synthesis was carried out using 1-3 µg of total RNA with oligo-dT and M-MLV SuperScript II reverse transcriptase (Gibco-BRL, Life Technologies Inc., Gaithersburg, MD, USA) in a total volume of 50 µl 1X buffer (Gibco-BRL, Life Technologies Inc., Gaithersburg, MD, USA) containing 10 mM DTT. Incubations were performed at 42°C for 50 min, 72°C for 5 min.

Primer design and characteristics

Primers used for the amplification of murine TCR BV regions include 18 primers specific for BV families 1-18 and a constant region primer, BC (Table 1). Murine TCR BV sequences in the GenBank database[20] were used together with the PCGENE FASTSCAN program (Intelligenetics, Palo Alto, CA, USA) to create library files for the BV families 1-18. Optimal primer sequences were found by using the computer program Oligo Version 3.4 (Medprobe, Oslo, Norway) aiming at a ΔG below -40.0 and a Tm between 50°C and 60°C[90]. Selected primer sequences were tested for match to all members of the respective families. Importantly, all sequences were

subsequently tested for potential homology to all other families, aiming at a minimum of 5 mismatches to non-relevant templates. All primers fulfill these criteria.

		ΔG	Tm	Pos	Size
BV1	5´-CGGTGCCCAGTCGTTTTATAC-3´	-40.8	53.8°C	-89	223bp
BV2	5´-CACACGGGTCACTGATACGGAG-3´	-41.0	56.7°C	-61	195bp
BV3	5´-CACCTTGCAGCCTAGAAATTCAG-3´	-42.5	54.9°C	-50	184bp
BV4	5´-CTGCCTCAAGTCGCTTCCAAC-3´	-41.2	56.3°C	-89	223bp
BV5	5´-TGARATGAACATGAGTGCCTTGG-3´	-41.3	56.4°C	-43	177bp
BV6	5´-TTCTCTCACTGTGACATCTGCCC-3´	-40.1	56.5°C	-42	176bp
BV7	5´-AAGGATACAGGGTCTCACGGAAG-3´	42.7	55.3°C	-80	214bp
BV8	5´-GATRTCCCTGATGGRTACAAGGC-3´	43.9	58.3°C	-40	174bp
BV8A	5´-TTGGCTTCCCTCTCTCAGACA-3´	-39.2	53.8°C	-27	161bp
BV9	5´-TCTCTCTACATTGGCTCTGCAGG-3´	-44.7	58,7°C	-42	176bp
BV10	5´-ATCAAGTCTGTAGAGCCGGAGG-3´	-41.1	54.1°C	-33	167bp
BV11	5´-AGGCACAAGGTGACAGGGAAG-3´	-40.4	55.5°C	-243	377bp
BV12	5´-ATGGTGGGGCTTTCAAGGATC-3´	-42.3	56.6°C	-98	232bp
BV13	5´-CTGTGAGGCCTAAAGGAACTAAC-3´	40.7	51.1°C	-68	202bp
BV14	5´-ACGACCAATTCATCCTAAGCAC-3´	-40.1	52.5°C	-53	187bp
BV15	5´-CCATCAGTCATCCCAACTTATCC-3´	-41.4	54.0°C	-69	203bp
BV16	5´-GTGACCCTCAATTGTGACCCAG-3´	-40.4	55.6°C	-213	347bp
BV17	5´-CACGATACCTGGTCAAAGAGAAAG-3´	-42.2	53.9°C	-245	379bp
BV18	5´-CGGCCAAACCTAACATTCTC-3´	-41.9	55.1°C	-63	215bp
BC	5´-GGGTAGCCTTTTGTTTGTTTGC-3´	-42.5	54.6°C	84	
BC-5`	5´-GCTACCTTCTGGCACAATCCTC-3`	-41.2	54.5°C	236	
BC-3`	5´-TAGGCATTTTCCAGGTCACAAG-3`	-40.6	53.5°C	699	463bp

GC-clamp: 5´-CGCCCGCCGCGCCCCGCGCCCGTCCCGCCGCCCCCGCCC-3´

Table 1. Primers used for the amplification of murine TCRBV regions include 18 primers specific for BV families 1-18 and a constant region primer, BC. Selected primer sequences were tested for match to all members of the respective families. Importantly, all sequences were subsequently tested for potential homology to all other families, aiming at a minimum of 5 mismatches to non-relevant templates. Position +1 is defined as the first nucleotide 5´ to the sequence coding for the conserved amino-acid sequence CASS in the proximal end of the variable region. The approximate size is calculated using an estimated length of the DJ region of 50 bp

TCR BV analysis and quantitation

Preliminary experiments were performed to certify that TCR BV analyses were performed in the exponential phase of the amplification, ensuring a proportional relationship between the amount of mRNA in the original sample and the amount of PCR product. cDNA was serially diluted (2 fold dilutions down to 1/512) and PCR amplified for 26 cycles with TCRBC specific primers (BC-5 and BC-3). The amount of TCR BC PCR product was quantitated using Imagequant software[91] and these results were used to ensure that all TCR BV analyses were carried out using an equal amount of TCR cDNA. Amplifications were performed twice in a total volume of 25 µl containing 5 pmol of each primer, 2.5 mM dNTPs (Pharmacia LKB, Uppsala,

Sweden) and 1.25 U Amplitaq polymerase (Perkin Elmer Cetus Corporation, U.S) in 1xPCR buffer (50 mM KCl, 20 mM Tris pH 8.4, 2.0 mM $MgCl_2$, 0.2 mM cresol, 12% sucrose, 0.005% (w/v) BSA (Boehringer-Mannheim, Mannheim, Germany.). Inclusion of sucrose and cresol red in the reaction buffer enables direct loading of aliquots on the gel [92]. Negative controls were samples without cDNA. TCR BV amplifications were performed by 30 cycles in a Perkin Elmer GeneAmp PCR System 9600 (Perkin Elmer Cetus Corporation, U.S.) using the following parameters: 94°C for 30 sec., 60°C for 30 sec. and 72°C for 60 sec. Taq polymerase and dNTPs were added to the reaction at an 80°C step between the denaturation and annealing steps of the first cycle (*hot start*)[93]. For quantitative PCR analysis the constant region primer (BC) was end-labeled with γ-[^{33}P]. Ten-microliter aliquots of PCR products were electrophoresed in a 2% NuSieve 3:1 agarose gel (FMC BioProducts, Rockland, ME) which was subsequently dried under vacuum and exposed to a Molecular Dynamics Storage Phosphor Screen (Molecular Dynamics, Sunnyvale, CA). Quantitation was accomplished using the Imagequant software[91].

DGGE

Melting maps were generated using the computer algorithm MELT87[94]. DGGE analyses were done in 6% polyacrylamide gels containing a gradient of urea and formamide from 20% to 80%[95]. Electrophoresis was performed at 160 V for 4.5 hours in 1x TAE buffer at a constant temperature of 58°C. After electrophoresis, the gels were stained with ethidium bromide and photographed under UV transillumination. In order to validate the resolving power of the method, BV regions selected for clonal analysis were cloned using the TA-cloning kit following the manufacturer's suggestions (Invitrogen, San Diego, CA, USA). Positive bacterial clones were PCR amplified for 35 cycles with the specific BV-primer together with the "GC-clamped" BC primer and 12-μl aliquots were analyzed using DGGE.

Sequencing reaction

Several PCR products were subjected to sequence analysis in order to investigate the clonality of the transcript using the Thermo Sequenase cycle sequencing kit (Amersham, Life Science, Cleveland, USA) according to the manufacturer's instructions. In brief, bands were excised from the denaturing gradient gel, and DNA was eluted in H_2O and reamplified. An aliquot (0.2 μl) of the PCR product was used

as template in a 40-cycle sequencing reaction with γ-[^{33}P]end-labeled BC as sequencing primer. Gels were dried under vacuum and exposed to a Phosphor Screen.

Results

Quantitative RT-PCR of TCR BV regions

The tumors used for investigation were induced by subcutaneous injection of either the parental B16 melanoma line G3.12[96] or the GD2 expressing melanoma line B78-D14 derived from the B16 melanoma cells by transfection with genes coding for β-1,4-N-acetylgalactosaminyltransferase and α-2,8-sialyltransferase[74]. Tumors were obtained from mice which were treated by i.v. administration of 8 μg ch14.18-IL2 fusion protein for 7 d. Therapy was initiated 10d after tumor cell inoculation. As controls, we used tumor samples obtained from mice receiving PBS instead of ch14.18-IL2. To analyze for the expression of TCR BV region expression in murine blood, skin and tumor tissues, we have designed 18 primers specific for murine TCR BV families 1-18. Prior to analysis of tumor lesions experiments were carried out to demonstrate that each amplified TCR BV product was obtained with the expected size (Table 1) and no spurious amplification products were observed. To validate the semi-quantitative RT-PCR methodology, serially diluted cDNA was PCR amplified for different numbers of cycles using the primers BV 1-18 together with the constant region primer BC end-labeled with γ-[^{33}P]. The data from these experiments were used to determine the amount of cDNA and the number of cycles through which the specific PCR products accumulated exponentially, enabling determination of the relative abundance of each TCR BV region. Furthermore, the accuracy and reproducibility of the method were investigated by repeated analyses of PBL indicating that the experimental variation represented 4-8% of the mean value. The relative expressions of TCR BV-regions in different tumors are shown in Table 2. The expression of each TCR BV family is given as the mean percentage (+/- SD) of the total TCR BV signal detected in the gel. As additional controls we analyzed the TCR BV1-18 expression in PBLs and skin from four healthy animals. Results from these analyses are shown in Table 2.

In general all analyses showed low expression of TCR BV17 and 18, and high expression of TCR BV8. One possible explanation for this observation is that most murine BV families are single member families whereas BV8 is a three-member family. A comparison of GD_2-expressing tumors in treated *versus* untreated animals indicates a significantly higher expression of BV5 in animals treated with the fusion protein (Table 3). The mean expression of BV5 in tumors derived from the untreated animals was 5.6% whereas it was 17.1% in tumors of animals treated with ch14.18-IL2. In several tumors, one or two additional BV families were expressed at levels ≥10%. This high expression was observed with the families BV1, 6, 11, 12 and 13. Like BV5, the high expression of BV12 is observed in several B16 G3.12 tumors, as well as B78-D14 tumors from both treated and untreated mice.

	animal 1		animal 1		animal 1		animal 1	
	PBL	Skin	PBL	Skin	PBL	Skin	PBL	Skin
	% SD	% SD	% SD	% SD	% SD	% SD	% SD	% SD
BV1	3.7 (1.1)	5.5 (0.7)	4.1 (0.0)	2.6 (1.0)	6.2 (1.0)	6.2 (0.8)	6.2 (1.0)	10.5 (2.1)
BV2	6.7 (0.8)	7.4 (0.1)	8.4 (1.8)	8.0 (1.3)	5.5 (0.0)	7.0 (0.7)	5.5 (0.0)	7.4 (2.4)
BV3	2.6 (0.2)	3.7 (1.0)	4.3 (0.8)	2.2 (0.7)	3.2 (0.0)	3.0 (0.4)	3.2 (0.0)	4.1 (1.2)
BV4	1.2 (0.8)	2.2 (0.4)	1.3 (0.0)	2.2 (0.3)	4.1 (0.3)	1.8 (0.9)	4.1 (0.3)	1.6 (0.4)
BV5	5.8 (0.3)	10.3 (1.2)	9.7 (0.5)	5.9 (0.5)	7.6 (2.2)	9.1 (0.9)	7.6 (2.2)	9.5 (0.0)
BV6	6.0 (2.3)	6.0 (0.1)	9.2 (4.1)	19.5 (0.6)	7.3 (0.2)	5.8 (0.7)	7.3 (0.2)	5.1 (0.9)
BV7	7.8 (1.3)	4.5 (1.2)	3.4 (1.8)	5.1 (0.3)	4.4 (0.7)	2.5 (1.1)	4.4 (0.7)	4.1 (0.3)
BV8	24.2 (3.8)	14.0 (3.0)	15.6 (2.2)	16.0 (0.0)	11.8 (2.0)	12.0 (5.3)	11.9 (2.0)	13.0 (1.1)
BV9	3.6 (0.1)	4.3 (0.2)	5.3 (1.0)	3.9 (1.5)	3.8 (0.5)	4.0 (1.4)	3.8 (0.5)	2.9 (1.3)
BV10	4.7 (0.1)	5.8 (0.8)	8.9 (1.4)	6.7 (1.4)	7.9 (1.8)	4.9 (2.4)	7.9 (1.8)	6.5 (0.2)
BV11	2.7 (0.3)	4.9 (0.6)	1.6 (1.4)	5.3 (1.0)	4.0 (1.0)	1.7 (0.3)	4.0 (1.0)	2.9 (0.5)
BV12	5.9 (0.7)	9.5 (0.0)	8.2 (3.0)	2.1 (1.1)	8.4 (1.3)	20.0 (2.6)	8.4 (1.3)	8.5 (0.5)
BV13	4.1 (0.3)	5.0 (0.2)	4.9 (1.1)	9.2 (1.8)	7.1 (0.1)	6.1 (0.5)	7.1 (0.1)	7.7 (1.5)
BV14	5.5 (0.4)	4.9 (1.1)	8.1 (0.6)	4.0 (1.4)	7.6 (1.2)	5.8 (0.9)	7.6 (1.2)	6.0 (0.9)
BV15	3.3 (0.1)	4.2 (0.4)	3.4 (2.2)	1.6 (0.6)	3.2 (0.4)	4.8 (1.4)	3.2 (0.4)	3.0 (0.3)
BV16	12.0 (0.7)	7.2 (0.6)	2.6 (1.7)	2.8 (0.2)	7.0 (0.0)	3.3 (0.1)	7.0 (0.0)	4.8 (0.3)
BV17	0.1 (0.1)	0.1 (0.1)	0.4 (0.0)	1.2 (1.0)	0.4 (0.1)	1.1 (0.1)	0.4 (0.1)	0.9 (0.5)
BV18	0.1 (0.1)	0.4 (0.0)	0.3 (0.3)	0.3 (0.1)	0.4 (0.0)	0.9 (0.7)	0.4 (0.0)	1.2 (1.1)

Table 2. TCRBV 1-18 expression in PBLs and skin from untreated animals. Preliminary experiments were performed to certify that TCRBV analyses were performed in the exponential phase of the amplification using an equal amount of TCR cDNA. TCRBV amplifications were performed by 30 cycles using the following parameters: 94°C for 30 sec., 60°C for 30 sec. and 72°C for 60 sec und *hot start* conditions. For quantitative PCR analysis the constant region primer (BC) was end-labeled with γ-[^{33}P]. PCR products were electrophoresed in a 2% NuSieve 3:1 agarose gel which was subsequently exposed to a Molecular Dynamics Storage Phosphor Screen. The expression of each BV region was calculated as a percentage of the sum of all BV spots.

	B16 / 7 days of PBS				B78-D14 / 7 days of PBS				B78-D14 / 7 days of ch14.18-IL2			
	Animal 1	Animal 2	Animal 3	Animal 4	Animal 1	Animal 2	Animal 3	Animal 4	Animal 1	Animal 2	Animal 3	Animal 4
	% (SD)	% (SD)	% (SD)	% (SD)	% (SD)	% (SD)	% (SD)	% (SD)	% (SD)	% (SD)	% (SD)	% (SD)
BV1	5.4 (0.4)	4.9 (1.4)	11.3 (ND)	5.2 (0.7)	10.9 (0.7)	2.8 (1.5)	9.4 (5.2)	4.3 (0.9)	6.1 (0.1)	3.4 (0.2)	4.4 (0.4)	6.8 (2.2)
BV2	4.2 (0.9)	5.1 (1.8)	4.1 (ND)	5.9 (1.8)	5.4 (0.7)	7.2 (1.9)	4.4 (1.7)	6.1 (0.3)	5.4 (0.6)	6.5 (1.1)	4.7 (0.7)	7.1 (0.4)
BV3	5.7 (0.5)	4.9 (1.4)	1.2 (ND)	2.7 (1.1)	2.9 (0.2)	3.6 (1.0)	4.0 (0.6)	2.6 (0.3)	2.5 (0.6)	1.4 (0.6)	2.7 (0.5)	4.5 (0.9)
BV4	1.6 (0.6)	4.2 (0.1)	2.5 (ND)	2.1 (0.5)	3.4 (0.0)	6.8 (3.2)	2.2 (0.2)	3.3 (0.3)	2.1 (0.6)	1.4 (0.1)	2.2 (0.1)	2.7 (1.3)
BV5	8.1 (0.6)	6.2 (0.3)	5.9 (ND)	7.7 (2.3)	4.7 (0.4)	6.2 (1.3)	5.2 (0.6)	6.3 (1.7)	11.6 (2.4)	28.8 (1.2)	17.5 (0.6)	10.3 (1.4)
BV6	12.7 (0.4)	6.4 (1.3)	19.9 (ND)	5.0 (0.1)	5.2 (1.7)	3.9 (0.4)	5.9 (0.8)	5.4 (0.8)	6.9 (0.4)	5.2 (0.8)	4.1 (0.1)	5.1 (0.3)
BV7	3.7 (1.2)	4.3 (0.6)	2.3 (ND)	3.5 (1.9)	2.9 (0.8)	2.8 (0.8)	3.4 (0.8)	3.6 (0.3)	6.0 (1.1)	4.6 (1.1)	6.8 (1.4)	5.8 (0.2)
BV8	13.2 (0.2)	5.3 (0.2)	10.5 (ND)	18.9 (1.7)	30.4 (4.0)	10.1 (0.7)	22.7 (1.1)	14.9 (1.4)	18.2 (0.4)	16.8 (0.5)	17.7 (0.7)	9.3 (3.1)
BV9	4.0 (1.2)	4.3 (1.3)	1.6 (ND)	3.7 (1.1)	4.0 (0.7)	3.0 (0.7)	6.0 (0.6)	3.7 (0.1)	5.8 (0.1)	3.8 (0.1)	3.3 (1.2)	5.2 (0.4)
BV10	3.1 (0.8)	7.4 (0.3)	3.1 (ND)	4.8 (0.3)	4.0 (0.1)	6.1 (0.3)	6.0 (1.0)	6.2 (0.6)	5.4 (1.1)	4.8 (1.3)	7.8 (0.5)	6.1 (0.6)
BV11	11.5 (2.6)	5.7 (0.1)	12.6 (ND)	9.0 (3.1)	7.1 (1.2)	5.4 (0.6)	2.5 (0.4)	5.4 (0.2)	5.2 (0.9)	6.1 (0.1)	4.7 (0.8)	5.3 (1.8)
BV12	5.8 (0.7)	8.4 (1.3)	10.8 (ND)	6.2 (0.0)	3.5 (1.3)	12.9 (0.5)	5.9 (1.0)	15.5 (0.0)	7.5 (1.9)	6.7 (1.6)	10.5 (0.6)	7.7 (1.1)
BV13	9.9 (4.0)	10.2 (1.4)	3.4 (ND)	5.1 (1.2)	2.3 (0.3)	4.4 (0.5)	3.3 (0.0)	4.7 (0.3)	6.5 (1.5)	3.8 (1.3)	4.1 (0.8)	6.8 (0.2)
BV14	2.8 (1.3)	7.5 (2.1)	2.4 (ND)	3.0 (0.1)	2.5 (0.5)	9.8 (0.2)	4.5 (0.7)	3.8 (1.0)	2.5 (0.0)	2.3 (0.5)	3.2 (0.3)	5.7 (0.4)
BV15	3.8 (1.0)	5.0 (1.0)	2.2 (ND)	4.5 (0.2)	5.0 (0.1)	6.6 (0.1)	9.3 (0.4)	6.2 (0.0)	2.0 (0.0)	1.4 (0.5)	2.1 (0.3)	4.5 (0.3)
BV16	3.9 (0.2)	5.9 (1.8)	4.6 (ND)	6.4 (0.8)	5.0 (0.2)	7.2 (1.0)	4.6 (0.9)	7.3 (2.3)	5.1 (0.1)	2.8 (0.2)	3.6 (0.4)	4.5 (0.3)
BV17	0.2 (0.1)	1.1 (0.9)	0.7 (ND)	0.4 (0.2)	0.1 (0.0)	0.3 (0.0)	0.4 (0.1)	0.1 (0.0)	0.5 (0.1)	0.3 (0.1)	0.4 (0.4)	0.2 (0.0)
BV18	0.4 (0.2)	3.3 (0.0)	0.5 (ND)	5.7 (0.9)	0.7 (0.1)	0.9 (0.7)	0.1 (0.1)	0.4 (0.0)	0.7 (0.4)	0.2 (0.1)	0.2 (0.1)	0.4 (0.1)

Table 3. Relative expression of TCRBV regions 1-18 in B16 G3.12 and B78-D14 tumors in PBS treated animals, as well as B78-D14 tumors in ch14.18-IL2 treated animals. Preliminary experiments were performed to certify that TCRBV analyses were performed in the exponential phase of the amplification using an equal amount of TCR cDNA. TCRBV amplifications were performed by 30 cycles using the following parameters: 94° C for 30 sec., 60° C for 30 sec. and 72° C for 60 sec und *hot start* conditions. For quantitative PCR analysis the constant region primer (BC) was end-labeled with γ-[^{33}P]. PCR products were electrophoresed in a 2% NuSieve 3:1 agarose gel which was subsequently exposed to a Molecular Dynamics Storage Phosphor Screen. The expression of each BV region was calculated as a percentage of the sum of all BV spots.

Denaturing gradient gel electrophoresis

To investigate the clonality of the transcripts, several PCR products from tumor tissues were sequenced directly through the CDR3 coding region of the receptor. A total of 21 different PCR products were sequenced, including BV5 from all 12 animals; BV8, BV11 and BV13 from animal 1 of the B16 G3.12/fusion protein group; BV1 and BV8 from animal 1, as well as BV8 and BV12 from animal 3 of the B78-D14/fusion protein group. These experiments revealed no indications of clonality. For a correct interpretation of this finding it is important to point out that clonally expanded T cells must account for at least 10% of the T-cell infiltrate in order to be detected by direct sequencing. Thus, we applied the DGGE methodology to resolve whether clonal T-cells might be present in the T-cell infiltrate at lower frequencies.

The melting properties of several TCR BV5, BV8 and BV12 sequences available, were evaluated by use of the computer program MELT 87 which predicts the melting of a double stranded DNA molecule on the basis of its base composition[20,94]. These calculations indicated that the DNA molecules amplified by the BV5 and BV12 primers were suited for denaturing gradient gel analysis, whereas the BV8 primer had to be changed (BV8A; Table 1). The subsequent attachment of a GC-rich sequence (GC-clamp) to the 5′-end of the constant region (Table 1) altered the melting profile of all tested sequences to generate the desired two-domain profile[97]. To validate the

resolving power of the method, cloned transcripts derived from TCR BV5, 8, and 12 were analyzed. In all cases clonal PCR products were resolved as distinct bands in the gel whereas analysis of polyclonal products revealed a smear (Figure 8). At least 8 different clonotypic transcripts were analyzed for each of the BV regions BV5, 8 and 12, and in all cases the products resolved at different positions in the gel.

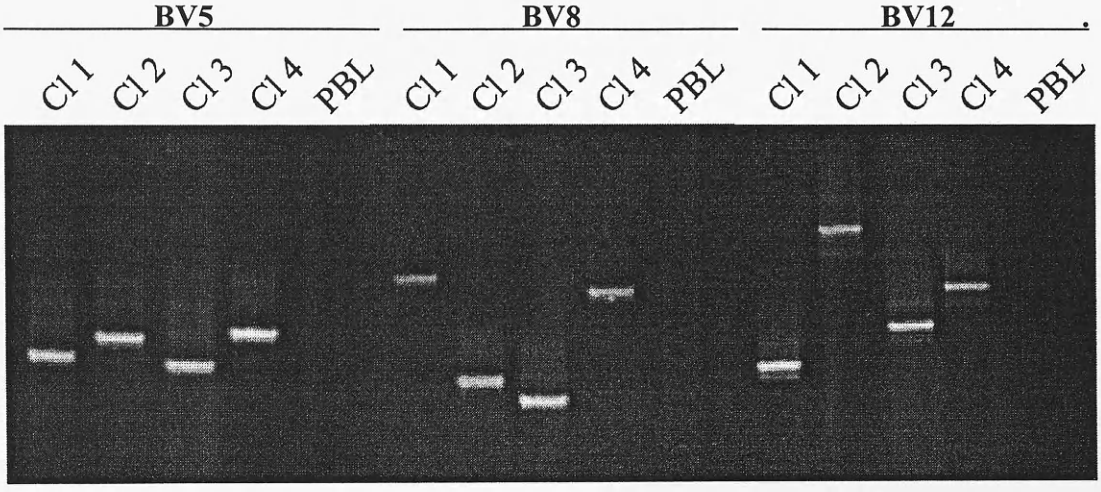

Figure 8. Denaturing gradient gel analysis of polyclonal (PBL) and clonal TCR transcripts covering BV5, BV8 and BV12. cDNA from peripheral blood lymphcytes was amplified with primers specific for BV families 5, 8 or 12, cloned into PCR^{TMII} (Invitrogen, San Diego, CA, USA) and reamplified. PCR products were loaded onto a 20% - 80% denaturing gradient gel and run for 4.5 hours at 160 Volts at a constant temperature of 58°C. DNA was stained with ethidium bromide and photographed under UV light.

Following this validation, we tested for the presence of clonotypic T-cells in different tumor samples. TILs from three groups, i.e., B16 G3.12 and B78-D14 tumors in PBS treated animals, as well as B78-D14 tumors in ch14.18-IL2 fusion protein treated animals were analyzed by DGGE for the presence of T-cell clonality in BV families 5, 8, and 12. Skin and PBLs from four disease free animals were analyzed as controls. Clonotypic transcripts were revealed in all tumors for at least one of the regions analyzed (Figure 9). In contrast, for skin and PBL samples in only one single case (skin sample no. 3) a clonal BV12 transcript could be detected (data not shown). Multiple DNA bands were recovered from the gels, re-amplified and sequenced in all cases verifying the clonality of the transcript. As shown in Figure 9, DGGE analysis demonstrated the presence of clonally expanded T-cells in B78-D14 tumors of animals receiving either ch14.18-IL2 or PBS. Furthermore, clonally expanded T-cells were also present in GD2 negative B16 G3.12 tumors; thus demonstrating the immunogenicity of the parental B16 line. In most lesions more than one clonal

transcript were detected, and in some lesions several clonal transcripts were found that carried the same BV-region.

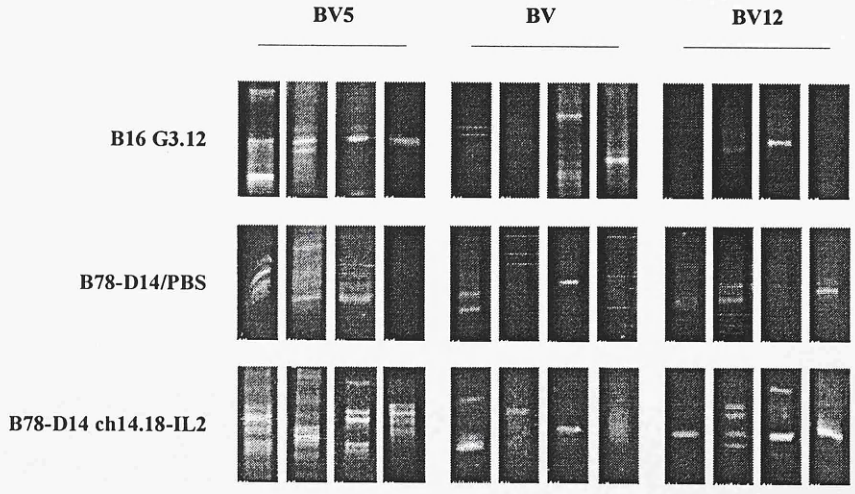

Figure 9. Denaturing gradient gel analysis for clonality in tumor infiltrating lymphocytes in B16 G3.12, B78-D14/PBS and B78-D14 ch14.18-IL2. From four animals in each group (left to right) cDNA from tumor biopsies were PCR amplified with primers specific for BV5, BV8 and BV12 together with the "GC"-clamped constant regions primer. Aliqouts were loaded onto a 20% - 80% denaturing gradient gel and run for 4.5 hours at 160 Volts at a constant temperature of 58°C. DNA was stained with ethidium bromide and photographed under UV light.

Discussion

The past decade has unveiled important insights into the role of T lymphocytes in the host's immune response to cancer in general and to melanoma in particular[84]. A number of MAA have been characterized which are specifically recognized by autologous T cell in the context of HLA molecules[98]. The notion that a functional and specific T-cell response is present in melanoma patients is corroborated by the observation that clonotypic T-cells exist in both primary and metastatic melanoma[86,99]. However, the unfavorable prognosis of metastatic melanoma clearly demonstrates that this immunological response is inadequate to eradicate the tumor.

Interleukin 2 which has a central role in the immune system has been widely used for the treatment of metastatic melanoma[62]. However, the systemic administration of this cytokine disregards its paracrine nature; thus resulting in limited anti-tumor responses and severe side effects[87]. Recently, we have tried to overcome these problems by developing antibody-IL2 fusion proteins that combine the unique targeting ability of antibodies with the multifunctional activity of cytokines. The therapeutic

effectiveness of such constructs for the treatment of established hepatic, pulmonary, and subcutaneous melanoma metastases has been documented in a number of different murine tumor models[71,76,100-102]. Detailed characterization in various tumor models revealed the superiority of antibody-IL2 fusion proteins over comparable amounts of IL2, the parental antibody, the combination of both or non-specific antibody-IL2 fusion proteins[71]. Even micrometastases displaying some degree of antigenic heterogeneity could be successfully addressed by this form of therapy. Several lines of evidence, i.e., immunohistology, *in vivo* depletion studies, adoptive transfer experiments, and cytotoxicity assays, indicated that this antitumor effect is largely dependent on CD8+ T cells[103]. However, the molecular basis of this T cell response remained elusive.

In the present study we scrutinized the nature of the T-cell response at the molecular level. Our aim was to test whether specific TCR BV regions were overexpressed in the T-cell infiltrate of tumors before and after targeted immunotherapy, followed by an analysis of these regions for clonality. The quantitative analysis of TCR BV1-18 in three groups of tumor samples, i.e. B16 G3.12 and B78-D14 tumors in PBS treated animals, as well as B78-D14 tumors in ch14.18-IL2 fusion protein treated animals, revealed an overexpression of BV5 in B78-D14 tumors after therapy with ch14.18-IL2 (Table 3). However, since the expression of BV5 was rather high in a limited number of skin samples (Table 2), it was not prudent to conclude that this overexpression was due to a clonal expansion of T cell induced by the applied immunotherapy. Hence, we subsequently analyzed the samples for clonally expanded T cells. This analysis was extended to cover not only BV5, but also the regions BV8 and BV12, which were highly expressed in some of the tumors. However, the initial approach to test for clonality by direct sequencing of PCR products was hampered by the inherent low sensitivity of this method. Thus, a DGGE-based method was established for the detection of clonotypic TCR transcripts in a murine system. We have recently described the use of DGGE for the detection of clonality in human T-cell populations. The sensitivity of this approach enables the detection of clonal transcripts constituting as low as 0.1% of the TCR transcripts in a mixed T-cell population[32]. As shown in Figure 9, DGGE analysis of both transfected and non-transfected tumors revealed the presence of clonotypic T-cells. These data suggest that the T-cells responsible for tumor clearance are recognizing TAAs expressed by the parental tumor cells and not antigens induced by the process of

transfection. In this regard, the murine analogues of human MART-1, gp100 and tyrosinase related protein 2 were recently cloned from a B16 melanoma cDNA library [104,105]. Furthermore, cytotoxic T-cell clones recognizing B16 melanoma, which exert their action in a tumor specific and MHC restricted manner have been raised from C57BL6 mice[106]. These data strongly suggest that clonal T-cell responses against melanoma associated antigens are a general feature of murine B16 melanoma. Although B16 melanoma is generally considered to be a weak or even non-immunogenic tumor, possibly because of a low expression of MHC class I molecules[107], these reports together with the data presented herein indicate that B16 melanoma fulfills the requirements to elicit a specific MHC restricted T-cell response. Such an immune response could have been boosted by targeted-IL2 therapy of established melanoma metastases. For all three TCR BV regions analyzed, more than one clonal transcript was present; this was most evident in treated tumors (Figure 9), e.g. BV5 analysis revealed the presence of 5-8 different clonal transcripts. This finding predicates that T-cell clones are present at levels which are not detectable prior to therapy, but are expanded by IL2 targeted to the tumor microenvironment by ch14.18-IL2. These data suggest that the majority of the T-cells present in the tumor subsequent to *in situ* IL2 therapy are tumor specific since their activation is dependent on both antigen recognition and the presence of IL2. However, at present it is not possible to confirm that the T cell clones detected *in situ* are directly implicated in the T-cell mediated anti-tumor immune response induced by targeted IL2 therapy. Although our knowledge and understanding of tumor-specific T cells have expanded considerably, current *in vitro* analysis may not reflect the *in vivo* immune status as *in vitro* culture steps may introduce major biases[108].

To date, only a limited number of studies have characterized TIL in tumors treated with IL2, at the molecular level. One of these studies suggested that regression of P815 tumors, induced by intratumoral injection of an adenoviral vector expressing IL2, was caused by a polyclonal non-specific T-cell population[109]. The means for assessing clonality in this study was based on analyzing infiltrating T-cells by the "Immunoscope" approach which uses CDR 3 size as a marker for clonality[34]. Consequently, a T-cell clone will be revealed by the presence of a high number of transcripts having the exact same length of CDR3. The inherent problems of this approach are obvious, i.e., a large number of different T-cell clones are difficult to distinguish simply by the length of CDR3. In contrast, the DGGE method reveals clonality on the basis of melting

properties, meaning that transcripts having the exact same length will be focused at different positions in the gel[32]. TCR transcripts of different lengths may, in theory, have similar melting properties and consequently may focus at the same position in a denaturing gradient gel. Sequencing a high number of individual bands has, however, revealed a single sequence in all cases, suggesting that co-focusing of different TCR transcripts be probably a rare event. The discrepancy of the data in these two studies is therefore most likely due to the different methods employed. An alternative explanation for this obvious discrepancy between these two studies could be the different means of IL2 administration.

A successful antitumor T cell response involves induction, recruitment, and effector functions of T cells. The presence of clonotypic T-cells in the B16 G3.12 and B78-D14 tumors without any specific therapy suggests that clonally expanded tumor-specific T-cells are present in the TIL population prior to therapy with the ch14.18-IL2 fusion protein; thus, targeted immune therapy seems to be involved in the modulation of later phases of a cellular immune response. Importantly, our results imply that anergized or otherwise inactive T-cells can be activated by means of targeted IL2 therapy without the requirement for specialized antigen-presenting cells or the induction of new or modified peptide antigens.

IN SITU CYTOKINE THERAPY: REDISTRIBUTION OF CLONALLY EXPANDED T-CELL CLONES

Summary

Immunity to tumors relies on re-circulating antigen-specific T cells. Whilst induction of antigen-specific T cells by immunotherapy has been convincingly proven, direct evidence for re-circulation of such cells is still lacking. Here, employing a recently established *in situ* immunotherapy model for murine melanoma we directly demonstrate the redistribution of therapeutic T-cell clones. In this model IL2 is targeted to the tumor microenvironment by means of specific antibody-IL2 fusion proteins resulting in the expansion of therapeutic T cells. The therapeutic effect of the fusion protein is not restricted to tumors expressing the targeted antigen, but extends to antigen negative variants of the tumor if present in the same animal. Analysis of the T-cell infiltrate by quantitative RT-PCR revealed the presence of highly expressed TCR BV-regions in both tumor variants. TCR clonotype mapping revealed that the high expressions of these regions were caused by clonal expansions and, notably, that these specific clonotypic TCR transcripts were identical in both tumors. Thus, therapeutic T-cell clones activated locally by targeted-IL2 therapy re-circulate and mediate eradication of distant tumor sites not subjected to *in situ* cytokine therapy.

Introduction

Malignant melanoma accounts for the majority of mortality from skin cancer, and the therapeutic options for advanced disease are limited. New treatment modalities are being explored, among which immunotherapy seems the most promising. IL2 has potent anti-tumor activity, and has been approved for treatment of metastatic melanoma[48]. However, systemic application of IL2 disregards the paracrine nature of this cytokine under physiological conditions[88]; hence, objective anti-tumor responses are insufficient and associated with severe side effects[64]. Targeting of IL2 directly to the tumor site can be accomplished with a tumor-specific antibody-IL2 fusion protein that retains both antigen binding and cytokine activity[68]. We have previously demonstrated that treatment with the ch14.18-IL2 fusion protein, which recognizes disialo-ganglioside GD2, can eradicate human melanoma metastases in SCID mice upon reconstitution with lymphokine-activated killer cells[71], as well as autologous murine B16 melanomas expressing the GD2 molecule[76]. The curative action of treatment with ch14.18-IL2 was shown to be dependent on $CD8^+$ T cells. Recently we demonstrated the presence of clonotypic T cells in tumor lesions of both IL2-fusion protein treated and in non-treated control mice indicating that such clonotypic T cells are activated and expanded by IL2 in the micro environment and subsequently are capable of controlling tumor growth[110].

In the current study we demonstrate the ability of targeted-IL2 therapy to eradicate not only targeted tumors, but also GD2-negative wtB16 tumors present in the same animal. TCR clonotype mapping in combination with comparative analyses DGGE revealed that clonotypic T cells were present in both B78-D14 and wtB16 tumors and that specific TCR transcripts in both tumors of the same animal were identical, thus, originating from the same T-cell expansion. Our data indicate that the effect of targeted IL2 therapy is mediated by activation of clonotypic T cells in the targeted GD2-expressing tumor and the subsequent migration of these T cells to the GD2-negative, wild type tumor.

Experimental Procedures

Animals

C57BL/6J mice were obtained from Jackson Laboratory at the age of 6 weeks. These animals were housed under specific pathogen-free conditions and all experiments were performed according to National Institute of Health guidelines for care and use of laboratory animals.

Cell lines, antibodies and fusion proteins

The murine melanoma cell lines, B16 G.3.12 and B78-D14, have been described[74,96]. B78-D14 was derived from B16 melanoma cells by transfection with genes coding for γ-1,4-N-acetylgalactosaminyltransferase and γ-2,8-sialyltransferase inducing a constitutive expression of the gangliosides GD2 and GD3. B16 melanoma cells were maintained as monolayers in RPMI 1640 medium supplemented with 10% fetal calf serum and 2 mM L-glutamine. The culture medium for B78-D14 cells was further supplemented with 400 μg G418 and 50 μg Hygromycin B per ml.

Mouse/human chimeric antibodies directed against GD2 (ch14.18) were constructed by joining the cDNA for the variable region of the murine antibodies with the constant regions of the γ1 heavy chain and the κ- light chain as previously described[71]. The antibody-IL2 fusion protein ch14.18-IL2, was constructed by fusion of a synthetic sequence coding for human IL2 to the carboxyl end of the human Cγ1 gene as described[68,76]. The fused genes were inserted into the vector pdHL2, which encodes for the dihydrofolate reductase gene. The resulting expression plasmids were introduced into Sp2/0-Ag14 cells and selected in Dulbecco's modified Eagle's medium supplemented with 10% fetal bovine serum and 100 nM methotrexate. The fusion proteins were purified over a protein A-Sepharose affinity column. All other antibodies used are commercially available and have been described in detail by the manufacturer (Pharmingen, La Jolla, CA).

Subcutaneous tumors

Tumors were induced by s.c. injection of 5 x 10^6 B78-D14 or 10^5 B16 G.3.12 tumor cells in RPMI 1640 resulting in tumors of approximately 40 μl volumes within 10 d.

Immunohistology

Frozen sections were fixed in cold acetone for 10 minutes followed by removal of endogenous peroxidase with 0.03% H_2O_2, and blocking of collagenous elements with 10% species specific serum in 1% BSA/PBS. The antibodies were then overlayed onto serial sections, at predetermined dilutions (usually 20 µg/ml), and the slides were incubated in a humid chamber for 30 minutes. With PBS washes between every step, a biotinylated link antibody was applied for 10 minutes followed by a streptavidin-linked enzyme, i.e. either peroxidase or alkaline phosphatase, for 10 minutes. After another wash, the substrate was added and the slides were incubated in the dark for 20 minutes. After a wash in PBS, the slides were counter stained, mounted and viewed using an Olympus BH2 microscope with photographic capabilities.

RNA extraction and RT-PCR

RNA was extracted using the Purescript Isolation Kit (Gentra Systems Inc. NC). Synthesis of cDNA was done with 1-3 µg of total RNA using oligo-dT and SuperScript II reverse transcriptase (Gibco-BRL, Life Technologies Inc., Gaithersburg, MD, USA) in a total volume of 50 µl 1X buffer (Gibco-BRL, Life Technologies Inc., Gaithersburg, MD, USA) containing 10 mM DTT. Incubations were performed at 42°C for 50 min, 72°C for 5 min. Primers used for the quantitative analysis of murine TCR BV regions include 18 primers specific for BV families 1-18 and a constant region primer, BC as described [110]. Prior to analysis, the total amount of TCR cDNA was quantitated by amplification of the constant part of the TCRB-chain, in order to normalize the amount of TCR cDNA. Amplifications were performed in duplicates by 30 cycles in a Perkin Elmer GeneAmp PCR System 9600 (Perkin Elmer Cetus Corporation, U.S.A.) using previously described conditions. Negative controls were samples without cDNA. For quantitative PCR analyses the constant region primer (BC) was end-labeled ^{33}P. Ten-microliter aliquots of PCR products were electrophoresed in a 2% NuSieve 3:1 agarose gel (FMC BioProducts, Rockland, ME) which was subsequently dried under vacuum and exposed to a Molecular Dynamics Storage Phosphor Screen (Molecular Dynamics, Sunnyvale, CA). Quantitation was accomplished using the Imagequant software.

TCR clonotype mapping

DGGE analyses for clonotype mapping of the BV regions BV5, BV8 and BV12 have been described[110]. In the present study we additionally evaluated the amplification products for the remaining BV regions by use of the computer program MELT87 which predicts the melting of a double stranded DNA molecule on the basis of its base composition[94]. These calculations indicated that the DNA molecules amplified by these primers were suited for denaturing gradient gel analysis without modifications. Exceptions were the primers BV11, BV16 and BV17 for which reason new primers were selected for the amplification of these regions (BV11A; 5′-GCC CAA TCA GTC GCA CTC AAC-3′, BV16A; 5′-CTC TGA AAA TCC AAC CCA CAG C-3′, BV17A; 5′-ATT CTC AGC TAA GTG TTC CTC GA-3′). The attachment of a 50 bp GC-rich sequence (GC-clamp) to the 5′-end of the constant region primer (BC1; 5′-TGG AGT CAC ATT TCT CAG ATC-3′) altered the melting profile of all tested sequences to generate the desired two-domain profile[97]. DGGE analysis was done in 6% polyacrylamide gels containing a gradient of urea and formamide from 20% to 80% [95]. Electrophoresis was performed at 160 V for 4.5 hours in 1x TAE buffer at a constant temperature of 54°C. After electrophoresis, the gels were stained with ethidium bromide and photographed under UV transillumination. In order to validate the resolving power of the method, amplification products were cloned using the TA-cloning kit following the manufacturer's suggestions (Invitrogen, San Diego, CA, USA). Positive bacterial clones were PCR amplified for 35 cycles with the specific BV-primer together with the "GC-clamped" BC primer and 10 µl aliquots were analyzed by DGGE.

Sequencing reaction

PCR products were subjected to sequence analysis using the Thermo Sequenase cycle sequencing kit (Amersham, Life Science, Cleveland, USA) following the manufacturer's instructions. Briefly, bands were excised from the denaturing gradient gel, and DNA was eluted in H_2O and reamplified. An aliquot (0.2 µl) of the PCR product was used as template in a 40-cycle sequencing reaction the BC primer labeled with ^{33}P as sequencing primer. Gels were dried under vacuum and exposed to a Phosphor Screen.

Results

Therapeutic Efficacy of the Antibody-IL2 Fusion protein

One major obstacle of antibody-based immunotherapy is the heterogeneity of target antigen expression. We previously demonstrated that successful treatment with antibody-IL2 fusion proteins is associated with the induction of a long-lived and transferable immunity[78]; thus, enabling this form of therapy to overcome heterogeneous expression of the target antigen within the tumor. However, the experimental design of these earlier studies could not rule out the possibility that this anti-tumor activity was due to a bystander effect since GD2-negative and GD2-positive tumor cells were located close to each other.

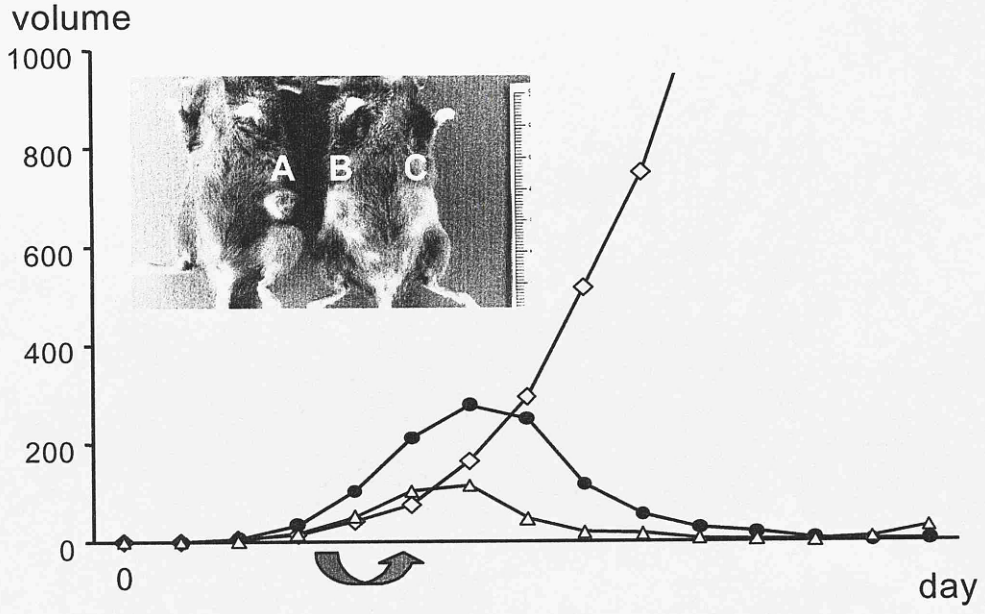

Figure 10. Therapeutic efficacy of ch14.18-IL2 on the growth of target-antigen negative tumors. Two groups consisting each of 8 animals were treated. In the first group only one tumor was induced by s.c. injection of 5 x 10^5 wtB16 melanoma cells resulting in a GD2-negative tumor (open diamonds; insert, A). In the second group of animals two different tumors were simultaneously induced: one by s.c. inoccultation of 5 x 10^5 wtB16 melanoma on the left flank of the animal (open triangle; insert, C), the second by s.c. injection of 5 x 10^6 B78-D14 melanoma cells on the right flank (closed circles; insert, B). The latter resulting in a GD2-expressing tumor. Initiation of treatment with 8µg ch14.18-IL2 at day 10 is indicated by an arrow; it was maintained for 7 days. The insert depicts a representative example of animals innoculated with (A) wtB16 tumor cells alone or (B) B78-D14 and (C) wtB16 tumor cells in the same animal as it was observed on day 35 after tumor cell inocculation.

To investigate whether antibody-IL2 fusion protein treatment might overcome antigen heterogeneity at distant metastatic sites, subcutaneous tumors were induced which either displayed or lacked expression of the target antigen of the ch14.18-IL2 fusion

protein, i.e., the ganglioside GD2 (Figures 10 and 11). Treatment with 8 µg ch14.18-IL2 administered intravenously was initiated after 10 d when tumors reached a volume of approximately 40 µl and was maintained for 7 d. This manipulation resulted in a dramatic reduction in size of both GD2-positive and -negative tumors if present in the same animal (Figure 10). In contrast, no therapeutic effect of ch14.18-IL2 was observed when administered to mice bearing only GD2-negative B16 melanoma. These tumors lacked any infiltration by lymphocytes following this treatment; whereas, the therapeutic effect of the fusion protein was associated with a marked infiltration by CD8+ T cells of both B78-D14 and wtB16 tumors if present in the same mouse (Figure11).

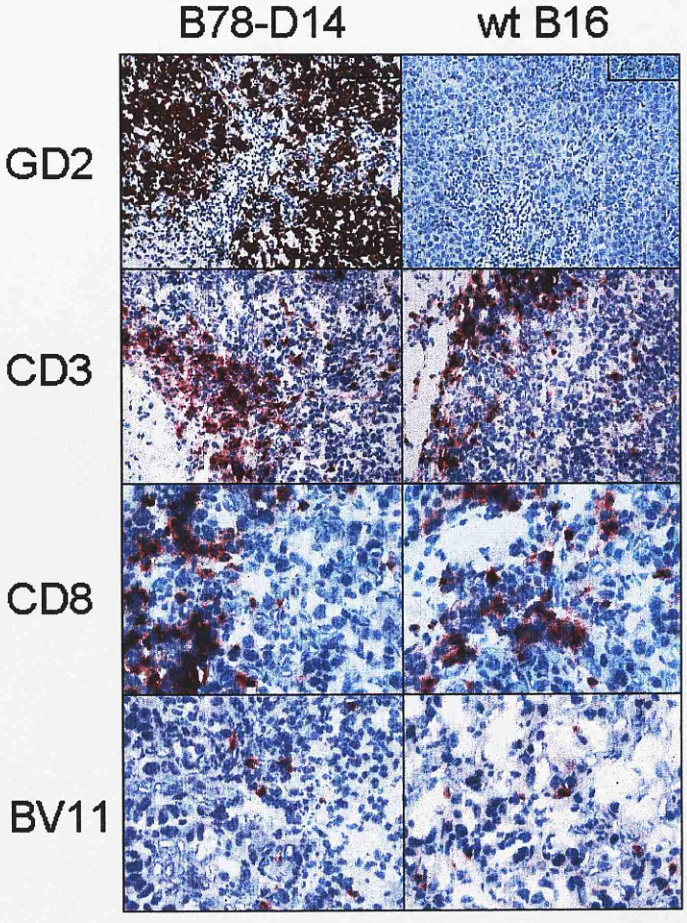

Figure 11. In situ IL2-therapy targeted to GD2-positive tumors induces T-cell infiltration in target-antigen negative tumors. Immunohistochemical characterization of B78-D14 and wtB16 tumors present in the same animal subsequent to 7 day therapy with 8 µg ch14.18-IL2 using antibodies with the indicated specificities, i.e., GD2, CD3, CD8 or TCR BV11. Representative examples for all mice (n=4) are given for GD2, CD3 and CD8. The lower panel depicts sections obtained from animal #4 subjected to immunostaining with an antibody specific for TCR BV11.

Quantitative RT-PCR of TCR BV regions

The eradication of wtB16 tumors is likely to be executed by redistribution of therapeutic T-cell clones that were expanded in the B78-D14 tumor due to the targeting of IL2 to this tumor. It is therefore likely that such expansions of identical T-cell clonotypes in both tumors would be detected by a semi-quantitative analysis of the BV regions in both tumors. Quantitative analyses of TCR BV regions in PBL and normal skin from 4 individual animals were used as baseline for the selection of highly expressed TCR BV regions for further analysis [110]. The relative expressions of the TCR BV regions 1-18 in GD2-positive and -negative tumors are given in Table 4. Individual BV regions were expressed at high levels compared to baseline, and some of these were expressed at elevated levels in both tumors from the same animal (Animal #1; BV15, Animal #4; BV11). In animal 4, this observation was subsequently confirmed using monoclonal antibodies against these highly expressed BV regions (Figure 11). Conversely, some regions were expressed at very different levels in the same animal (i.e. BV12 animal #3).

	animal 1				animal 2				animal 3				animal 4			
	B16wt		B78-D14		B16wt		B78-D14		B16wt		B78-D14		B16wt		B78-D14	
	Exp. %	#	Exp. %	#	Exp. %	#	Exp. %	#	Exp. %	#	Exp. %	#	Exp. %	#	Exp. %	#
BV1	5.5 (1.2)	2	3.9 (0.3)	1	4.7 (1.0)	1	5.2 (0.2)	2	5.0 (0.9)	2	4.9 (0.6)	2	8.6 (0.6)	2	6.3 (1.3)	2
BV2	3.2 (0.5)	0	5.8 (0.8)	1	4.7 (2.2)	0	4.2 (1.0)	1	5.9 (1.8)	0	4.6 (1.1)	0	2.7 (0.1)	0	5.5 (0.9)	1
BV3	2.0 (0.0)	1	2.4 (0.4)	>4	3.0 (0.0)	0	2.9 (0.4)	4	2.1 (0.1)	2	2.9 (0.3)	0	2.0 (0.2)	1	2.9 (0.4)	>4
BV4	2.4 (0.1)	3	2.9 (1.0)		1.5 (0.5)	2	2.0 (1.3)	3	1.4 (0.4)	0	1.9 (1.0)	4	1.9 (0.2)	0	2.1 (0.1)	3
BV5	14.2 (2.1)	1	13.0 (2.2)	0	14.5 (0.1)	0	12.8 (3.7)	1	15.3 (3.1)	0	16.2 (1.6)	0	8.0 (0.8)	0	16.3 (0.7)	1
BV6	11.9 (1.6)	2	5.5 (0.9)	2	5.4 (1.9)	1	4.0 (1.7)	2	4.5 (0.3)	0	4.7 (1.4)	0	9.4 (1.5)	0	3.3 (0.2)	>4
BV7	2.9 (0.2)	1	5.4 (0.3)	3	4.4 (0.1)	1	4.8 (2.0)	4	6.1 (0.8)	1	4.8 (1.2)	1	2.7 (0.5)	0	6.1 (1.1)	2
BV8	13.6 (2.3)	1	14.2 (4.4)	>4	18.5 (0.7)	0	20.9 (1.0)	3	28.3 (1.7)	0	14.5 (0.9)	0	11.8 (0.6)	0	10.5 (3.0)	2
BV9	2.1 (0.1)	1	9.6 (3.0)	1	4.7 (0.8)	0	5.9 (1.3)	>4	3.2 (0.7)	1	4.3 (0.4)	0	1.6 (0.1)	0	2.5 (0.7)	>4
BV10	3.7 (0.1)	0	7.1 (0.1)	0	7.1 (1.1)	0	4.6 (0.8)	0	5.0 (2.0)	1	5.4 (3.3)	0	6.0 (0.4)	2	3.2 (0.6)	1
BV11	4.1 (0.5)	1	4.8 (1.1)	1	4.1 (0.4)	0	3.2 (1.9)	3	4.7 (0.4)	1	6.2 (2.2)	0	18.3 (1.5)	1	12.2 (1.1)	>4
BV12	4.6 (1.3)	1	7.9 (2.6)	1	6.7 (0.1)	1	6.5 (2.1)	4	4.9 (0.1)	2	11.4 (0.2)	2	6.5 (0.6)	1	6.8 (0.2)	1
BV13	3.2 (0.6)	1	6.8 (1.8)	0	6.1 (0.7)	1	5.5 (0.8)	1	4.5 (2.0)	1	5.7 (0.6)	0	5.3 (0.0)	2	8.0 (0.6)	1
BV14	1.1 (0.0)	0	3.8 (1.5)	2	3.1 (0.6)	0	5.2 (0.2)	1	1.7 (0.2)	0	3.6 (0.1)	3	1.0 (0.7)	0	2.5 (0.0)	1
BV15	22.8 (2.1)	2	23.1 (1.2)	1	5.8 (0.2)	1	5.2 (0.5)	3	3.5 (1.3)	2	3.0 (0.9)	2	6.1 (1.2)	1	4.6 (0.3)	3
BV16	2.4 (0.2)	3	2.9 (1.4)	0	5.3 (0.6)	0	5.9 (0.4)	0	3.2 (0.5)	0	5.0 (0.4)	0	8.1 (0.5)	1	6.6 (1.2)	0
BV17	< 1	1	< 1	1	< 1	2	< 1	0	< 1	>4	< 1	1	< 1	3	< 1	0

Table 4. Expression of TCRBV-regions and presence of T-cell clonotypes in wtB16 and B78-D14 tumors in four animals.Relative expression of the TCRBV families 1-18 in the individual tumors (wtB16 and B78-D14) in four animals. The expression of each TCRBV family is given as the mean percentage (+/- SD) of the total TCRBV signal detected in the gel. The number of T-cell clonotypes determined by TCR clonotype mapping is given in a separate column for each tumor.

TCR clonotype mapping

To thoroughly examine the T-cell infiltrates of wtB16 and B78-D14 tumors for the presence of clonotypic T cells, we adopted a "TCR clonotype mapping" strategy

based on RT-PCR coupled with DGGE. This method physically separates and visually displays clonotypic TCR transcripts in complex T-cell infiltrates[32]. We have previously utilized a TCR clonotype mapping assay to establish the profile and extent of T-cell clonality in the TCR infiltrates of human melanoma[111]. To establish an assay for the murine system, all 18 BV regions were rendered amenable to DGGE analysis by computer modeling of DNA melting and appropriate "GC-clamping"[94]. Subsequent to this theoretical validation, the resolving power of the method was tested using cloned PCR products. In all cases clonal PCR products were resolved as distinct bands in the gel, whereas analysis of polyclonal PCR products for the same BV regions revealed a smear. At least 8 different clonotypic transcripts were analyzed for each of the BV regions and in all cases the products resolved at different positions in the gel. Furthermore, we analyzed PBL, skin and spleen of healthy animals and found that each individual BV region only rarely is represented by a clonotype, and that PBL, skin, and spleen in normal mice comprise from 0 – 5 T-cell clonotypes.

Following this validation, we tested for the presence of clonotypic T cells in the tumor samples. This analysis revealed that clonotypic transcripts for several BV regions were present in all tumors. A representative result is depicted in Figure 12 showing the TCR clonotype map of the GD2-expressing tumor from animal #2. The numbers of clonotypic transcripts in each tumor ranged from 9 to more than 30 (Table 4). Notably, clonotypic transcripts were detected in most BV regions, irrespective of the level of expression. Even regions expressed at a level below 1% contained clonotypic TCR transcripts. Conversely, clonotypic TCR transcripts were absent in some BV regions expressed at high levels, demonstrating that a high level of expression does not necessarily imply the presence of clonally expanded T-cells.

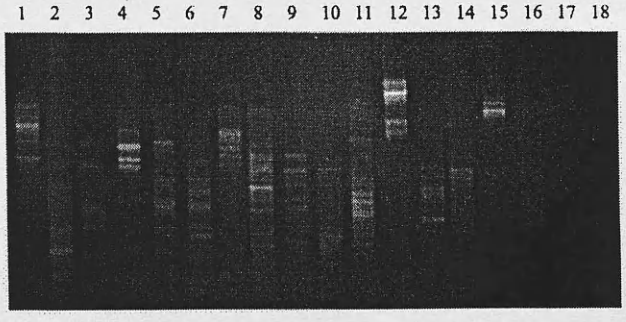

Figure 12. TCR clonotype mapping of the T-cell infiltrate B78-D14 from animal #2, covering the BV families 1-18. PCR products were loaded onto a 20% - 80% denaturing gradient gel and run for 4.5 hours at 160 Volts at a constant temperature of 54°C. DNA was stained with ethidium bromide and photographed under UV light.

Comparative DGGE

In some cases T-cell clonotypes expressing identical BV regions were detected in both tumors from the same animal. To resolve whether these clonotypes were identical, RT-PCR was repeated and samples were loaded onto a denaturing gradient gel in adjacent lanes. Since DGGE separates DNA molecules on the basis of their melting properties, identical DNA sequences will resolve at the same position in the gel. Initially, BV15 from animal #1 and BV11 from animal #4 were compared as these regions were highly expressed in both tumors of the respective animals. This analysis demonstrated the identity of clonotypic transcripts in GD2-positive and GD2-negative tumors (Figure 13).

Figure 13. Identity of T cell clonotypes among overexpressed TCR BV familes present in GD2-positive and GD2-negative tumors. Comparative TCR BV region analysis of selected T-cell clonotypes present in both tumor variants of animals #1 and #4. Sequence analysis was subsequently used to verify identity.

The presence of identical T-cell clonotypes in wtB16 and B78-D14 tumors strongly suggests that these T cells contributed to the translocation of the therapeutic antitumor effect. However, the migration of a single T-cell clone from B78-D14 to the wtB16 tumor as detected in animals #1 and #4, would possibly be insufficient to mediate the regression of a fast growing tumor. We therefore found it of interest to investigate whether the presence of identical T-cell clonotypes in both GD2-positive and GD2-negative tumors from the same animal is a phenomenon confined to single T-cell clones present at high numbers or may also occur for less pronounced clonotypes. Accordingly, a complete comparison of all T-cell clonotypes (BV1, BV3, BV11, BV12, BV15, and BV16) in the tumors from animal #4 was conducted. Data from this analysis demonstrated that half of the transcripts (BV11, BV15, and BV16) were identical

whereas the remaining were not (Figure 14). The finding that some of them were expressed at intermediate levels suggests that the redistribution of T cells is not dependent on high cell numbers.

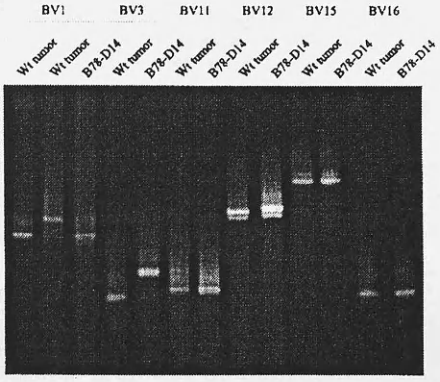

Figure 14. Identity of T cell clonotypes among TCR BV familes expressed at low levels present in GD2-positive and GD2–negative tumors. Comparative TCR BV region analysis of the clonotypes detected in both tumors of animal #4. Subsequent sequence analysis revealed identity of the clonotypes belonging to the BV11, BV15, and BV16 families.

Sequencing

PCR products corresponding to potentially identical T-cell clonotypes were sequenced to verify identity. In all cases sequence identity was confirmed. The nucleotide sequences of the CDR3 region for the BV15 T-cell clone of animal #1, and the BV11, BV15 and BV16 T-cell clones detected in both tumors from animal #4, are given in Table 5.

Animal #1

TCRBV15S1 ← → CDR3 ←→ Joining 2.7 ← → Constant region

tgt ggt gct gga ctg ggg ggg cga gaa cag tac ttc ggt ccc ggc acc agg ctc acg gtt tta gag gat ctg aga aat gtg

cys gly ala gly leu gly gly arg glu gln tyr phe gly pro gly thr arg leu thr val leu glu asp leu arg asn val

Animal #4

TCRBV11 ← → CDR3 ←→ Joining 2.4 ← → Constant region

tgt gca agc agc tta gcc cct ggt caa aac acc ttg tac ttt ggt gcg ggc acc cga cta tcg gtg cta gag gat ctg aga aat gtg

cys ala ser ser leu ala pro gly gln asn thr leu tyr phe gly ala gly thr arg leu ser val leu glu asp leu arg asn val

TCRBV15S1 ← → CDR3 ←→ Joining 2.5 ← → Constant region

tgt ggt gct agg gac ccg gat aac caa gac acc cag tac ttt ggg cca ggc act cgg ctc ctc gtg tta gag gat ctg aga aat gtg

cys gly ala arg asp pro asp asn gln asp thr gln tyr phe gly pro gly thr arg leu leu val leu glu asp leu arg asn val

TCRBV16S1 ← → CDR3 ←→ Joining 2.5 ← → Constant region

tgt gcc agc agc cag act ggg aaa gac acc cag tac ttt ggg cca ggc act cgg ctc ctc gtg tta gag gat ctg aga aat gtg

cys ala ser ser gln thr gly lys asp thr gln tyr phe gly pro gly thr arg leu leu val leu glu asp leu arg asn val

Table 5. TCR/CDR3 nucleotide sequence and deduced amino acid sequence of T-cell clonotypes detected in both wtB16 tumors and B78-D14 tumors from animal #1 and #4.

Discussion

The induction of a persistent tumor-specific immunity by antibody-targeted IL2 therapy, which is mediated by circulating CD8+ T cells, explains its high therapeutic efficacy against disseminated metastases displaying a substantial heterogeneity of antigen expression, notably, the target antigen. We have previously shown the capability of the therapy to eradicate tumors consisting of a mixed population of wtB16 and B78-D14 cells[77]. In the present study, B78-D14 and wtB16 tumors were induced by separate s.c. injection of tumor cells on the left and the right side of the animal resulting in individual tumors either expressing or lacking the GD2-target antigen of the fusion protein. Our data demonstrate that boosting the immune response by targeting IL2 to one localized tumor is sufficient to promote a powerful response against non-targeted tumors. The experimental design of this study definitely excludes that the curative response against the wtB16 tumor is a bystander effect of the response against the B78-D14 cells. This finding is highly significant for future clinical trials since heterogeneity of gene expression is a characteristic of many tumors and their subsequent metastases. In fact, loss of antigen was suggested to be a major mechanism of immune escape in melanoma[112]. The achieved eradication of tumor masses despite the lack of targeting due to lack of the GD2 antigen expression strongly emphasizes the curative potential of this therapy in a clinical setting.

T cells are the main effector cells induced by antibody-IL2 fusion proteins in our animal model. The eradication of distant wtB16 tumors strongly indicates a systemic involvement of this T-cell response, i.e., that T cells activated in the targeted GD2-positive B78-D14 tumor entered the periphery and migrated to the GD2-negative wtB16 tumor. Such a scenario is reflected by the high expression of identical BV regions in both tumors in the same animals. Quantitative analyses demonstrated high expression of BV5 and BV8 in all tumors. However, BV8 is over-expressed not only in tumors but also in PBL and skin from healthy mice suggesting that its over-expression be neither related to the tumor nor the treatment[110]. Nevertheless, the restricted over-expression of BV5 in TIL, but not in skin or blood, indicates that these T cells are indeed involved in the anti-tumor response. Since BV5 was found to be over-expressed in both B78-D14 and wtB16 tumors following therapy with ch14.18-IL2, this high expression of BV5 in the GD2 negative tumor seems to be a result of ch14.18-IL2 therapy targeted to the GD2 positive tumor. Likewise, the regions BV15 in animal #1, and BV11 in animal #4 were

both expressed at equally high levels in TIL from both tumors. However, such conclusions are only presumptive unless they are based on identification of the same clonotypes in the different tumor lesions. Therefore, we extended our studies by using DGGE based TCR clonotype mapping which is capable of detecting T-cell clonotypes in a polyclonal background[32]. The detailed analysis of the T-cell infiltrate demonstrated the presence of 9 to 36 T-cell clonotypes in each tumor. This is in corroboration with a recent analysis of human melanoma revealing that T-cell responses comprise an even higher number of clonotypes, ranging from 40 to more than 60[111]. The gradual difference between humans and mice could be related to the fact that murine cells express only a single MHC Class I molecule. Focusing initially on highly expressed, i.e., BV15 and BV11, and subsequently on the remaining TCR BV regions, we demonstrated the presence of identical T cell clonotypes in both tumors in the same animal.

An important issue relates to the characterization of the target structures recognized by these T cells. With the present data it cannot formally be excluded that some of the T-cell clones in the B78-D14 tumor recognize antigens derived from the GD2 molecule. Our data do however indicate that the therapeutic T-cell clones recognize identical antigens on B78-D14 and wtB16 melanoma cells; hence, although the antigens recognized by these T cells *in situ* are not known, it is unlikely that they are derived from or related to the GD2 molecule. As further proof of this notion we have previously shown that protection against B16 does not induce protection against the syngeneic GD2+ EL-4 thymoma cells[78]. Antigens that are possibly recognized by T cells on murine melanoma tumors have recently been identified. These include the murine homologues of MART1, gp100, and tyrosinase-related protein 2 (TRP-2) [104,105]. Interestingly, the TRP-$2_{181\text{-}188}$ peptide has been identified as a tumor rejection antigen for B16 melanoma[105], and recently, a CTL line expressing exclusively BV11 which recognizes the TRP-$2_{181\text{-}188}$ was reported to exert anti-tumor reactivity[113]. In half of our animals TIL of both tumors comprised clonotypic BV11 TCR transcripts, indicating the involvement of BV11 in the recognition of melanoma associated epitopes, possibly the TRP-$2_{181\text{-}188}$ peptide.

Studies of the T-cell response against human melanoma have suggested that a functional dissociation exist between local and systemic immune responses[114]. Recently, we provided evidence that the *in situ* T-cell response against human melanoma is mainly comprised by localized T-cell clonotypes which neither enter the

periphery nor home to other metastatic sites. Although similar studies have not been conducted in untreated, tumor bearing mice, it leads to the hypothesis that IL2 based immunotherapy with antibody-IL2 fusion proteins induces a migrating capacity in T cells.

In conclusion we demonstrate that administration of an antibody-IL2 fusion protein induces a specific T-cell response in B57BL/6 mice, which results in eradication, not only of targeted tumors but also distant, antigen-negative wtB16 tumors. Furthermore, the presence of identical T-cell clonotypes in targeted and non-targeted tumors from the same animal strongly indicates that the activation of tumor specific T cells in targeted tumors, and the subsequent migration of these T cells to non-targeted tumor lesions accomplish tumor eradication. The present data not only emphasize the curative potential in a clinical setting, but also stress the relevance of re-circulation of tumor specific T cells, one of the axioms of immunosurveillance.

TARGETING OF LYMPHOTOXIN-α TO THE TUMOR MICROENVIRONMENT ELICITS AN EFFICIENT IMMUNE RESPONSE BY INDUCTION OF A PERIPHERAL LYMPHOID-LIKE TISSUE

Summary

A recombinant antibody-lymphotoxin-α fusion protein induced an adaptive immune response protecting mice from melanoma. Importantly, this fusion protein elicited the formation of a lymphoid-like tissue in the tumor microenvironment containing L-selectin$^+$ T cells, MHC class II$^+$ antigen presenting cells and lymph node-like T- and B-cell areas. Furthermore, PNAd$^+$/TCA4$^+$ high endothelial venules were observed within the tumor, suggesting entry channels for naïve T-cell infiltrates. Over the course of therapy, a marked clonal expansion of certain TCR specificities occurred among tumor infiltrating lymphocytes which displayed reactivity against melanoma cells and the TRP-$2_{180\text{-}188}$ peptide. Consequently, naive T cells may have been recruited to as well as primed and expanded in the lymphoid-like tissue induced by the lymphotoxin-α fusion protein at the tumor site.

Introduction

A variety of tumors have proven to be immunogenic and for melanoma, several tumor-associated antigens have been identified, some of which are recognized by specific T cells. However, in most cases despite detectable anti-tumor responses, these do not control established tumor growth. Therefore, many anti-tumor therapy strategies aim at enhancing these existing T-cell based immune responses[47,115]. In this regard, earlier studies have shown that the genetic fusion of a tumor-specific antibody with a cytokine is a powerful tool to enrich the cytokine in the tumor environment, thus taking the paracrine working mechanism of cytokines into account[116]. We previously demonstrated that antibody-mediated targeting of IL2 to the tumor microenvironment mounts an effective cellular response against murine melanoma[76,110].

However, detailed studies revealed that, although antibody-IL2 fusion proteins were able to boost a pre-existing T-cell response, the induction of additional tumor-specific T cells was not achieved[110]. Since it has been reported that tumor-antigen-specific T cells can be rendered anergic by the tumor[117], priming of additional T cells may be particularly critical for the initiation of a successful anti-tumor immune response. Therefore, we wanted to test the efficacy of targeting cytokines to the tumor site that are likely to promote the induction of new tumor-specific T cells. We chose lymphotoxin-α (LTα) because it is a potent mediator of proinflammatory and tumoricidal activities as well as lymphoid genesis[118-121].

LTα exists either as a soluble or membrane-bound molecule. The soluble form is a homotrimer and binds to the receptors TNFRI and TNFRII[122], for which TNFα is also a ligand, whereas the membrane-bound form of LTα is a heterotrimer complexed with the transmembrane protein lymphotoxin-β (LTβ)[123]. The LTα/β complex ($LT\alpha_1/LT\beta_2$) can not bind to either of the TNF-receptors, but instead serves as a ligand for the LTβ-receptor (LTβR)[124].

Several studies revealed the important function of lymphotoxin in lymph node genesis. Notably, LTα/β-LTβR interactions seem to be most relevant, as disruption of either the LTβ or LTβR genes led to the absence of Peyer's patches and most lymph

nodes[125,126]. In comparison, in mice treated with antibodies against LTβR and TNFRI as well as in LTα knock-out mice no lymph nodes were observed at all[118,127], implying that LTα-TNFRI interactions rescued some of the lymph node genesis in LTβ knock-out mice. Furthermore, it has been shown that expression of LTα under the control of a rat insulin promoter induced a lymphoid-like tissue at the site of expression in transgenic mice, designated a tertiary lymphoid organ[128]. This lymphoid neogenesis was mediated by LTα through induction of several adhesion molecules as well as chemokines in endothelial cells[129].

Initial studies of a tumor-specific antibody-LTα fusion protein were performed in a xenograft melanoma model where this treatment was effective in eliminating pulmonary metastases[130]. Additional experiments in mice with different immune defects demonstrated a dependence of the therapeutic effect on B lymphocytes and NK cells. These results encouraged us to examine the effect of the antibody-LTα fusion protein in an autologous murine melanoma model and thereby to scrutinize the working mechanisms of directed LTα therapy.

We demonstrate that antibody-LTα fusion protein therapy is an effective treatment resulting in the eradication of established pulmonary metastases and subcutaneous tumors. Furthermore, our results suggest an improved T-cell immune response, which is most likely evoked by the induction of peripheral lymphoid tissue at the tumor site. In fact, the functional significance of this tertiary lymphoid tissue at tumor sites was confirmed by immunohistologic and electron microscopic analysis of endothelial/lymphocyte interactions as well as TCR clonotype mapping providing evidence for the induction of new T-cell clones among TIL, which were shown to specifically lyse melanoma cells and to produce IFNγ in response to a TRP-2 derived peptide.

Experimental Procedures

Animals.

C57BL/6J mice were obtained from Charles River Laboratories (Sulzfeld, Germany) at the age of 6 weeks. These animals were housed under specific pathogen-free

conditions and all experiments were performed according to National Institute of Health guidelines for care and use of laboratory animals.

Cell line, antibodies and fusion proteins

The murine melanoma cell line B78-D14 has been described previously[74]. B78-D14 was derived from B16 melanoma by transfection with genes coding for β-1,4-N-acetylgalactosaminyltransferase and α-2,8-sialyltransferase inducing a constitutive expression of the disialogangliosides GD2 and GD3. B78-D14 melanoma cells were maintained as monolayers in RPMI 1640 medium supplemented with 10% fetal calf serum, 2mM L-glutamine, 400 µg/ml G418 and 50 µg/ml Hygromycin B. Cells were passaged when sub-confluent.

The mouse/human chimeric antibody directed against GD2 (ch14.18) was constructed by joining the cDNA for the variable region of the murine 14.18 antibody with the constant regions of the human γ1 heavy chain and the κ light chain. From this, the ch14.18-LTα fusion protein was constructed by fusion of a synthetic sequence coding for human LTα - lacking the leader peptide - to the carboxyl end of the human Cγ1 gene[67]. The fused genes were inserted into the vector pdHL2 that encodes for the dihydrofolate reductase gene. The resulting expression plasmids were introduced into Sp2/0-Ag14 cells and selected in Dulbecco's modified Eagle's medium supplemented with 10% fetal bovine serum and 100 nM methotrexate. The fusion proteins were purified over a protein A-Sepharose affinity column.

All other antibodies used (anti-CD4, clone RM4-5; anti-CD8, clone 53-6.7; anti-CD45R/B220, clone RA3-6B2; anti CD62L, clone MEL-14; anti-PNAd, clone MECA-79 [Pharmingen, San Diego, CA]; anti-MHC-class II, clone M5/114 [ATCC, Rockville, MD] and anti-TCA-4; AF457 [R&D Systems, Wiesbaden, Germany]) are commercially available and have been described in detail by the manufacturer.

Experimental lung metastases

Single cell suspensions of 2.5 x 10^6 B78-D14 cells were injected into the lateral tail vein. To prevent pulmonary embolism caused by injection of tumor cells, mice were anaesthetized by halothane inhalation; tumor cells were suspended in 500 µl PBS containing 0.1% BSA and administered i.v. over a period of 60 s. After 7 days micrometastases were disseminated throughout the lungs invading the pulmonary

alveoli. At day 28, grossly visible metastases were present on the surface of the organ. At day 35 lungs were fixed in Bouin fixative and examined under a low magnification microscope for tumor foci on their surface. Sections from the lungs were stained with hematoxylin/eosin and examined histologically.

Subcutaneous tumors

Tumors were induced by s.c. injection of 2.5 x 10^6 B78-D14 melanoma cells in RPMI 1640, which resulted in tumors of approximately 40 µl volume within 14 days.

Treatment schedule

Soluble LTα or the ch14.18-LTα fusion protein were administered daily either by i.p. injections for pulmonary metastases or by i.v. injections for subcutaneous tumors. For pulmonary metastases therapy was maintained for 5, for subcutaneous tumors for 7 days. The applied dose is specified for each individual experiment in the result section. Murine anti-human antibodies directed against the chimeric fusion protein do occur but are likely to have only an impact on additional cycles of therapy.

Immunohistology

Frozen sections were fixed in cold acetone for 10 minutes followed by removal of endogenous peroxidase with 0.03% H_2O_2, and blocking of collagenous elements with 10% species-specific serum in 1% BSA/PBS. The biotinylated antibodies were then overlaid onto serial sections at predetermined dilutions (usually 20 µg/ml). Slides were incubated in a humid chamber for 30 minutes. The streptavidin-peroxidase complex (DAKO, Hamburg, Germany) was applied for 30 minutes after a wash with PBS. Following another wash, the substrate was added and the slides were incubated in the dark for 20 minutes. After a wash in PBS, the slides were counter stained, mounted and viewed using a Zeiss Axiophot microscope with photographic capabilities.

Electron microscopy

Tumors were dissected in 0.1 M of cold sodium cacodylate buffer (pH 7.2) containing 3% glutaraldehyde and 1.7 mM $CaCl_2$. After washing in the same buffer supplemented with 3% sucrose, the tissue was postfixed for 1 h on ice with 2% osmium tetroxide and 1% potassium ferrocyanide in sodium cacodylate buffer. Subsequently the tissue was washed first with cacodylate buffer, and then with 200

mM of sodium acetate buffer (pH 5.2). After staining for 1 h with 1% uranyl acetate in sodium acetate buffer, the sample was dehydrated in ethanol, after which it was infiltrated with and embedded in EMBED 812 (EM Sciences, Gibbstown, NJ). Thin sections were examined with a Leo 906 electron microscope (Leo Electron Microscopy Ltd, Oberkochen, Germany).

TCR clonotype mapping by denaturing gradient gel electrophoresis (DGGE)

DGGE analysis for clonotype mapping of the murine TCR BV regions 1-16 has been described[110]. Briefly, RNA was extracted using the Purescript Isolation Kit (Gentra Systems Inc. NC) and synthesis of cDNA was carried out using 1-3 μg of total RNA, oligo-dT and SuperScript II reverse transcriptase (Gibco-BRL, Gaithersburg, MD). cDNA was amplified using primers specific for BV families 1-16 and a constant region primer. Amplified sequences were evaluated using the computer program MELT87 that predicts the melting of a double stranded DNA molecule on the basis of its base composition[94]. These calculations indicated that the DNA molecules amplified were suited for denaturing gradient gel analysis by the attachment of a 50 bp GC-rich sequence to the 5′-end of the constant region primer. Amplifications were performed in a GeneAmp PCR System 9700 (Applied Biosystems, Weiterstadt, Germany) using previously described conditions. DGGE analysis was done in 6% polyacrylamide gels containing a gradient of urea and formamide from 20% to 80%. Electrophoresis was performed at 160 V for 4.5 hours in 1x TAE buffer at a constant temperature of 54°C.

ELISPOT assay

The ELISPOT assay described by Taguchi *et al.* was modified to detect $TRP2_{180-188}$ specific CD8 T cells [131]. First, 96-well filtration plates (Millipore) were coated with rat anti-mouse IFNγ antibody (clone R4–6A2, Pharmingen). Peptide-pulsed target cells were generated by incubating RMA-S cells, a TAP-deficient T cell lymphoma line derived from C57BL/6J mice (B6, H-2^b), with the appropriate concentration of peptide for 45 min at room temperature. $CD8^+$ T cells were isolated from PBL or TIL as described[76], kept in culture for 5 days in complete medium supplemented with 10 units/well of recombinant human IL2 (Chiron, Ratingen, Germany) before being added at indicated numbers to 5 x 10^4 target cells. After 24 hr, the plates were washed followed by incubation with biotinylated anti-mouse IFNγ antibody (clone XMG 1.2,

Pharmingen). Spots were developed using freshly prepared substrate buffer (0.3 mg/ml amino-9-ethyl-carbazole and 0.015% H_2O_2 in 0.1 M sodium acetate [pH 5]).

Results

Therapeutic effect of antibody-LTα fusion proteins on pulmonary metastases

Initially, we confirmed that the ch14.18-LTα fusion protein exerts direct cytotoxic effects against a number of tumor cell-lines *in vitro* as well as its antigen-specific binding to the disialoganglioside GD_2. Additionally, we established that the specific activity of the ch14.18-LTα fusion protein was three logs less than soluble LTα (sLTα) as measured by killing of L929 cells.

In subsequent series of experiments, we tested the *in vivo* anti-tumor effect of this fusion protein upon experimental pulmonary metastases of B16 melanoma cells, genetically engineered to express GD_2, in syngeneic C57BL/6J mice. The results of these experiments are summarized in Table 6. Initially, the effect of different doses of ch14.18-LTα fusion protein was established. Treatment was initiated on day 3 after tumor cell injection and maintained for 5 consecutive days. The lungs of control mice revealed a heavy metastatic burden when exposed to either 10ng of sLTα - which corresponds to more than 10 times the lytic activity of ch14.18-LTα - , to 32μg of the parental antibody ch14.18, or to 32μg of an antibody-LTα fusion protein directed to an irrelevant antigen, i.e., ch225-LTα recognizing the human EGF-receptor (Figures 15A, 15B and Table 6). In contrast, mice receiving 16μg of ch14.18-LTα fusion protein already showed a reduction in size and number of the metastatic foci indicated by lower lung weights. Moreover, at higher doses, i.e., 32μg, almost all animals (14 of 16) exhibited lungs completely free of metastases (Figure 15C), a finding which was confirmed by hematoxylin/eosin stained sections (Figure 15D). An increase in the dose of ch14.18-LTα to 64μg did not further improve the therapeutic effect. After establishing 32μg as the amount of ch14.18-LTα necessary for successful treatment of pulmonary metastases, we performed kinetic studies to investigate the effect of ch14.18-LTα at various stages of tumor progression. These experiments revealed that treatment with ch14.18-LTα could be delayed up to one week after induction of

pulmonary metastases, whilst still achieving a complete inhibition of tumor growth in 75% of the animals. However, the number of cured animals was reduced to 25% when therapy was started on day 10 and no therapeutic effect was observed at this dose level when therapy began on day 14. These observations indicate that either changes in the microenvironment of tumors, established for more than 10 days, or the mere size of the tumor burden at that stage of disease counteracted the effects induced by ch14.18-LTα.

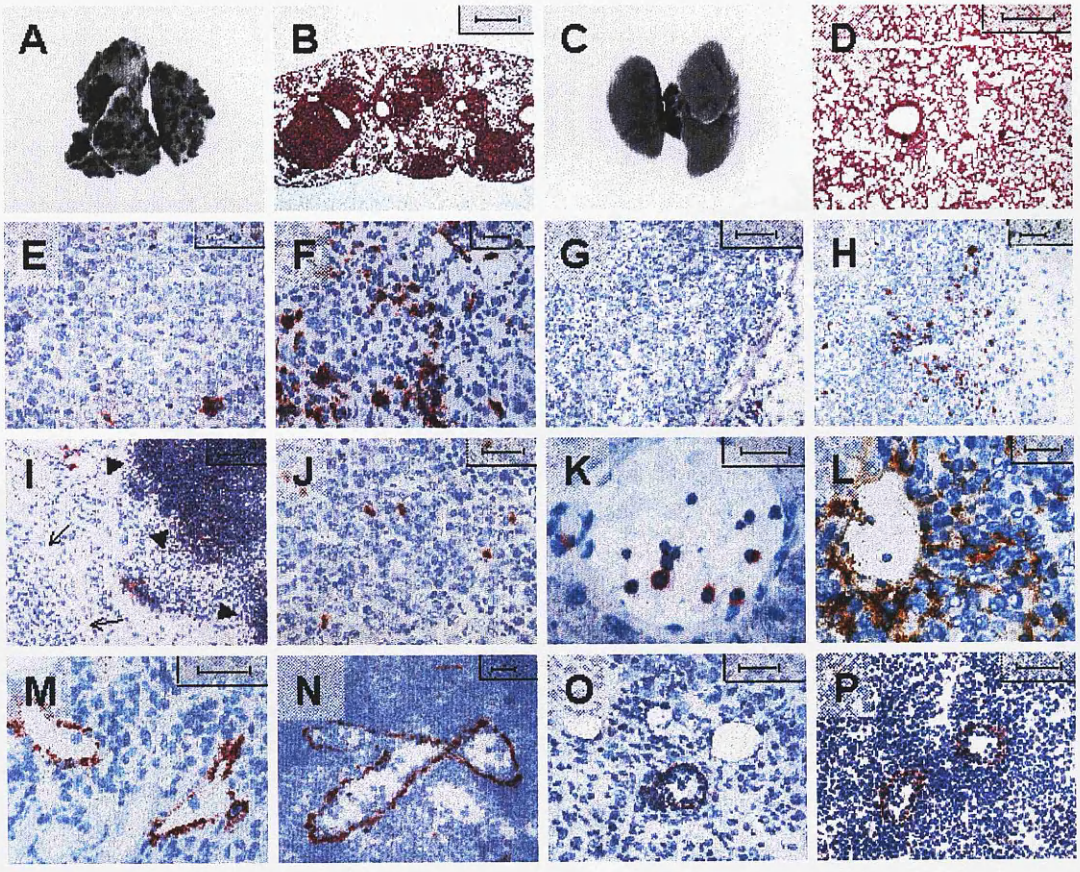

Figure 15. Macroscopic, histological and immunohistological characterization of tumor specimens. Pulmonary metastases (A–D) were induced by i.v., subcutaneous tumors (E–M and O) by s.c. injection of 2.5 x 10^6 B78-D14 cells. For pulmonary metastases treatment was administrated from day 3 through 7, consisting of 10ng sLTα (A and B) or 32µg ch14.18-LTα (C and D). For subcutaneous tumors, treatment was provided from day 14 through 21 with either 10ng of sLTα (E and G) or 64µg ch14.18-LTα (F, H, I–M and O). On day 35, lungs were removed, their macroscopic appearance documented (A and C) and sections subsequently subjected to hematoxylin/eosin staining (B and D). Subcutaneous tumors were excised on day 21 (E–I, K–M, and O) or day 28 (J) after tumor induction. In addition lymph nodes of normal mice (N and P) were obtained. Sections were subjected to staining with antibodies directed against CD4 (E and F), CD8 (G and H), CD45R/B220 (I), CD62L (J and K), MHC class II (L), PNAd (M and N) and TCA-4 (O and P). In (I) the B cell areas are indicated by closed arrowheads, the tumor by arrows. Scalebars: 25 µm (K), 100µm (G-I, and P), 200 µm (D), 400 µm (B) or 50 µm (all others).

In order to test whether the ch14.18-LTα fusion protein exerted its anti-tumor effect either directly or indirectly via the immune system, we examined the effect of ch14.18-LTα on pulmonary metastases in immune deficient C57BL/6J *scid/scid* mice lacking mature B and T lymphocytes. Treatment of these animals even at doses as high as 128μg had no therapeutic benefit (Table 6).

	TREATMENT			LUNG
MICE [a]	INITIATION [d] [b]	DOSE [c]	NO. OF FOCI [d]	WEIGHT [g]
C57BL/6J *scid/scid* [e]	3	10 ng sLTα	72, >200, >200, >200	0.58 ± 0.11
		32 μg ch14.18-LTα	91, >200, >200, >200	0.62 ± 0.16
		64 μg ch14.18-LTα	52, >200, >200, >200	0.55 ± 0.15
		128 μg ch14.18-LTα	65, 112, >200, >200	0.59 ± 0.13
C57BL/6J [f]	3	10 ng sLTα	79, 101, >200, >200, >200, >200, >200, >200	0.60 ± 0.13
	3	32 μg ch14.18	86, 134, 142, >200 >200, >200, >200, >200	0.54 ± 0.11
		32 μg ch225-LT	49, 71, 102, 148, >200, >200, >200, >200	0.48 ± 0.14
		16 μg ch14.18-LTα	0, 74, 89, >200, >200, >200, >200, >200	0.42 ± 0.11
		32 μg ch14.18-LTα	0, 0, 0, 0, 0, 0, 0, 8	0.22 ± 0.04
		64 μg ch14.18-LTα	0, 0, 0, 0, 0, 0, 0, 43	0.29 ± 0.08
	3	32 μg ch14.18-LTα	0, 0, 0, 0, 0, 0, 0, 13	0.30 ± 0.09
	7		0, 0, 0, 0, 0, 0, 16, 34	0.37 ± 0.10
	10		0, 0, 16, 37, 52, 102, >200, >200	0.53 ± 0.17
	14		87, 101, 113, >200, >200, >200, >200, >200	0.66 ± 0.10

Table 6. Effect of the ch14.18-LTα fusion protein on experimental lung metastases depending on immune status of mice, dose and time of initiation of therapy. [a]Experimental pulmonary metastases were induced in C57BL/6J *scid/scid* or normal mice by i.v. injection of 2.5 x 10^6 B78-D14 cells. [b]Treatment was initiated at the indicated days after tumor cell inoculation. [c]The therapy was administered by daily i.p. injections for 5 consecutive days. [d]Animals were sacrificed and the metastatic score evaluated 35 days after tumor induction. [e]Each group consisted of 4 animals. [f]Each group consisted of 8 animals.

Eradication of subcutaneous tumors

The second series of experiments evaluated the effect of ch14.18-LTα therapy on subcutaneous tumors. Macroscopic examination on day 28 revealed that treatment of animals with 64μg ch14.18-LTα from day 14 through 20 after tumor cell inoculation resulted in flattened and necrotic tumors (Figure 16A). Such an effect on subcutaneous tumors was never observed in control animals receiving comparable amounts of sLTα. This finding was confirmed by measurements of mean tumor volume over the course of the experiment where 3 groups of 8 mice each either

received 10ng sLTα, or 32μg and 64μg antibody-LTα, respectively. The mean tumor volume of the control group constantly increased over the time course of therapy (Figure 16B). In contrast, tumor growth in ch14.18-LTα treated animals leveled off after a few days of therapy. On day 21 the mean subcutaneous tumor volume of the ch14.18-LTα treated groups started to decrease and on day 28 the reduction in tumor volume between treated and control groups was significant ($p < 0.017$) at a dose of 64μg ch14.18-LTα as compared to 10ng sLTα. As was observed for pulmonary metastases, the effect of ch14.18-LTα on subcutaneous tumors was dose dependent.

It should be noted that the mean tumor volume started to increase again 9 days after therapy was stopped. Analysis of the individual tumor volumes, however, provided a more detailed picture. In fact, in 5 of 8 mice treated with 64μg ch14.18-LTα the tumor regressed completely in response to ch14.18-LTα administration and did not reoccur within the observation period of the experiment. The remaining 3 animals revealed tumor regressions persisting for several days before the tumor started to grow again (Figure 16C).

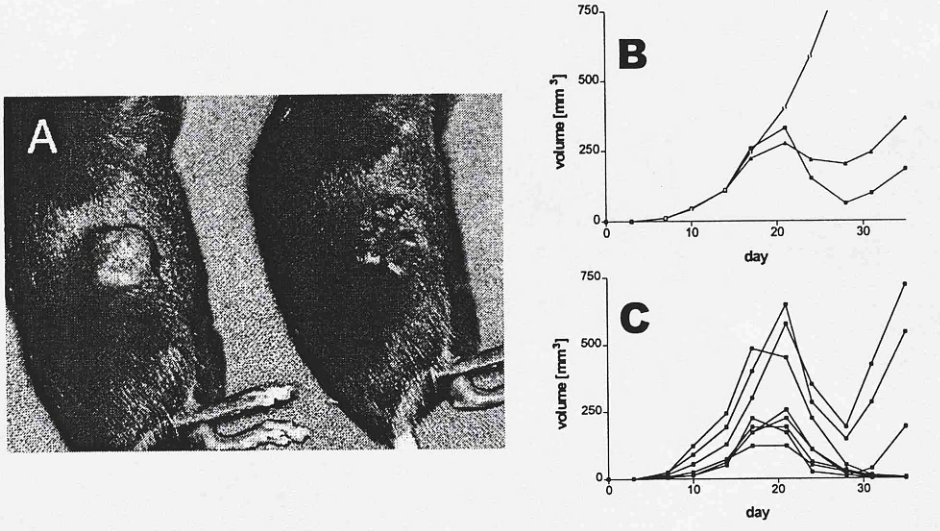

Figure 16. Effect of ch14.18-LTα therapy on subcutaneous tumors. C57BL/6J mice were injected s.c. with 2.5 x 10^6 B78-D14 melanoma cells. Therapy with either 32μg or 64μg ch14.18-LTα for 7 consecutive days was started at day 14 after tumor cell inoculation. Control animals received 10ng sLTα. Macroscopic appearance of the tumor on day 28 in an animal treated with 10ng sLTα (left) or 64μg ch14.18-LTα (right) (A). Mean tumor volumes of animals (n=8) receiving 10 ng sLTα (open circles), 32μg (closed triangles) a nd 64μg (closed squares) ch14.18-LTα, respectively (B). Individual tumor volumes of all animals treated with 64μg ch14.18-LTα are given separately (C).

Antibody-LT α fusion protein treatment prolongs survival

Survival studies were performed to determine whether the observed anti-tumor effect of the antibody-LTα fusion protein would translate into a prolonged survival, as previously shown for the antibody-IL2 fusion protein[76]. Each experimental group consisted of 6 animals. The control group was treated with 10ng sLTα, whereas the therapy group received 32μg ch14.18-LTα. Treatment was started 3 days after the induction of pulmonary metastases and was administered for 5 consecutive days. In the control group, death started to occur at day 47. In contrast, at day 62 when the last mouse of the control group had died, all of the ch14.18-LTα treated mice still remained alive. In fact, only one animal in the ch14.18-LTα treated group had died (day 85), prior to termination of the experiment on day 112 (Figure 17).

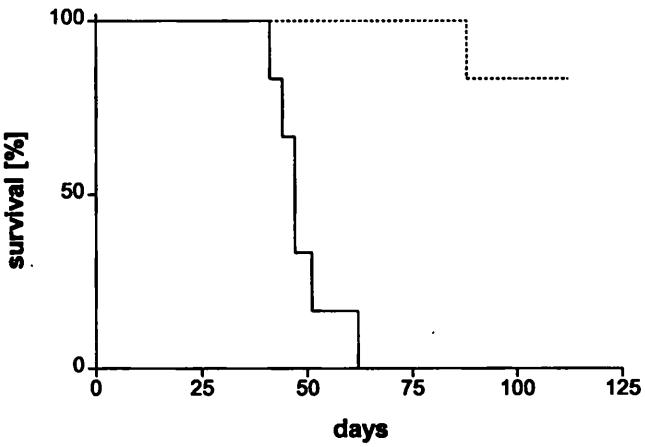

Figure 17. Kaplan-Meier plot demonstrating the effect of ch14.18-LTα fusion protein on the life span of C57BL/6J mice bearing pulmonary metastases. Each group consisted of six animals. The control group received 10ng of sLTα (solid line), the therapy group 32μg ch14.18-LTα fusion protein (dashed line) from days 3 through 7 after tumor inoculation. The experiment was terminated on day 112.

Infiltration of naive T cells into ch14.18-LTα treated tumors

Several experiments were performed to delineate the mechanisms involved in the observed anti-tumor effect of the antibody-LTα fusion protein. Knowing that ch14.18-LTα did not exert any anti-tumor effects in SCID mice, we started to characterize the TIL by immunohistology with an emphasis on T cells. When tumor sections were stained with antibodies against CD4 and CD8, few if any positive cells were observed in tumors obtained from control animals (Figures 15E and 15G). In contrast, ch14.18-LTα treated mice revealed a marked infiltration of $CD4^+$ T cells

throughout the tumor whereas $CD8^+$ T cells accumulated at the tumor periphery (Figures 15F and 15H). We performed flow cytometry to quantitate the difference in inflammatory infiltrates between control animals and ch14.18-LTα treated mice. To this end, in addition to the larger magnitude of inflammatory infiltrate, we found a much higher percentage of both $CD4^+$ and $CD8^+$ T cells in TIL from ch14.18-LTα treated mice, whereas in control animals the infiltrate was dominated by NK cells. Detection of B cells by immunohistochemistry with the CD45R/B220 monoclonal antibody revealed their presence in the tumor starting on day 21. Notably, 7 days later, B cells were compartmentalized in a lymphoid like pattern adjacent to the tumor in the majority of analyzed samples (Figure 15I). To determine whether the infiltrate resembled the cellular composition of a lymphoid tissue, we stained sections of the tumor with an antibody directed against MHC class II to identify antigen presenting cells. MHC class II^+ cells were found dispersed throughout the tumor and many displayed dendritic cell-like morphology (Figure 15L). We further stained for L-selectin since this molecule is expressed on a subset of lymphocytes' composed of mainly naive T cells for which it serves as a homing receptor to lymph nodes. Indeed, L-selectin$^+$ cells were found throughout the tumor (Figure 15J). Furthermore, at higher magnification, L-selectin$^+$ cells were detected in close contact with endothelial cells (Figure 15K), suggesting expression of L-selectin ligands on tumor vessels subsequent to ch14.18-LTα therapy. Tissues of control animals stained essentially negative for the antibodies tested.

HEV characteristics of blood vessels of ch14.18-LTα treated tumors

Migration of L-selectin$^+$ cells into tissue occurs through specialized blood vessels, the high endothelial venules (HEV), which normally are limited to lymph nodes and Peyer's patches. As described above, we obtained evidence that naive T cells may adhere and migrate through tumor blood vessels after therapy with ch14.18-LTα. Therefore, we stained for PNAd, an adhesion molecule restricted to HEV, which serves as ligand for L-selectin. About 30% of the vessels in tumors of ch14.18-LTα treated mice (Figure 15M) were stained in a similar pattern as HEV in lymph nodes (Figure 15N), the signal covering the internal surface of the vessel. A further mandatory step for migration of naive T cells through HEV is the activation of the lymphocytes via chemokine receptor CCR7 mediated by TCA-4 (Exodus-2, SLC,

6Ckine) present in the glycocalyx of HEV. Indeed, anti-TCA-4 antibodies revealed identical staining patterns for blood vessels in tumors of ch14.18-LTα treated mice and HEV in lymph nodes of normal mice (Figures 15O and 15P).

To confirm that some of the blood vessels penetrating the tumor were HEV, we performed electron microscopy studies. Blood vessels in all untreated tumors possessed the phenotype of peripheral capillaries with flat endothelia (Figure 18A). In contrast, tumors treated with antibody-LTα fusion protein harbored vessels with HEV morphology, i.e., endothelial cells of cuboidal shape (Figure 18B). In addition, we observed lymphocytes transmigrating out of the vessel lumen through the junctions between high endothelial cells (Figure 18C). At higher magnification, interactions between high endothelial venules and lymphocytes were observed to take place via microvilli (Figure 18D).

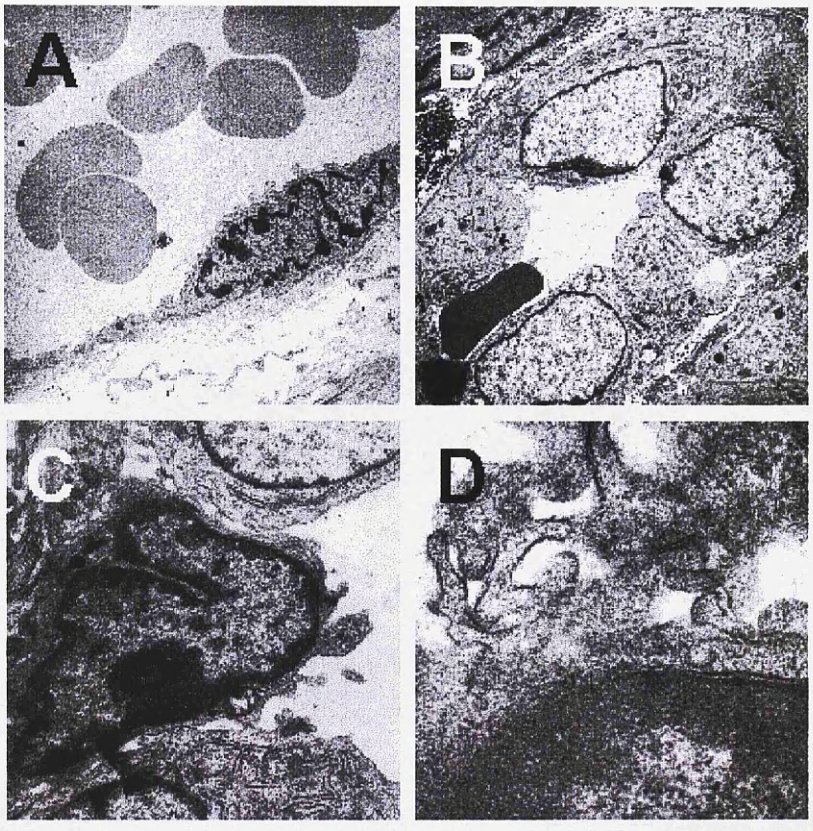

Figure 18. Electron microscopy of tumor blood vessels. Subcutaneous tumors were induced by s.c. injection of 2.5 x 10^6 B78-D14 cells in C57BL/6J mice. After 14 days animals received either 10ng of sLTα (A) or 64µg ch14.18-LTα (B–D) for 7 consecutive days. Endothelial cells in tumors of control animals appear flat (A, x3000), while those of the therapy group display a cuboidal shape (B, x3000). At higher magnification lymphocytes migrating through the vessel wall (C, x12000) and lymphocyte-endothelial interaction mediated by microvilli (D, x24000) are depicted.

Clonotype mapping reveals an increase in the number of T-cell clones during the course of therapy

Since we detected lymphoid like tissue, HEVs and the infiltration of $CD62L^+$ T cells in tumors subsequent to ch14.18-LTα administration, we tested the hypothesis that this treatment indeed alters the T-cell response against the tumor by priming, and subsequently expanding newly recruited cells. Such a change should translate into differences in the TCR repertoire among TIL. Consequently, we analyzed the relative expression of all TCR BV regions prior to and after therapy. This was done by semi-quantitative PCR with specific primers for each murine TCR BV family which demonstrated that treatment with ch14.18-LTα induced a relative over-expression of some TCR BV families differing between animals (data not shown). In addition to these differences in the relative over-expression we also observed a major increase in the magnitude of the inflammatory infiltrate in general, and in the number of infiltrating T cells, in particular (Figure 15F and 15H). However, since we observed previously that clonal expansion of T cells is not restricted to over-expressed TCR BV families, but also occurs in non over-expressed regions[111], we established the clonotype maps of BV regions 1-16 within the same tumor over the course of the experiment. The variable regions BV 17 and 18 were excluded since previous work indicated that these families comprise less than 0.5% each of the total TCR transcripts[110]. For these experiments, treatment was started 8 days after tumor cell inoculation for 7 consecutive days and biopsies of the same tumor were obtained on days 7, 14 and 21. Figure 19A depicts as an example the TCR clonotype map of BV regions 1-16, generated by RT-PCR/DGGE analysis of one ch14.18-LTα treated animal at day 21. Each distinct band represents an individual T-cell clone. In some BV regions, such as BV 5, only one or two clones were detected, whereas in others there were up to 7, e.g., BV 8. Comparative analysis of serial tumor biopsies demonstrated the dynamics in the TCR repertoire of TIL (Figure 19B). In fact, not only the persistence and the induction of T cell clonotypes over the course of the experiment was observed, but also the disappearance of clonotypes present in TIL prior to therapy. To illustrate the changes in the occurrence of clones, we provide the ratios of the number of clones on day 14 and day 21 compared to day 7 (Figures 190C and 19D). For ch14.18-LTα treated animals TCR clonotype mapping revealed an increase in the number of T-cell clones among TIL. These clones covered the majority

of BV regions. However, the increase in the number of T-cell clones varied between the BV regions, ranging from 1 (BV 2) to up to 7 (BV 15). In contrast, although the occurrence of T-cell clones in control animals was also diverse, there was no general increase in the number of T-cell clonotypes.

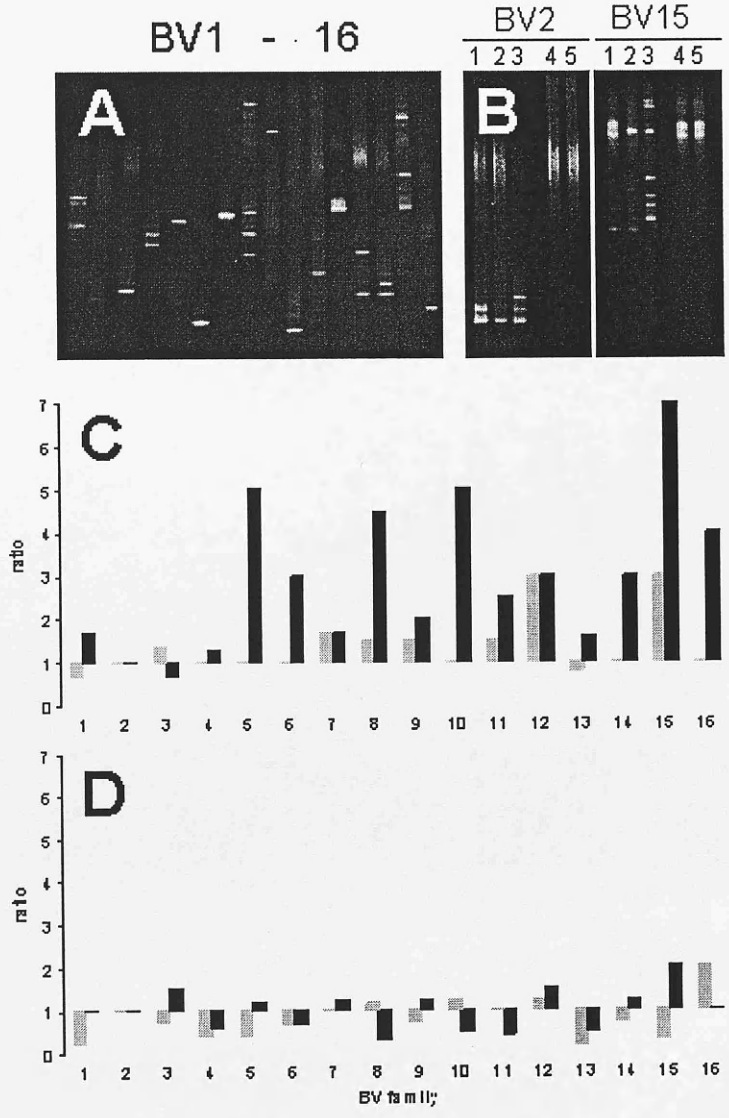

Figure 19. TCR repertoire changes of TIL over the course of therapy. Subcutaneous tumors were induced by s.c. injection of 2.5 x 10^6 B78-D14 cells in C57BL/6J mice. Treatment was administered from day 8–14 in form of 64µg ch14.18-LTα (A-C) or 10ng of sLTα (D). Biopsies of tumors were taken 7, 14 and 21 days after tumor cell inoculation and analyzed by TCR clonotype mapping. Example of a TCR clonotype map of TIL on day 21 of a ch14.18-LTα treated tumor covering BV regions 1-16 (A). Comparative TCR analysis for BV families 2 and 15. Samples were obtained from the same tumor localized on the right flank on day 7 (lane 1), day 14 (lane 2) and day 21 (lane 3) as well as by excision of the inguinal lymph nodes on day 21 (left and right, lanes 4 and 5, respectively) (B). The variation in number of T-cell clones for BV regions 1-16 is given as the ratio of the number of clones on day 14 (gray) or 21 (black) to the number of clones on day 7 for ch14.18-LTα (C) and sLTα (D) treated animals.

In addition to tumor biopsies, the draining lymph nodes were also analyzed at day 21. Even when all TCR BV regions were taken into account in these lymph nodes, RT-PCR/DGGE clonotype mapping showed at most a few faint bands (Figure 19B). This finding implies that the T-cell population in the lymph nodes is either largely polyclonal or that the clonal expansion is below the detection level of the applied method. RT-PCR/DGGE clonotype mapping, however, is generally able to detect a T-cell clone in a mixed population at a fraction of 0.1%[32]. Besides, in rare cases where T-cell clones were present, these never matched with those clonotypes found in the tumor.

Induction of a specific T-cell response by ch14.18-LTα therapy

The immunological changes induced by ch14.18-LTα therapy, including an altered inflammatory infiltrate, infiltration of $CD62L^+$ T cells into tumors as well as the clonal expansion of certain TCR BV specifities subsequent to ch14.18-LTα therapy, prompted us to examine if these would indeed translate into a functional active and specific T cell response. This was done by cytotoxicity and ELISPOT assays. The cytotoxicity assays revealed that PBL or TIL obtained from ch14.18-LTα treated mice after therapy were at least twice as efficient in killing B78-D14 melanoma cells compared to lymphocytes derived from control animals (Figures 20A and 20B). The specific killing of B78-D14 was MHC class I restricted as it could be inhibited by the presence of a surplus of C3H antibody directed against the MHC I molecules $H2\text{-}K^b$and $H2\text{-}D^b$.

Thereafter we analyzed the ability of the $CD8^+$ T cells among PBL and TIL to react against a defined tumor-associated antigen, i.e., TRP-2, a melanocyte differentiation antigen. This reactivity was measured in the ELISPOT assay by the production of IFN-γ induced in response to RMA-S cells pulsed with the $TRP\text{-}2_{180\text{-}188}$ epitope. Reactivity against this TRP-2 peptide epitope was present in both, control animals and mice treated with ch14.18-LTα. This observation indicates that the presence of B78-D14 melanoma alone induces a detectable cellular immune response, a notion substantiated by the presence of clonally expanded T cells in untreated tumors [132]. The amount of reactive T cells, however, was more than three times higher among samples derived from animals treated with ch14.18-LTα than those of control animals receiving 10ng sLTα. In PBL from ch14.18-LTα treated mice we detected an average

of 208 TRP-2 peptide specific spots per 10^5 $CD8^+$ cells. In contrast, for sLTα treated control animals this number was only 36 (Figure 20C). The specific reactivity of $CD8^+$ cells obtained from TIL was more than one log higher than those from PBL. Thus, the ELIPOT assay performed with only 10^4 $CD8^+$ T cells revealed 293 TRP-$2_{180\text{-}188}$ peptide specific spots for ch14.18-LTα treated and 91 for control animals (Figure 20D). The background reactivity against unpulsed RMA-S cells in the assays performed with TIL was rather high and is most likely due to remaining T cell epitopes derived from contaminating tumor cells in the T-cell preparation.

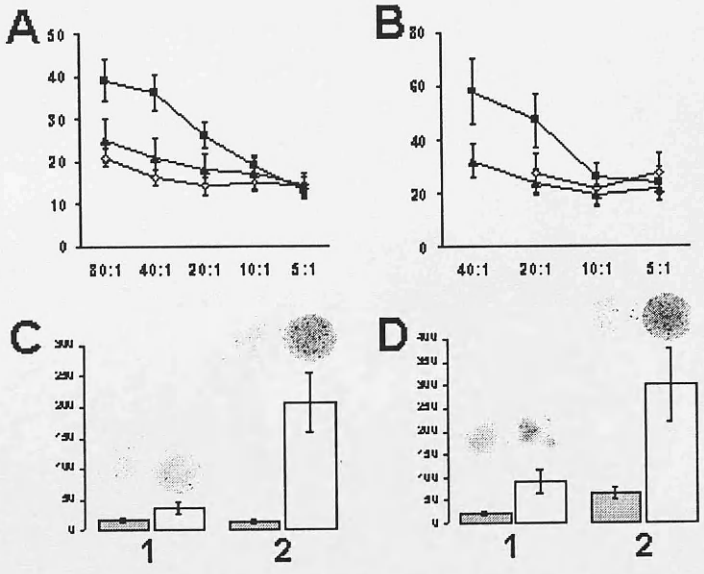

Figure 20. Presence of specific cytotoxic and IFN-γ-producing T cells in PBL and TIL. The percentage of lysed B78-D14 melanoma cells by PBL (A) or TIL (B) was measured at different effector to target ratios in a 51Cr release assay as previously described[76]. Effector cells were obtained subsequent to treatment with either 10ng sLTα (open diamonds) or 64μg ch14.18-LTα (closed squares). For cells obtained from ch14.18-LTα treated animals the assay was also performed in the presence of the anti-H2-Kb/H2-Db monoclonal antibody C3H (closed triangles). In the ELISPOT assay either 10^5 CD8+ T cells isolated from PBL (C) or 10^4 CD8+ cells from TIL (D) obtained after treatment with either 10ng sLTα (1) or 64μg ch14.18-LTα (2) were analyzed after 5 days of *in vitro* culture for their reactivity against the TRP-$2_{180\text{-}188}$ epitope. Each spot represents an IFN-γ-producing cell. Graphs depict the quantification of reactive cells; gray columns represent the average number of IFN-γ-producing cells in the absence of peptide, white bars in the presence of the TRP-$2_{180\text{-}188}$ peptide.

Discussion

We previously reported the therapeutic effect of a tumor-specific antibody-LTα fusion protein in a xenograft tumor model[130]. Here, we demonstrate the efficacy of this immunocytokine against B16 melanoma, leading to the eradication of both pulmonary metastases and subcutaneous tumors in a syngeneic tumor model. In the xenograft model the effect of the antibody-LTα fusion protein was found to be dependent on B and NK cells. However, in xenograft tumor models multiple confounding factors may obscure the actual working mechanism of immunomodulatory agents[133]. Thus, a syngeneic model was required to delineate such mechanisms in more detail. To this end, we observed a marked infiltrate of T lymphocytes subsequent to therapy with ch14.18-LTα in the syngeneic model. Additional lines of evidence indicating that T cells are the principal effector cells induced by targeted-LTα therapy included (i) the lack of any therapeutic effect of the ch14.18-LTα fusion protein in SCID mice, (ii) the presence of MHC class I restricted B78-D14 specific cytotoxic T cells, as well as (iii) the detection of TRP-$2_{180\text{-}188}$ reactive IFN-γ-producing cells in PBL and TIL. The latter observation is of particular interest since it rules out the possibility that the induced T-cell response is only directed against the target antigen of the ch14.18-LTα fusion protein, i.e., the disialoganglioside GD2. The difference in recruitment of effector cells in the xenograft and syngeneic tumor models are likely due to a xenogeneic response in the former[134].

Immunohistological staining did not only reveal a marked T-cell infiltrate, but also indicated the arrangement of T and B cells in a lymphoid like pattern adjacent to and within the tumor. This observation prompted us to test the hypothesis that targeted LTα therapy may induce the neogenesis of lymphoid tissue at the tumor site allowing the recruitment of naive T cells. In this regard, L-selectin can be used as a marker for naive T cells which serves them as a homing receptor to HEV in secondary lymphoid organs via its interaction with the adhesion molecule PNAd[135]. Subsequent to ch14.18-LTα treatment, L-selectin$^+$ cells were found dispersed all over the tumor as well as being in direct contact with endothelial cells. In addition, many of the vessels

within the tumor expressed PNAd which is normally restricted to HEV. Moreover, the lumen of the vessels was covered with TCA-4 (Exodus-2, SLC, 6Ckine), another molecule largely confined to HEV. TCA-4 reacts with the CCR7 chemokine receptor on T cells and upregulates LFA-1[136]; this activation is mandatory for the firm arrest of T cells after their initial rolling during the process of extravasation of naive T cells from the blood stream into lymphoid tissues[136,137]. Further evidence was provided by electron microscopy studies which clearly confirmed the HEV morphology of ~30% of blood vessels in the tumor. Taken together, these findings imply that naive T cells migrated from blood into the tumor microenvironment subsequent to ch14.18-LTα therapy. These observations are consistent with a report by Kratz *et al.* stating that the basis of the chronic inflammation caused by lymphotoxin is lymphoid neogenesis[128]. These investigators demonstrated that the structures generated by the transgenic expression of LTα under the control of a rat insulin promoter resembled lymph nodes with regard to cellular composition, delineated T- and B-cell areas, primary and secondary follicles, and characteristic morphologic as well as antigenic features of HEV. Thus, it appears likely that treatment with the antibody-LTα fusion protein induces a lymphoid-like tissue at the site of LTα accumulation in the tumor. It has previously been shown that the presence of inflammation induced by transgenic expression of LTα is not dependent on LTβ expression, although its cellular composition is influenced by this cytokine[121,138]. Since sLTα can be generated by the cleavage of a plasmin site in the ch14.18-LTα fusion protein, $LT\alpha_1\beta_2$ complexes may form at the tumor site subsequent to ch14.18-LTα therapy. Therefore, future experiments in LTβ knock-out mice are planned to address the question whether $LT\alpha_1\beta_2$ complexes are involved in the therapeutic effect of ch14.18-LTα.

Lymphoid tissue is the prime environment for initiating T-cell responses[139], as naive T cells are only able to encounter antigen in such tissues[140]. Hence, the question whether the lymphoid tissue induced by antibody-LTα fusion protein therapy would promote the clonal expansion of infiltrating T cells was of pertinent importance. To this end, analysis of the T-cell clonality by RT-PCR/DGGE clonotype mapping revealed an increase in the number of clones over the course of treatment. This was not observed in control animals. Comparative clonotype analysis demonstrated that this increase in the number of clonally expanded T cells is due to both the persistence as well as the occurrence of new clones. It should be noted, that the clonotypic

composition of TIL in untreated tumors was not static either, but neither quantitative nor qualitative analysis could divulge a significant change during the course of the experiment. It is not possible to establish with certainty whether clones emerging during the course of treatment are truly "new" or represent the amplification of pre-existing clones which were previously below the level of detection. However, large numbers of polyclonal transcripts hamper the detection of a T-cell clonotype leaving a clone more likely to be left undetected in treated tumors which were characterized by a brisk infiltration of T cells. Conversely, even minor expansions are readily detected in untreated tumors showing a limited infiltration of polyclonal T cells[132]. Furthermore, T-cell clones detected in lymph nodes draining the tumor were never detected recurrently in the tumor. This observation together with the immunohistological and electron microscopical evidence for the occurrence of HEV and interaction of lymphocytes with the endothelia provides strong presumptive evidence that the therapy-induced tertiary lymphoid organ is functional and allows for priming of naive lymphocytes at the tumor site. Thus, the effects of antibody-LTα therapy differ substantially from the effects induced by the antibody-IL2 fusion protein therapy which only boosted a pre-existing T-cell response[110]. Nevertheless, for both therapies the eradication of B78-D14 tumors is mediated via clonally expanded tumor-specific T cells rather than a polyclonal, non-specific T-cell population. As in the case of antibody-IL2 treatment, targeted-LTα therapy is closely linked to tumor regression, raising the question whether the emergence of new clones is directly related to the treatment or a secondary phenomenon reflecting the immunological rejection. However, separate analysis of regressive and progressive parts of human melanoma lesions did not reveal differences in the numbers of clonotypic T cells indicating that immunological rejection is not coupled to the presence of higher numbers of clonotypic T cells[42]. Moreover the last tumor samples for TCR clonotype mapping were obtained at day 21, a time when the progressive growth of the tumor just started to level off; thus, the presence of clonally expanded T cells is at least not caused by tumor necrosis but rather is a therapy-induced immune response.

The finding that almost no clones were discovered in the draining lymph nodes further suggests that priming occurred in the tumor and not in the lymph node. Furthermore, even when we were able to detect an occasional clonal expansion within these lymph nodes, none of these were identical to those present in the tumor (Figure

19B). Our results agree with those of a recent report by Shrikant and Mescher who demonstrated that transferred, transgenic cytotoxic T lymphocytes only expand at the site of antigen[141]. This holds also true for viral infections where virus-specific $CD8^+$ T cells are only predominating the T-cell pool at sites of viral replication[142]. In humans, we were able to detect identical T-cell clonotypes in the primary tumor and in the sentinel lymph node (unpublished results) whereas in the present murine model this was not possible. While most human melanoma tumor cells have the capacity to disseminate and to cause metastases, the B78-D14 cell line used in the present murine model was derived from a B16 subline which does not spontaneously metastasize [143]. Therefore, melanoma cells present in the sentinel lymph node of patients may cause primed T cells to expand, whereas in our mouse model no tumor cells were found in the lymph node.

The induction of lymphoid tissues at the tumor site should provide the means to overcome two of the major obstacles to prolonged immune responses to weakly immunogenic tumors, i.e., clonal anergy and clonal exhaustion[144]. It may avoid T cell anergy by provision of a suitable cytokine and cellular environment together with a high antigen load. Clonal exhaustion may be prevented as new, naive T cells can be continuously primed. The function and specificity of the resulting T-cell response was conclusively shown. Nevertheless, the recurrent observation that even high doses of ch14.18-LTα fusion protein did not cure all animals, may be due to differences in the quality and/or quantity of clonal T-cell responses. The magnitude of a T-cell response is at least theoretically dependent on the frequency of suitable T-cell precursors[145]. Animals which can not be cured may possess a lower frequency of T-cell precursors or the induced T-cell response may be characterized by insufficient antigen binding specificity. In addition, other immune escape mechanisms have to be taken into consideration[146].

Antibody-LTα dependent lymphoid neogenesis may improve anti-tumor responses in several ways. The possibility that naive T cells can be primed next to the tumor by a tertiary lymphoid organ should lead to (i) a larger number of primed tumor-specific T cells since tumor-specific antigens predominate[142], (ii) a reduction in the time between priming and expansion as well as the risk of primed T cells not reaching the tumor and (iii) ongoing T-cell responses that react more readily and quickly to changes in the antigen expression profile of the tumor. In addition, it may stop lymphocytes from

leaving the tumor microenvironment which is beneficial, since it has been suggested that effective immunotherapy depends more on sustaining an immune response at the appropriate location than on its initiation[141]. Thus, the effectiveness of tumor-targeted LTα therapy appears to be due to direct clonal expansion of tumor-specific T cells through the formation of peritumoral lymphoid tissue.

Concluding Remarks and Perspectives

By RT-PCR/DGGE based *in situ* TCR clonotypic mapping the T cell responses to melanoma was scrutinized by analyzing metastatic lesions obtained from mice receiving different forms of targeted immunotherapy for the presence of clonotypic T cells. The first revelation from this study was the presence of multiple (from 40 to more than 60) clonotypic T cells in all lesions which were derived from T-cell receptor β-variable regions expressed both at high and low levels. Secondly, comparison of T-cell clonotypes present in the different lesions from the same animal demonstrated that, in general, individual clonotypes were exclusively detected in only one lesion. Hence, anti-melanoma T-cell responses are much more heterogeneous than previously appraised and accommodate a predominance of strictly localized T-cell clonotypes. In addition, the overexpression of certain TCR β-variable regions, as well as the clonal expansion of individual T-cells among tumor infiltrating lymphocytes subsequent to targeted-IL2 administration was demonstrated. However, clonally expanded T-cells were also detectable prior to therapy, suggesting that IL2 acts as a modulator rather than an inducer of an anti-tumor T-cell responses. Further studies in the same tumor model indicated IL2 enables the redistribution of clonally expanded therapeutic T cells.

The second cytokine analyzed for its *in situ* immune modulating capacities was LT-α. The eradication of established melanoma metastases caused by LT-α was accompanied by neogenesis of a lymphoid-like tissue at the tumor site containing L-selectin$^+$ T cells, MHC class II$^+$-APCs and lymph node-like B and T cell areas. This peritumoral-lymphoid tissue showed a marked clonal expansion of certain TCR specificities over the course of LT-α therapy, suggesting that naïve T cells were recruited, as well as primed and expanded at the tumor site. This observation is significant, since the induction of lymphoid tissues at the tumor site provides the means to overcome two of the major obstacles of prolonged immune responses to weakly immunogenic tumors, namely clonal anergy and clonal exhaustion of T cells. Thus, antibody-LT-α-dependent lymphoid neogenesis may improve anti-tumor responses by i) a greater number of tumor-specific T cells; ii) reducing the time interval between priming and expansion and the risk of primed T cells not reaching

the tumor; and iii) facilitating ongoing T cell responses to react more quickly to changes in antigen expression by the tumor.

In conclusion, *in situ* analysis of cellular immune responses to solid tumors has proven to be a valuable tool to monitor immune modulating therapies. This value becomes particular obvious in several clinical reports demonstrating a lack of correlation between T-cell reactivity measured in peripheral blood and the course of neoplastic disease. These findings emphasize the need to analyze not only the peripheral blood but also the tumor site as well as secondary and tertiary lymphatic tissues for the presence and activation status of tumor-reactive T cells in order to obtain more adequate insights into immune responses to solid tumors (Figure 21).

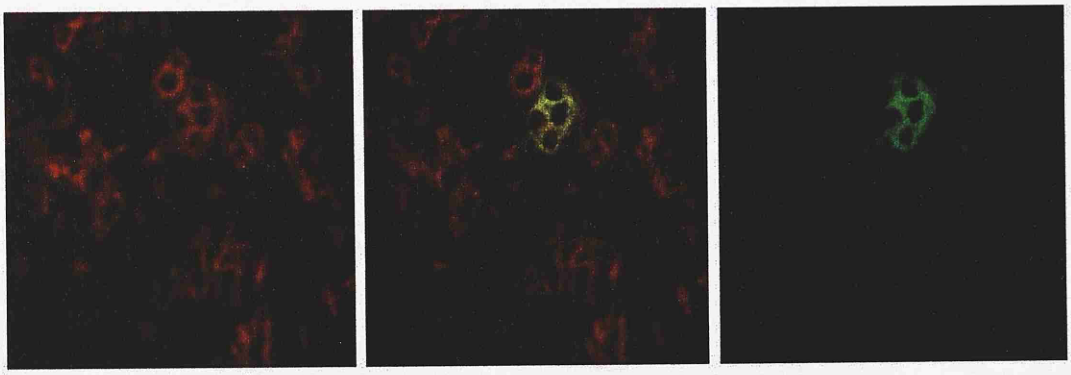

Figure 21. In situ detection of tumor-reactive CTL in a sentinel lymphnode from a stage III melanoma patient. Confocal laser scanning microscopy was used to detect CTL reacting with an Cy3-conjugated anti-CD8 antibody (red chanel) and/or an FITC-conjugated multimeric MHC/peptide construct.

References

1. Tada T. The immune system as a supersystem. Annu Rev Immunol 1997;15:1-13.
2. Janeway CA, Jr., Medzhitov R. Introduction: the role of innate immunity in the adaptive immune response. Semin Immunol 1998 Oct;10(5):349-50.
3. Dutton RW, Bradley LM, Swain SL. T cell memory. Annu Rev Immunol 1998;16:201-23.
4. Nemazee D. Receptor selection in B and T lymphocytes. Annu Rev Immunol 2000;18:19-51.
5. Fu YX, Chaplin DD. Development and maturation of secondary lymphoid tissues. Annu Rev Immunol 1999;17:399-433.
6. Moss PA, Rosenberg WM, Bell JI. The human T cell receptor in health and disease. Annu Rev Immunol 1992;10:71-96.
7. Banchereau J, Briere F, Caux C, Davoust J, Lebecque S, Liu YJ, Pulendran B, Palucka K. Immunobiology of dendritic cells. Annu Rev Immunol 2000;18:767-811.
8. McDevitt HO. Discovering the role of the major histocompatibility complex in the immune response. Annu Rev Immunol 2000;18:1-17.
9. Carosella ED, Rouas-Freiss N, Paul P, Dausset J. HLA-G: a tolerance molecule from the major histocompatibility complex. Immunol Today 1999 Feb;20(2):60-2.
10. Engelhard VH. Structure of peptides associated with class I and class II MHC molecules. Annu Rev Immunol 1994;12:181-207.
11. Rock KL, Goldberg AL. Degradation of cell proteins and the generation of MHC class I-presented peptides. Annu Rev Immunol 1999;17:739-79.
12. Watts C. Capture and processing of exogenous antigens for presentation on MHC molecules. Annu Rev Immunol 1997;15:821-50.
13. Fischer WH, thor Straten P, Terheyden P, Becker JC. Function and dysfunction of CD4(+) T cells in the immune response to melanoma. Cancer Immunol Immunother 1999 Oct;48(7):363-70.
14. Elliott T. How does TAP associate with MHC class I molecules? Immunol Today 1997 Aug;18(8):375-9.
15. Alfonso C, Karlsson L. Nonclassical MHC class II molecules. Annu Rev Immunol 2000;18:113-42.
16. Garcia KC, Teyton L, Wilson IA. Structural basis of T cell recognition. Annu Rev Immunol 1999;17:369-97.
17. Frank SJ, Engel I, Rutledge TM, Letourneur F. Structure/function analysis of the invariant subunits of the T cell antigen receptor. Semin Immunol 1991 Sep;3(5):299-311.
18. Zhang W, Samelson LE. The role of membrane-associated adaptors in T cell receptor signalling. Semin Immunol 2000 Feb;12(1):35-41.
19. Livak F, Tourigny M, Schatz DG, Petrie HT. Characterization of TCR gene rearrangements during adult murine T cell development. J Immunol 1999 Mar;162(5):2575-80.
20. Arden B, Clark SP, Kabelitz D, Mak TW. Mouse T-cell receptor variable gene segment families. Immunogenetics 1995;42(6):501-30.
21. McBlane F, Boyes J. Stimulation of V(D)J recombination by histone acetylation. Curr Biol 2000 Apr;10(8):483-6.
22. Gascoigne NR, Alam SM. Allelic exclusion of the T cell receptor alpha-chain: developmental regulation of a post-translational event. Semin Immunol 1999 Oct;11(5):337-47.
23. Candeias S, Muegge K, Durum SK. Junctional diversity in signal joints from T cell receptor beta and delta loci via terminal deoxynucleotidyl transferase and exonucleolytic activity. J Exp Med 1996 Nov;184(5):1919-26.

24. Matsui K, Boniface JJ, Reay PA, Schild H, Fazekas dS, Davis MM. Low affinity interaction of peptide-MHC complexes with T cell receptors. Science 1991 Dec;254(5039):1788-91.

25. Gunzer M, Schafer A, Borgmann S, Grabbe S, Zanker KS, Brocker EB, Kampgen E, Friedl P. Antigen presentation in extracellular matrix: interactions of T cells with dendritic cells are dynamic, short lived, and sequential [In Process Citation]. Immunity 2000 Sep;13(3):323-32.

26. Valitutti S, Muller S, Cella M, Padovan E, Lanzavecchia A. Serial triggering of many T-cell receptors by a few peptide-MHC complexes. Nature 1995 May;375(6527):148-51.

27. Viola A, Lanzavecchia A. T cell activation determined by T cell receptor number and tunable thresholds . Science 1996 Jul;273(5271):104-6.

28. Schraven B, Marie-Cardine A, Hubener C, Bruyns E, Ding I. Integration of receptor-mediated signals in T cells by transmembrane adaptor proteins. Immunol Today 1999 Oct;20(10):431-4.

29. Viola A, Schroeder S, Sakakibara Y, Lanzavecchia A. T lymphocyte costimulation mediated by reorganization of membrane microdomains . Science 1999 Jan;283(5402):680-2.

30. Becker JC, Brabletz T, Kirchner T, Conrad CT, Brocker EB, Reisfeld RA. Negative transcriptional regulation in anergic T cells. Proc Natl Acad Sci U S A 1995 Mar;92(6):2375-8.

31. Lanzavecchia A, Sallusto F. From synapses to immunological memory: the role of sustained T cell stimulation. Curr Opin Immunol 2000 Feb;12(1):92-8.

32. thor Straten P, Barfoed A, Seremet T, Saeterdal I, Zeuthen J, Guldberg P. Detection and characterization of alpha-beta-T-cell clonality by denaturing gradient gel electrophoresis (DGGE). Biotechniques 1998 Aug;25(2):244-50.

33. Nitta T, Oksenberg JR, Rao NA, Steinman L. Predominant expression of T cell receptor V alpha 7 in tumor- infiltrating lymphocytes of uveal melanoma. Science 1990 Aug;249(4969):672-4.

34. Pannetier C, Even J, Kourilsky P. T-cell repertoire diversity and clonal expansions in normal and clinical samples. Immunol Today 1995 Apr;16(4):176-81.

35. Guldberg P, Guttler F. A simple method for identification of point mutations using denaturing gradient gel electrophoresis. Nucleic Acids Res 1993 May;21(9):2261-2.

36. Koh HK. Cutaneous melanoma. N Engl J Med 1991 Jul;325(3):171-82.

37. Balch CM, Buzaid AC, Atkins MB, Cascinelli N, Coit DG, Fleming ID, Houghton A, Jr., Kirkwood JM, Mihm MF, Morton DL, Reintgen D, Ross MI, Sober A, Soong SJ, Thompson JA, Thompson JF, Gershenwald JE, McMasters KM. A new American Joint Committee on Cancer staging system for cutaneous melanoma. Cancer 2000 Mar;88(6):1484-91.

38. Cochran AJ, Balda BR, Starz H, Bachter D, Krag DN, Cruse CW, Pijpers R, Morton DL. The Augsburg Consensus. Techniques of lymphatic mapping, sentinel lymphadenectomy, and completion lymphadenectomy in cutaneous malignancies. Cancer 2000 Jul;89(2):236-41.

39. Becker JC, thor Straten P. T-cell clonality in immune responses. Immunol Today 2000 Feb;21(2):107.

40. Romero P, Dunbar PR, Valmori D, Pittet M, Ogg GS, Rimoldi D, Chen JL, Lienard D, Cerottini JC, Cerundolo V. Ex vivo staining of metastatic lymph nodes by class I major histocompatibility complex tetramers reveals high numbers of antigen- experienced tumor-specific cytolytic T lymphocytes. J Exp Med 1998 Nov;188(9):1641-50.

41. Becker JC, Terheyden P, Brocker EB. Molecular basis of T-cell dysfunction in melanoma. Melanoma Res 1997 Aug;7 Suppl 2:S51-S57.

42. thor Straten P, Becker JC, Seremet T, Brocker EB, Zeuthen J. Clonal T cell responses in tumor infiltrating lymphocytes from both regressive and progressive regions of primary human malignant melanoma. J Clin Invest 1996 Jul;98(2):279-84.

43. Brinckerhoff LH, Thompson LW, Slingluff CL, Jr. Melanoma vaccines. Curr Opin Oncol 2000 Mar;12(2):163-73.

44. Nielsen MB, Marincola FM. Melanoma vaccines: the paradox of T cell activation without clinical response. Cancer Chemother Pharmacol 2000;46 Suppl:S62-S66.

45. thor Straten P, Becker JC, Guldberg P, Zeuthen J. In situ T cells in melanoma. Cancer Immunol Immunother 1999 Oct;48(7):386-95.

46. Lazar-Molnar E, Hegyesi H, Toth S, Falus A. Autocrine and paracrine regulation by cytokines and growth factors in melanoma. Cytokine 2000 Jun;12(6):547-54.

47. Keilholz U, Eggermont AM. The emerging role of cytokines in the treatment of advanced melanoma. For the EORTC Melanoma Cooperative Group. Oncology 2000 Feb;58(2):89-95.

48. Atkins MB, Lotze MT, Dutcher JP, Fisher RI, Weiss G, Margolin K, Abrams J, Sznol M, Parkinson D, Hawkins M, Paradise C, Kunkel L, Rosenberg SA. High-dose recombinant interleukin 2 therapy for patients with metastatic melanoma: analysis of 270 patients treated between 1985 and 1993. J Clin Oncol 1999 Jul;17(7):2105-16.

49. Lode HN, Xiang R, Becker JC, Gillies SD, Reisfeld RA. Immunocytokines: a promising approach to cancer immunotherapy. Pharmacol Ther 1998 Dec;80(3):277-92.

50. Ehrlich P. The Coonian lecture: On immunity. Proc.R.Soc.London 66, 423-437. 1900. Ref Type: Journal (Full)

51. Milstein C, Brownlee GG, Cartwright EM, Jarvis JM, Proudfoot NJ. Sequence analysis of immunoglobulin light chain messenger RNA. Nature 1974 Nov;252(5482):354-9.

52. Maloney DG, Grillo-Lopez AJ, Bodkin DJ, White CA, Liles TM, Royston I, Varns C, Rosenberg J, Levy R. IDEC-C2B8: results of a phase I multiple-dose trial in patients with relapsed non-Hodgkin's lymphoma. J Clin Oncol 1997 Oct;15(10):3266-74.

53. Cheresh DA, Honsik CJ, Staffileno LK, Jung G, Reisfeld RA. Disialoganglioside GD3 on human melanoma serves as a relevant target antigen for monoclonal antibody-mediated tumor cytolysis. Proc Natl Acad Sci U S A 1985 Aug;82(15):5155-9.

54. Gruber R, Holz E, Riethmuller G. Monoclonal antibodies in cancer therapy. Springer Semin Immunopathol 1996;18(2):243-51.

55. Riethmuller G, Holz E, Schlimok G, Schmiegel W, Raab R, Hoffken K, Gruber R, Funke I, Pichlmaier H, Hirche H, Buggisch P, Witte J, Pichlmayr R. Monoclonal antibody therapy for resected Dukes' C colorectal cancer: seven-year outcome of a multicenter randomized trial. J Clin Oncol 1998 May;16(5):1788-94.

56. Handgretinger R, Anderson K, Lang P, Dopfer R, Klingebiel T, Schrappe M, Reuland P, Gillies SD, Reisfeld RA, Neithammer D. A phase I study of human/mouse chimeric antiganglioside GD2 antibody ch14.18 in patients with neuroblastoma. Eur J Cancer 1995;31A(2):261-7.

57. George AJ, Spooner RA, Epenetos AA. Applications of monoclonal antibodies in clinical oncology. Immunol Today 1994 Dec;15(12):559-61.

58. Ghetie MA, Ghetie V, Vitetta ES. Immunotoxins for the treatment of B-cell lymphomas. Mol Med 1997 Jul;3(7):420-7.

59. Goldenberg DM, Larson SM, Reisfeld RA, Schlom J. Targeting cancer with radiolabeled antibodies. Immunol Today 1995 Jun;16(6):261-4.

60. Zhu H, Baxter LT, Jain RK. Potential and limitations of radioimmunodetection and radioimmunotherapy with monoclonal antibodies. J Nucl Med 1997 May;38(5):731-41.

61. Maas RA, Dullens HF, Den Otter W. Interleukin-2 in cancer treatment: disappointing or (still) promising? A review. Cancer Immunol Immunother 1993;36(3):141-8.

62. Rosenberg SA. Immunotherapy of cancer using interleukin 2: current status and future prospects. Immunol Today 1988 Feb;9(2):58-62.

63. Forni G, Giovarelli M, Santoni A, Modesti A, Forni M. Interleukin 2 activated tumor inhibition in vivo depends on the systemic involvement of host immunoreactivity. J Immunol 1987 Jun;138(11):4033-41.

64. Kammula US, White DE, Rosenberg SA. Trends in the safety of high dose bolus interleukin-2 administration in patients with metastatic cancer. Cancer 1998 Aug;83(4):797-805.

65. Nanni P, Rossi I, De Giovanni C, Landuzzi L, Nicoletti G, Stoppacciaro A, Parenza M, Colombo MP, Lollini PL. Interleukin 12 gene therapy of MHC-negative murine melanoma metastases. Cancer Res 1998 Mar;58(6):1225-30.

66. Reisfeld RA, Mueller BM, Handgretinger R, Yu AL, Gillies SD. Potential of genetically engineered anti-ganglioside GD2 antibodies for cancer immunotherapy. Prog Brain Res 1994;101:201-12.

67. Gillies SD, Young D, Lo KM, Foley SF, Reisfeld RA. Expression of genetically engineered immunoconjugates of lymphotoxin and a chimeric anti-ganglioside GD2 antibody. Hybridoma 1991 Jun;10(3):347-56.

68. Gillies SD, Reilly EB, Lo KM, Reisfeld RA. Antibody-targeted interleukin 2 stimulates T-cell killing of autologous tumor cells. Proc Natl Acad Sci U S A 1992 Feb;89(4):1428-32.

69. Tao MH, Levy R. Idiotype/granulocyte-macrophage colony-stimulating factor fusion protein as a vaccine for B-cell lymphoma [see comments]. Nature 1993 Apr;362(6422):755-8.

70. Sabzevari H, Gillies SD, Mueller BM, Pancook JD, Reisfeld RA. A recombinant antibody-interleukin 2 fusion protein suppresses growth of hepatic human neuroblastoma metastases in severe combined immunodeficiency mice. Proc Natl Acad Sci U S A 1994 Sep;91(20):9626-30.

71. Becker JC, Pancook JD, Gillies SD, Mendelsohn J, Reisfeld RA. Eradication of human hepatic and pulmonary melanoma metastases in SCID mice by antibody-interleukin 2 fusion proteins. Proc Natl Acad Sci U S A 1996 Apr;93(7):2702-7.

72. Hornick JL, Khawli LA, Hu P, Lynch M, Anderson PM, Epstein AL. Chimeric CLL-1 antibody fusion proteins containing granulocyte- macrophage colony-stimulating factor or interleukin-2 with specificity for B-cell malignancies exhibit enhanced effector functions while retaining tumor targeting properties. Blood 1997 Jun;89(12):4437-47.

73. Chen TT, Tao MH, Levy R. Idiotype-cytokine fusion proteins as cancer vaccines. Relative efficacy of IL-2, IL-4, and granulocyte-macrophage colony-stimulating factor. J Immunol 1994 Nov;153(10):4775-87.

74. Haraguchi M, Yamashiro S, Yamamoto A, Furukawa K, Takamiya K, Lloyd KO, Shiku H, Furukawa K. Isolation of GD3 synthase gene by expression cloning of GM3 alpha-2,8-sialyltransferase cDNA using anti-GD2 monoclonal antibody. Proc Natl Acad Sci U S A 1994 Oct;91(22):10455-9.

75. Yamashiro S, Haraguchi M, Furukawa K, Takamiya K, Yamamoto A, Nagata Y, Lloyd KO, Shiku H, Furukawa K. Substrate specificity of beta 1,4-N-acetylgalactosaminyltransferase *in vitro* and in cDNA-transfected cells. GM2/GD2 synthase efficiently generates asialo-GM2 in certain cells. J Biol Chem 1995 Mar;270(11):6149-55.

76. Becker JC, Pancook JD, Gillies SD, Furukawa K, Reisfeld RA. T cell-mediated eradication of murine metastatic melanoma induced by targeted interleukin 2 therapy. J Exp Med 1996 May;183(5):2361-6.

77. Becker JC, Varki N, Gillies SD, Furukawa K, Reisfeld RA. An antibody-interleukin 2 fusion protein overcomes tumor heterogeneity by induction of a cellular immune response. Proc Natl Acad Sci U S A 1996 Jul;93(15):7826-31.

78. Becker JC, Varki N, Gillies SD, Furukawa K, Reisfeld RA. Long-lived and transferable tumor immunity in mice after targeted interleukin-2 therapy. J Clin Invest 1996 Dec;98(12):2801-4.

79. Sprent J. Antigen-presenting cells. Professionals and amateurs. Curr Biol 1995 Oct;5(10):1095-7.

80. Zhang X, Sun S, Hwang I, Tough DF, Sprent J. Potent and selective stimulation of memory-phenotype CD8+ T cells *in vivo* by IL-15. Immunity 1998 May;8(5):591-9.

81. Banchereau J, Steinman RM. Dendritic cells and the control of immunity. Nature 1998 Mar;392(6673):245-52.

82. Nestle FO, Alijagic S, Gilliet M, Sun Y, Grabbe S, Dummer R, Burg G, Schadendorf D. Vaccination of melanoma patients with peptide- or tumor lysate-pulsed dendritic cells. Nat Med 1998 Mar;4(3):328-32.

83. Rosenberg SA, Yang JC, Schwartzentruber DJ, Hwu P, Marincola FM, Topalian SL, Restifo NP, Dudley ME, Schwarz SL, Spiess PJ, Wunderlich JR, Parkhurst MR, Kawakami Y, Seipp CA, Einhorn JH, White DE. Immunologic and therapeutic evaluation of a synthetic peptide vaccine for the treatment of patients with metastatic melanoma [see comments]. Nat Med 1998 Mar;4(3):321-7.

84. Boon T, van der BP. Human tumor antigens recognized by T lymphocytes. J Exp Med 1996 Mar;183(3):725-9.

85. Castelli C, Rivoltini L, Mazzocchi A, Parmiani G. T-cell recognition of melanoma antigens and its therapeutic applications. Int J Clin Lab Res 1997;27(2):103-10.

86. Salvi S, Segalla F, Rao S, Arienti F, Sartori M, Bratina G, Caronni E, Anichini A, Clemente C, Parmiani G. Overexpression of the T-cell receptor beta-chain variable region TCRBV14 in HLA-A2-matched primary human melanomas. Cancer Res 1995 Aug;55(15):3374-9.

87. Dummer R, Gore ME, Hancock BW, Guillou PJ, Grobben HC, Becker JC, Oskam R, Dieleman JP, Burg G. A multicenter phase II clinical trial using dacarbazine and continuous infusion interleukin-2 for metastatic melanoma. Clinical data and immunomonitoring [see comments]. Cancer 1995 Feb;75(4):1038-44.

88. Pardoll DM. Paracrine cytokine adjuvants in cancer immunotherapy. Annu Rev Immunol 1995;13:399-415.

89. Chomczynski P, Sacchi N. Single-step method of RNA isolation by acid guanidinium thiocyanate- phenol-chloroform extraction. Anal Biochem 1987 Apr;162(1):156-9.

90. Rychlik W, Rhoads RE. A computer program for choosing optimal oligonucleotides for filter hybridization, sequencing and *in vitro* amplification of DNA. Nucleic Acids Res 1989 Nov;17(21):8543-51.

91. Johnston RF, Pickett SC, Barker DL. Autoradiography using storage phosphor technology. Electrophoresis 1990 May;11(5):355-60.

92. Hoppe BL, Conti-Tronconi BM, Horton RM. Gel-loading dyes compatible with PCR. Biotechniques 1992 May;12(5):679-80.

93. Mullis K, Faloona F, Scharf S, Saiki R, Horn G, Erlich H. Specific enzymatic amplification of DNA *in vitro*: the polymerase chain reaction. Cold Spring Harb Symp Quant Biol 1986;51 Pt 1:263-73.

94. Lerman LS, Silverstein K. Computational simulation of DNA melting and its application to denaturing gradient gel electrophoresis. Methods Enzymol 1987;155:482-501.

95. Guldberg P, Guttler F. 'Broad-range' DGGE for single-step mutation scanning of entire genes: application to human phenylalanine hydroxylase gene. Nucleic Acids Res 1994 Mar;22(5):880-1.

96. Stackpole CW. Intrapulmonary spread of established B16 melanoma lung metastases and lung colonies. Invasion Metastasis 1990;10(5):267-80.

97. Sheffield VC, Cox DR, Lerman LS, Myers RM. Attachment of a 40-base-pair G + C-rich sequence (GC-clamp) to genomic DNA fragments by the polymerase chain reaction results in improved detection of single-base changes. Proc Natl Acad Sci U S A 1989 Jan;86(1):232-6.

98. Van den Eynde BJ, Boon T. Tumor antigens recognized by T lymphocytes. Int J Clin Lab Res 1997;27(2):81-6.

99. Scholler J, thor SP, Birck A, Siim E, Dahlstrom K, Drzewiecki KT, Zeuthen J. Analysis of T cell receptor alpha beta variability in lymphocytes infiltrating melanoma primary tumours and metastatic lesions. Cancer Immunol Immunother 1994 Oct;39(4):239-48.

100. Pancook JD, Becker JC, Gillies SD, Reisfeld RA. Eradication of established hepatic human neuroblastoma metastases in mice with severe combined immunodeficiency by antibody-targeted interleukin-2. Cancer Immunol Immunother 1996 Feb;42(2):88-92.

101. Lode HN, Xiang R, Varki NM, Dolman CS, Gillies SD, Reisfeld RA. Targeted interleukin-2 therapy for spontaneous neuroblastoma metastases to bone marrow. J Natl Cancer Inst 1997 Nov;89(21):1586-94.

102. Xiang R, Lode HN, Dolman CS, Dreier T, Varki NM, Qian X, Lo KM, Lan Y, Super M, Gillies SD, Reisfeld RA. Elimination of established murine colon carcinoma metastases by antibody-interleukin 2 fusion protein therapy. Cancer Res 1997 Nov;57(21):4948-55.

103. Becker JC, Varki N, Brocker EB, Reisfeld RA. Lymphocyte-mediated alopecia in C57BL/6 mice following successful immunotherapy for melanoma. J Invest Dermatol 1996 Oct;107(4):627-32.

104. Zhai Y, Yang JC, Spiess P, Nishimura MI, Overwijk WW, Roberts B, Restifo NP, Rosenberg SA. Cloning and characterization of the genes encoding the murine homologues of the human melanoma antigens MART1 and gp100. J Immunother 1997 Jan;20(1):15-25.

105. Bloom MB, Perry-Lalley D, Robbins PF, Li Y, el Gamil M, Rosenberg SA, Yang JC. Identification of tyrosinase-related protein 2 as a tumor rejection antigen for the B16 melanoma. J Exp Med 1997 Feb;185(3):453-9.

106. Wang RF, Robbins PF, Kawakami Y, Kang XQ, Rosenberg SA. Identification of a gene encoding a melanoma tumor antigen recognized by HLA-A31-restricted tumor-infiltrating lymphocytes [published erratum appears in J Exp Med 1995 Mar 1;181(3):1261]. J Exp Med 1995 Feb;181(2):799-804.

107. Hara I, Nguyen H, Takechi Y, Gansbacher B, Chapman PB, Houghton AN. Rejection of mouse melanoma elicited by local secretion of interleukin- 2: implicating macrophages without T cells or natural killer cells in tumor rejection. Int J Cancer 1995 Apr;61(2):253-60.

108. Faure F, Even J, Kourilsky P. Tumor-specific immune response: current *in vitro* analyses may not reflect the *in vivo* immune status. Crit Rev Immunol 1998;18(1-2):77-86.

109. Levraud JP, Duffour MT, Cordier L, Perricaudet M, Haddada H, Kourilsky P. IL-2 gene delivery within an established murine tumor causes its regression without proliferation of preexisting antitumor-specific CTL. J Immunol 1997 Apr;158(7):3335-43.

110. thor Straten P, Guldberg P, Seremet T, Reisfeld RA, Zeuthen J, Becker JC. Activation of preexisting T cell clones by targeted interleukin 2 therapy. Proc Natl Acad Sci U S A 1998 Jul;95(15):8785-90.

111. thor Straten P, Guldberg P, Gronbaek K, Hansen MR, Kirkin AF, Seremet T, Zeuthen J, Becker JC. In situ T cell responses against melanoma comprise high numbers of locally expanded T cell clonotypes. J Immunol 1999 Jul;163(1):443-7.

112. Pawelec G, Zeuthen J, Kiessling R. Escape from host-antitumor immunity. Crit Rev Oncog 1997;8(2-3):111-41.

113. Harada M, Tamada K, Abe K, Li T, Onoe Y, Tada H, Tatsugami K, Ando T, Kimura G, Nomoto K. Characterization of B16 melanoma-specific cytotoxic T lymphocytes. Cancer Immunol Immunother 1998 Dec;47(4):198-204.

114. Lee KH, Panelli MC, Kim CJ, Riker AI, Bettinotti MP, Roden MM, Fetsch P, Abati A, Rosenberg SA, Marincola FM. Functional dissociation between local and systemic immune response during anti-melanoma peptide vaccination. J Immunol 1998 Oct;161(8):4183-94.

115. Rosenberg SA. Cancer vaccines based on the identification of genes encoding cancer regression antigens. Immunol Today 1997 Apr;18(4):175-82.

116. Reisfeld RA, Becker JC, Gillies SD. Immunocytokines: a new approach to immunotherapy of melanoma. Melanoma Res 1997 Aug;7 Suppl 2:S99-106.

117. Staveley-O'Carroll K, Sotomayor E, Montgomery J, Borrello I, Hwang L, Fein S, Pardoll D, Levitsky H. Induction of antigen-specific T cell anergy: An early event in the course of tumor progression. Proc Natl Acad Sci U S A 1998 Feb;95(3):1178-83.

118. De Togni P, Goellner J, Ruddle NH, Streeter PR, Fick A, Mariathasan S, Smith SC, Carlson R, Shornick LP, Strauss-Schoenberger J. Abnormal development of peripheral lymphoid organs in mice deficient in lymphotoxin. Science 1994 Apr;264(5159):703-7.

119. von Boehmer H. Lymphotoxins: from cytotoxicity to lymphoid organogenesis. Proc Natl Acad Sci U S A 1997 Aug;94(17):8926-7.

120. Cuff CA, Schwartz J, Bergman CM, Russell KS, Bender JR, Ruddle NH. Lymphotoxin alpha3 induces chemokines and adhesion molecules: insight into the role of LT alpha in inflammation and lymphoid organ development. J Immunol 1998 Dec;161(12):6853-60.

121. Sacca R, Cuff CA, Lesslauer W, Ruddle NH. Differential activities of secreted lymphotoxin-alpha3 and membrane lymphotoxin-alpha1beta2 in lymphotoxin-induced inflammation: critical role of TNF receptor 1 signaling. J Immunol 1998 Jan;160(1):485-91.

122. Loetscher H, Pan YC, Lahm HW, Gentz R, Brockhaus M, Tabuchi H, Lesslauer W. Molecular cloning and expression of the human 55 kd tumor necrosis factor receptor. Cell 1990 Apr;61(2):351-9.

123. Browning JL, Ngam-ek A, Lawton P, DeMarinis J, Tizard R, Chow EP, Hession C, O'Brine-Greco B, Foley SF, Ware CF. Lymphotoxin beta, a novel member of the TNF family that forms a heteromeric complex with lymphotoxin on the cell surface. Cell 1993 Mar;72(6):847-56.

124. Crowe PD, VanArsdale TL, Walter BN, Ware CF, Hession C, Ehrenfels B, Browning JL, Din WS, Goodwin RG, Smith CA. A lymphotoxin-beta-specific receptor. Science 1994 Apr;264(5159):707-10.

125. Rennert PD, Browning JL, Mebius R, Mackay F, Hochman PS. Surface lymphotoxin alpha/beta complex is required for the development of peripheral lymphoid organs. J Exp Med 1996 Nov;184(5):1999-2006.

126. Koni PA, Sacca R, Lawton P, Browning JL, Ruddle NH, Flavell RA. Distinct roles in lymphoid organogenesis for lymphotoxins alpha and beta revealed in lymphotoxin beta-deficient mice. Immunity 1997 Apr;6(4):491-500.

127. Rennert PD, James D, Mackay F, Browning JL, Hochman PS. Lymph node genesis is induced by signaling through the lymphotoxin beta receptor. Immunity 1998 Jul;9(1):71-9.

128. Kratz A, Campos-Neto A, Hanson MS, Ruddle NH. Chronic inflammation caused by lymphotoxin is lymphoid neogenesis. J Exp Med 1996 Apr;183(4):1461-72.

129. Ruddle NH. Lymphoid neo-organogenesis: lymphotoxin's role in inflammation and development. Immunol Res 1999;19(2-3):119-25.

130. Reisfeld RA, Gillies SD, Mendelsohn J, Varki NM, Becker JC. Involvement of B lymphocytes in the growth inhibition of human pulmonary melanoma metastases in athymic nu/nu mice by an antibody- lymphotoxin fusion protein. Cancer Res 1996 Apr;56(8):1707-12.

131. Taguchi T, McGhee JR, Coffman RL, Beagley KW, Eldridge JH, Takatsu K, Kiyono H. Detection of individual mouse splenic T cells producing IFN-gamma and IL-5 using the enzyme-linked immunospot (ELISPOT) assay. J Immunol Methods 1990 Mar;128(1):65-73.

132. Moerch U, Schrama D, Guldberg P, Seremet T, Zeuthen J, Becker JC, thor-Straten P. Comparative delineation of T cell clonotypes in coexisting syngeneic B16 melanoma. Cancer Immunol Immunother 49, 426-432. 2000.

133. Robson SC, Schulte am Esch J, Bach FH. Factors in xenograft rejection. Ann N Y Acad Sci 1999 Jun;875:261-76.

134. Brouard S, Gagne K, Blancho G, Soulillou JP. T cell response in xenorecognition and xenografts: a review. Hum Immunol 1999 Jun;60(6):455-68.

135. Salmi M, Hellman J, Jalkanen S. The role of two distinct endothelial molecules, vascular adhesion protein-1 and peripheral lymph node addressin, in the binding of lymphocyte subsets to human lymph nodes. J Immunol 1998 Jun;160(11):5629-36.

136. Stein JV, Rot A, Luo Y, Narasimhaswamy M, Nakano H, Gunn MD, Matsuzawa A, Quackenbush EJ, Dorf ME, von Andrian UH. The CC Chemokine Thymus-derived Chemotactic Agent 4 (TCA-4, Secondary Lymphoid Tissue Chemokine, 6Ckine, Exodus-2) Triggers Lymphocyte Function-associated Antigen 1-mediated Arrest of Rolling T

Lymphocytes in Peripheral Lymph Node High Endothelial Venules. J Exp Med 2000 Jan;191(1):61-76.

137. Campbell JJ, Hedrick J, Zlotnik A, Siani MA, Thompson DA, Butcher EC. Chemokines and the arrest of lymphocytes rolling under flow conditions. Science 1998 Jan;279(5349):381-4.

138. Cuff CA, Sacca R, Ruddle NH. Differential induction of adhesion molecule and chemokine expression by LTalpha3 and LTalphabeta in inflammation elucidates potential mechanisms of mesenteric and peripheral lymph node development. J Immunol 1999 May;162(10):5965-72.

139. Lakkis FG, Arakelov A, Konieczny BT, Inoue Y. Immunologic 'ignorance' of vascularized organ transplants in the absence of secondary lymphoid tissue. Nat Med 2000 Jun;6(6):686-8.

140. Cyster JG. Chemokines and cell migration in secondary lymphoid organs. Science 1999 Dec;286(5447):2098-102.

141. Shrikant P, Mescher MF. Control of syngeneic tumor growth by activation of CD8+ T cells: efficacy is limited by migration away from the site and induction of nonresponsiveness. J Immunol 1999 Mar;162(5):2858-66.

142. Flynn KJ, Belz GT, Altman JD, Ahmed R, Woodland DL, Doherty PC. Virus-specific CD8+ T cells in primary and secondary influenza pneumonia. Immunity 1998 Jun;8(6):683-91.

143. Stackpole CW. Distinct lung-colonizing and lung-metastasizing cell populations in B16 mouse melanoma. Nature 1981 Feb;289(5800):798-800.

144. Fields P, Fitch FW, Gajewski TF. Control of T lymphocyte signal transduction through clonal anergy. J Mol Med 1996 Nov;74(11):673-83.

145. Bousso P, Kourilsky P. A clonal view of alphabeta T cell responses. Semin Immunol 1999 Dec;11(6):423-31.

146. Marincola FM, Jaffee EM, Hicklin DJ, Ferrone S. Escape of human solid tumors from T-cell recognition: molecular mechanisms and functional significance. Adv Immunol 2000;74:181-273.